INTERNATIONAL UNION OF CRYSTALLOGRAPHY

IUCr Newsletter

Volume 32 · Issue 4

Collected archival edition
Original article text and available illustrations

Contents

Letter from the President

President's Letter – Winter 2024 3

Editorial

Editorial 5

IUCr activities

International Tables Volume C Second Edition - Data Mining Chapters 7

Feature article

Methods in molecular photocrystallography 9

On the importance of crystal structures for organic thin film transistors 38

Commentary

The structure of Chlamydomonas LOV1 as revealed by time-resolved serial synchrotron crystallography 57

AI-enhanced X-ray diffraction analysis: towards real-time mineral phase identification and quantification 60

Unity gives strength: combining Bertaut's and Belov's concepts and the formalism of aperiodic crystals to solve magnetic structures of unprecedented complexity 63

Associates news

Japan-Taiwan Bilateral Seminar on Crystallography: "Frontier of Crystallography" 66

Outreach

11th Polish Crystal Growing Competition for Schools 2024 68

Meeting report (IUCr supported)

ACA2024 Meeting 72

Meeting report

SCANZ Crystal 35 Meeting Report – Going West! 76

Notice

Results of the 7th CSP blind test published - overcoming pharmaceutical and other materials issues before they exist 80

Press release

Setting the pace in non-ambient XRD: a new benchmark for environmental heating 83

Feature article

Tribute to the support groups in the quasicrystal discovery – a 40-year anniversary 86

IUCr supported events

IUCr supported meetings 95

Meetings calendar

Meetings calendar 96

LETTER FROM THE PRESIDENT

President's Letter – Winter 2024



Santiago García-Granda

As we bid farewell to the year 2024 and look forward to the beginning of 2025, I write this brief note for the winter *Newsletter* of the IUCr with best wishes to the people who make up this scientific family.

2024 has been a busy year in terms of scientific meetings of our regional associations, all of them very successful, the last and most recent being the Asian Crystallographic Association (AsCA) meeting in Kuala Lumpur, Malaysia. The regional impact of the IUCr is one of the most effective ways to bring the IUCr closer to the scientific societies related to structural science. Once again we have witnessed the awarding of a Nobel Prize directly related to structural science and macromolecular crystallography. Our community has produced some very creative videos with ingenious ideas for the crystallization competitions that are held in many countries. The new EC Outreach Committee is overseeing support for proposed outreach initiatives around the world. We have also boosted the prominence and leadership of women scientists in our community resulting in an impact on global science.

The reorganization of staff in our Chester office is being completed successfully, both in the editorial, administrative and outreach sections, with Kezia Bowman now looking after the *IUCr Newsletter* and the addition of Harriet Jackson in the office. There are great expectations for an increase in our editorial strength with the addition of the new Head of Publishing Strategy, who is expected to join the Chester editorial team in the new year.

The Executive Committee met virtually on 12 November, and the Finance Committee will meet virtually on 18 December. The Finance Committee will meet in person in Lund, Sweden, on 24-25 March 2025, just after the annual meeting of the Journals Management Board, which will take place in Chester on 20-21 March. It is a priority for the Executive Committee to return the activity levels of our journals to those in 2019 and to recover their capacity to produce the resources to cover the funding of our projects, especially the support to young scientists and the promotion of structural science in less developed geographical areas. In this endeavor, it is also important that the Finance Committee is able to identify the most productive and secure investments for the future of our financial health.

2025 will be a year of consolidation of the organization of the Congress and the 27th General Assembly in Calgary, Canada. As with every congress, the participation and support of our commercial partners will be very important in order to be able to organise a commercial exhibition as attractive as our scientific congress. It is important that no participation is hampered by bureaucratic or other issues, and we will strive to facilitate the widest possible participation and, in particular, to promote the presence and influence of younger researchers.

All IUCr Commissions are proposing members of the International Programme Committee (IPC) and selecting the more attractive speakers for the Plenary and Keynote Lectures, as well as the most

appealing Microsymposia, showing the impact of crystallography and structural science in solving the challenges of the present and future of our planet.

The International Science Council (ISC) Elections for the shortlist of candidates for renewal of the ISC Governing Board will take place in Oman, in the framework of the Muscat Global Knowledge Dialogue and Third ISC General Assembly, in January 2025. The IUCr will be represented by our Vice-President Professor Graciela Díaz de Delgado.

Following its inaugural meeting, the IUCr Early Career Scientist Division (ECSD) met on 18 November 2024, and several decisions were taken to develop this important division of IUCr. The first elected Chair and Co-chair were Rebecca Clulow (ECA) and Orbett Alexander (AfCA). Kara Zielinski (ACA) was nominated as a member of the Division to serve on the International Program Committee (IPC). Actions were planned to increase the visibility of the new IUCr Division in the existing communities and to organize meetings for young scientists in the field of structural sciences. All of the initial group are actively producing new ideas and developing the framework and networks to have a major impact on the present and the future of IUCr.

As usual, I end this letter with deep gratitude to all those who form and make our organisation work, the Regional Associates, the IUCr Commissions and Committees, Editors, Co-editors, referees and authors of our journals, our Chester staff and all individual structural scientists, women and men.

Thanks to *IUCr Newsletter* Editor Mike Glazer, and his team, and thanks to all contributors for making possible, as with every issue, a new issue that continues to be the reference communication for our community.

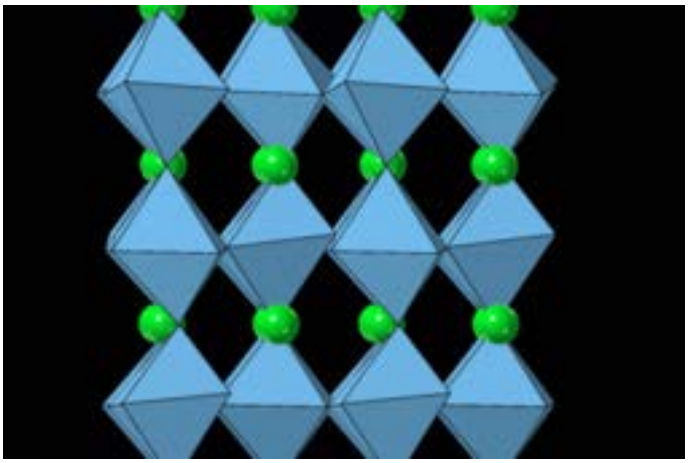
Thank you all for helping to keep the momentum of the IUCr going, wherever you are in the world.

Enjoy the holiday season with your families, colleagues and friends!

Best wishes for the best personal and professional development in 2025.

EDITORIAL

Editorial



Mike Glazer

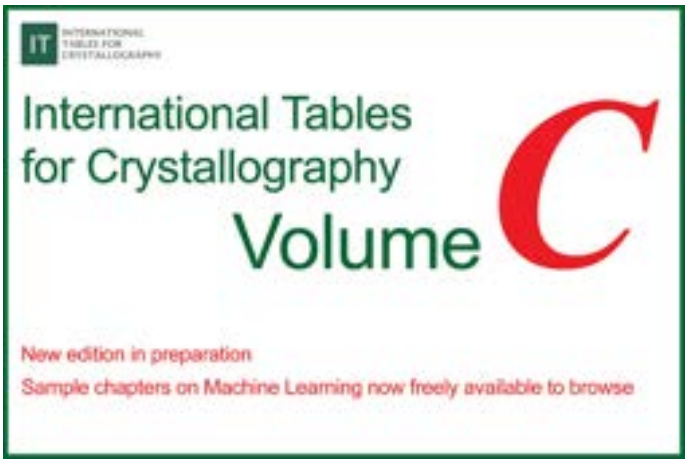
I recently attended a meeting of the Biographical Memoirs Committee of the Royal Society where a discussion was had about how to promote the Memoirs to the wider public. I was reminded that some time ago we ran an article (https://www.iucr.org/news/newsletter/etc/articles?issue=147154&result_138339_result_page=24) on the memoirs of crystallographers who were Fellows of the Royal Society. When one considers the great successes of crystallographers since the initial work of Laue in Germany and the Braggs, father and son, in England in 1912, together with the extraordinary number of Nobel Prizes awarded for research in or related to crystallography (roughly 30), it is not surprising to find so many biographical memoirs of crystallographers in the Royal Society archives. So, for those of you who missed the earlier article, I thought it would be worth recalling that there is a wealth of interesting material available on the Royal Society website. Since that list was published in the *Newsletter*, we have to add the memoirs of Michael Woolfson, who died in 2019 (https://royalsocietypublishing.org/doi/10.1098/rsbm.2021.0018), and Louise Johnson, who died in 2012 (https://royalsocietypublishing.org/doi/10.1098/rsbm.2021.0038).

It is not often that a particular science suddenly has most of its basic tenets overthrown, but that is exactly what occurred 40 years ago in Crystallography. I recall how surprised (shocked?) I was to hear then that some crystals had been discovered that completely overturned the received dogma on the nature of symmetry in crystals. Like most crystallographers, I had been brought up in the belief that crystals could not have 5-fold rotational symmetry and that, according to the so-called Crystallographic Restriction Theorem, only 1 (*i.e.* no symmetry), 2, 3, 4 and 6-fold symmetry were allowed. Dan Schechtman's discovery and subsequent Nobel Prize (2011) made crystallographers rethink what they thought they knew about crystal symmetry. In this issue of the *Newsletter*, Istvan Hargittai has written an article for us (https://www.iucr.org/news/newsletter/volume-32/number-4/tribute-to-the-support-groups-in-the-quasicrystal-discovery-a-40-year-anniversary) recording some aspects of that discovery and how it came to be in collaboration with others at the time. Today, the existence of so-called *quasicrystals* is completely accepted, and numerous papers and books have been written on this subject. However, this is mainly of an academic nature since quasicrystals have yet to find much application, and the Restriction Theorem still applies to most crystals that we study. Quasicrystals belong to a class of crystals known in general as aperiodic crystals, where the usual concept of periodicity (*i.e.* repetition of atoms or molecules to define what we call the *crystal structure*) breaks down in three dimensions. However, when one considers periodicity occurring in a higher dimension (mathematicians have no problem with this!), typically in a 6-dimensional space, quasicrystals then become understandable as a projection down onto our 3-dimensional world. So, when we think of what a crystal means, we have to revise previously held views. See, for example, https://www.iucr.org/news/newsletter/etc/articles?issue=151351&result_138339_result_page=17. It is

interesting to note that some clever scientists, such as Roger Penrose and, especially, the crystallographer Alan Mackay at Birkbeck College London, had already been playing around with these ideas long before the discovery of quasicrystals. I recall, as a young PhD student, attending lectures by Alan, who taught us how to draw different crystal shapes, and he introduced some rather unusual thoughts on crystal symmetry, but I have to admit that I did not appreciate his ideas at the time!

IUCR ACTIVITIES

International Tables Volume C Second Edition - Data Mining Chapters



Ludmila Kuleshova, Detlef Hofmann

Crystallography has been (and still remains) one of the most multidisciplinary sciences that links together frontier areas of research and has, directly or indirectly, produced the largest number of Nobel Laureates throughout history (up to 29 Prizes for 48 Laureates now). It is therefore not surprising that the recent Nobel Prizes for Physics and Chemistry in 2024 once again highlight the groundbreaking advancements made in the field of crystallography. This time, the award was given for the development of methods to predict protein structures using methods of machine learning.

Crystallographers were among the first scientists to recognize the importance of collecting data on crystal structures. The subsequent explosive growth has been caused by the accumulation of huge amounts of data and the growing ability of computers to store them. Data mining has appeared as the tool of choice when extracting hidden patterns and new knowledge from data by using computing power and applying new techniques of machine learning. This has been aided by such precedent discoveries in computer science as neural networks (1943), clustering, genetic algorithms (1950s), decision trees (1960s) and support vector machines (1980s). Even if the key algorithms used in data mining today were known in mathematics as early as the beginning of the last century, data mining is still a young field of science with the rapid evolution of methods and tools and the explosive growth of computational possibilities. Partly for this reason, it is very difficult to find a unified terminology and presentation within the huge amount of specialized literature, like in handbooks on data mining. Therefore, to navigate between tasks, algorithms and their applications as used in crystallography, the new edition of *International Tables for Crystallography* (*Volume C: Mathematical, Physical and Chemical Tables*) will include two new chapters: 'Data mining. I. Machine learning in crystallography' and 'Data mining. II. Prediction of protein structure and optimization of protein crystallizability'.

The first chapter, written by D. W. M. Hofmann and L. N. Kuleshova, introduces readers to the concept, terminology and overall scheme of machine learning as it is used today. Then, the main tasks of machine learning, such as clustering, anomaly detection, classification, regression and summarization (dimensionality reduction), are characterized and specified in relation to actual problems of crystallography. For example, together with an overview of clustering algorithms and methods of similarity detection (also known as pattern recognition), several important applications of crystal structure clustering are described. Clustering of polymorphs defined at non-ambient conditions reveals significant structural changes and the need to take into account additional descriptors (temperature and pressure) during Crystal Structure Prediction.

The presented mathematical concept behind the tasks of classification and regression is illustrated using examples drawn from crystal-density estimation and force-field development. The new approach for the refining of the model and parameters of a force field allows one to handle any types of atoms including metals and ions, and to take into account external conditions. It helps improve significantly the predictability of Crystal Structure Prediction, which belongs one of the high level primary goals of machine learning.

The summarization (dimensionality reduction) task is illustrated in the chapter by calculation and prediction of solubility, the property that is of crucial importance for pharmaceutical developments and drug discovery, as are estimates of the crystal energy for monitoring the stability of proposed new drugs.

The importance of the anomaly (outlier) detection task is also highlighted. Since all methods of machine learning are very sensitive to data quality, they can easily detect anomalies and outliers. An accurate analysis of any outliers is very often worthwhile as it can indicate the kinds of problems present: erroneous data, or the inefficiency or unsuitability of the models. Furthermore, several cleansers have been developed for use during data pre-processing in addition to the two cleansers used at present in the Cambridge Structural Database, the first of which, *enCIFer* (CCDC, 2016), checks the syntax of the data, while the second, *PLATON* (Spek, 2016), checks the reasonableness of the structure and, for instance, annotates the records of structures that contain large voids. It is also illustrated how the data cleansers develop during machine learning work within the algorithms and how they can be used for database cleansing. The removal of anomalous data from a dataset often results in a significant increase in the accuracy of data-mining procedures.

The second chapter, written by A. Kloczkowski *et al.*, is dedicated to the application of machine learning techniques to extract predictive information from the protein, DNA and RNA databases. Mining for information in biological databases involves various forms of data analysis such as clustering, sequence homology searches, structure homology searches, examination of statistical significance, *etc*. In particular, the data mining of structural fragments of proteins from known structures in the Protein Data Bank (PDB) significantly improves the accuracy of secondary structure prediction. Accordingly, in the chapter, an original method (fragment data mining, FDM) is discussed. The method mines the structural segments from the PDB and utilizes structural information by matching the sequence of these structural fragments with the aim of improving the prediction of secondary structure. Consequently, further improvements are discussed that combine FDM with the classical GOR V secondary structure prediction method. This one is based on information theory and Bayesian statistics, coupled with evolutionary information from multiple sequence alignments. The newer and more accurate approach for secondary structure predictions is also introduced: the SPINE-X method based on a machine learning methodology to predict secondary structures by mining protein sequences and structures. The obtained results strongly suggest that data mining can be an efficient and accurate approach for secondary structure prediction in proteins. The last part of this second chapter discusses applications of data mining to the problem of optimizing protein crystallization conditions. Machine learning can be used to improve the yield and quality of protein crystals, and thus aid in solving protein structures by X-ray crystallography. There is a vast amount of data for protein structures, sequences and crystallization conditions that can be mined to aid in structure prediction and structure determination.

We hope that the methods and concepts presented in these chapters will make data mining and machine learning more accessible to the general practitioner in crystallography, and allow new applications in the field and the discovery of non-trivial and scientifically relevant knowledge.

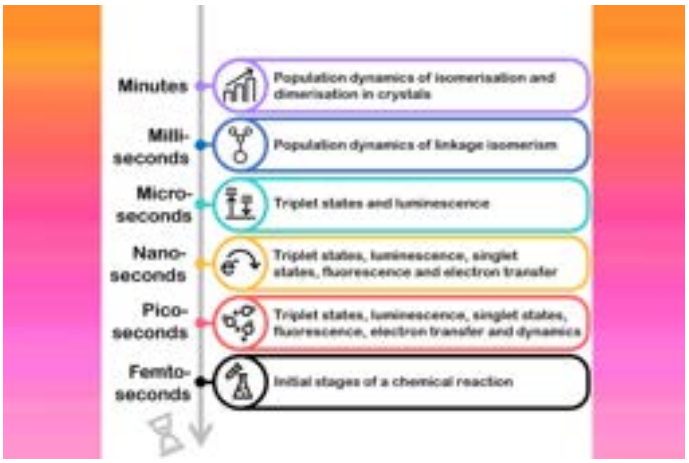
References

Spek, A. (2016). *PLATON*, University of Utrecht, The Netherlands.

CCDC (2016). *enCIFer*, Cambridge Crystallographic Data Centre, UK.

FEATURE ARTICLE

Methods in molecular photocrystallography



Lauren E. Hatcher, Mark R. Warren, Paul R. Raithby

This article is part of the collection Best practice in crystallography.

Over the last three decades, the technology that makes it possible to follow chemical processes in the solid state in real time has grown enormously. These studies have important implications for the design of new functional materials for applications in optoelectronics and sensors. Light–matter interactions are of particular importance, and *photocrystallography* has proved to be an important tool for studying these interactions. In this technique, the three-dimensional structures of light-activated molecules, in their excited states, are determined using single-crystal X-ray crystallography. With advances in the design of high-power lasers, pulsed LEDs and time-gated X-ray detectors, the increased availability of synchrotron facilities, and most recently, the development of XFELs, it is now possible to determine the structures of molecules with lifetimes ranging from minutes down to picoseconds, within a single crystal, using the photocrystallographic technique. This review discusses the procedures for conducting successful photocrystallographic studies and outlines the different methodologies that have been developed to study structures with specific lifetime ranges. The complexity of the methods required increases considerably as the lifetime of the excited state shortens. The discussion is supported by examples of successful photocrystallographic studies across a range of timescales and emphasises the importance of the use of complementary analytical techniques in order to understand the solid-state processes fully.

1. Background

The term *Photocrystallography* has been used since the 1990s to describe diffraction experiments in which the structure of a metastable or excited state species within a crystalline solid is determined by crystallography when the material is activated by light (Cole, 2008; Coppens, 2017). The term was first used by Philip Coppens (Carducci *et al.*, 1997), one of the pioneers in the research area, and is now used to refer to a wide range of experiments in which photochemical and crystallographic techniques are used to study dynamic processes in crystalline solids. An analogous term *X-ray photodiffraction* (Naumov, 2012) has also been used to describe experiments in which diffraction has been used to study the salient effects of dynamic crystals which undergo a rapid phase transition upon exposure to light (photo-salient), causing the crystalline sample to rapidly move or in some cases jump (Naumov *et al.*, 2020). Heat (thermo-salient) or localized pressure (mechano-salient) effects can also initiate rapid movement in crystalline samples.

Photocrystallography brings the dimension of time into the crystallographic experiment (Raithby, 2007). In a conventional single-crystal X-ray crystallographic experiment, while the interaction of a single X-ray

photon with the electron density is very fast, of the order of 10^{-18} s, in order to solve and refine the crystal structure, the collection of the intensities from all the reflections (Bragg peaks) is required and results in an overall experiment time on a scale of minutes to hours. The resulting three-dimensional (3D) structure is, therefore, both a time average across the total experiment and a space average over the whole diffracting crystal. The development of time-resolved diffraction techniques, coupled with dramatic advances in numerous contingent technologies, including the increases in intensity and brightness of X-ray sources, the rapidity and accuracy of modern X-ray detectors, improvements in cryogenics and laser technology, and increased computing power and data storage capacity, has changed the situation hugely. These advances have opened up the field of Time-Resolved Single-Crystal X-ray Diffraction (TR-SCXRD), allowing the use of 3D X-ray methods to study dynamic processes as they occur in crystalline materials, with applications across the physical and life sciences.

Time-resolved crystallography was developed for macromolecular systems before molecular systems because of the interest in and importance of many biological processes. Biological crystals are more susceptible to X-ray damage than molecular crystals, so faster data collection strategies are beneficial to minimize this effect. As a result, the first macromolecular studies were carried out using Laue diffraction techniques, where the crystal is irradiated with a continuum of X-ray wavelengths from a polychromatic, or `white', X-ray beam (Drenth, 2007). This methodology makes more efficient use of the X-ray beam, with many more reflections being collected in a single diffraction image than is possible with monochromatic radiation. However, experimental techniques needed to be developed to reach the short timescales required to study the biological processes of interest.

In 1996, Moffat and co-workers reported the first light-induced nanosecond-resolved crystallographic investigation on the photodissociation mechanism of CO in carbon monoxy-myoglobin (MbCO) (Šrajer *et al.*, 1996). The reaction in solution had already been studied in detail using ultra-fast spectroscopic methods (Lim *et al.*, 1995), and in the diffraction study, Moffat and co-workers showed that the diffraction data correlated well with the solution studies. Using a pump–probe strategy, they found that, with probe delays (τ) of between 4 ns and 1 µs after the initial pump (activation) pulse, there was a reduction in electron density at the expected position of the CO ligand bound to the Fe centre. This indicated that photoactivation of the CO had occurred causing the CO to dissociate from the metal centre and begin to move away, within the confines of the crystalline environment. In a later study by the same group, with probe delays of between τ = 1 ns and 1 µs, the positions of transient docking sites for the photodissociated CO ligand were identified, and the pathway for the photodissociation process identified (Srajer *et al.*, 2001). Since these pioneering studies, there has been an explosion in investigations into the dynamic structures and reactivity of proteins and other macromolecules using synchrotrons and X-ray free electron lasers (XFELs) (Spence *et al.*, 2012; Chapman, 2019; Levantino *et al.*, 2021).

For molecular systems, photoinduced changes in crystals have been studied since the 1960s, well before the term *photocrystallography* was coined. Schmidt and Cohen studied the irreversible [2 + 2] photodimerization within crystals of a series of *trans*-cinnamic acid derivatives, using sunlight to photoactivate them (Cohen & Schmidt, 1964; Cohen *et al.*, 1964; Schmidt, 1964), and powder and single-crystal X-ray diffraction to monitor the dimerization. The authors analysed the crystalline environment in which the dimerization occurred. They highlighted a set of criteria that must be satisfied if single-crystal-to-single-crystal transformations were to occur. They put forward their *Topochemical Postulate* stating that `*the photoreaction will follow a minimum energy pathway that imparts the lowest level of steric strain on the surrounding crystal array*'. While there have been subsequent improvements (Cohen, 1975) and the identification of some exceptions (Natarajan & Bhogala, 2011), the *Topochemical Postulate* remains an effective guideline for designing systems that will undergo high levels of solid-state photoconversion.

Building on this *Postulate* and by examining single-crystal-to-single-crystal reactions and their kinetics, Ohashi proposed the idea of a *reaction cavity* (Ohashi *et al.*, 1981). Since, for a single-crystal-to-single-crystal transformation to occur, the crystal integrity must be maintained, it follows that there must be a void space around the reactive groups that allows the required movement

without disrupting the wider crystalline lattice. It further follows that the available void space essentially controls the reactivity of the crystal. In his pioneering work on a series of cobaloxime complexes, Ohashi showed that the *reaction cavity* displayed flexibility through the process of the reaction and that changes in temperature could significantly affect the reaction, lowering the temperature and causing lattice contraction, reducing the *cavity* size and thus terminating the process (Ohashi, 2013). These ideas can readily be related to the types of intermolecular interactions present within the crystalline environment, including hydrogen bonding and π–π stacking interactions, and *Crystal Engineering* concepts have proved helpful in the interpretation of *photocrystallographic* experiments (Hatcher, Bigos *et al.*, 2014; Naumov *et al.*, 2020; Hatcher *et al.*, 2023).

2. Planning a single-crystal *photocrystallographic* experiment

When planning a *photocrystallographic* experiment on a molecular crystal system, there are a whole series of contributing factors to consider. Some of these factors are associated with the molecular photochemistry of the material being studied and others are associated with its crystal structure. What has been learned is that it is unwise to attempt a photocrystallographic experiment unless a whole range of complementary experimental and computational techniques have been applied to the chemical process and its nature in the crystalline state is well understood.

2.1. Complementary techniques

Firstly, when considering the photochemistry of the molecule, it is important to establish the nature of the reaction process, the reaction products, the wavelengths of light that cause the photoactivation, the timescale of the reaction and the quantum yield of the reaction. These may already be known for the process in solution, but we are specifically considering the solid-state (preferably crystalline-state) process. That process may not be the same as is observed in solution. If the spectroscopic studies have not already been determined for the solid-state material, they should be carried out as a first step. Spectroscopy and computational investigations might include:

– A full photophysical analysis (optical absorption spectroscopy/fluorescence spectroscopy) will provide information on the photochemistry of the crystals.

– Time-averaged absorption spectra can inform the choice of irradiation wavelength to be used. When exciting a crystal with light, it is prudent not to irradiate the crystal at the absorption maximum (λ_{max}) because the size of the crystal may exceed the penetration depth of the light at that wavelength, that is, the light beam may be stopped within a few nanometres of the crystal surface and molecules deeper in the crystal will not be excited, limiting the level of conversion possible. In crystals, it is better to irradiate with a wavelength of light that is within the absorption peak but is half to two-thirds towards the absorption maximum in the tail of the band, as this radiation will penetrate more deeply into the crystal (Enkelmann *et al.*, 1993). If there is an overlap of the absorption of the ground state and photoexcited state species, then, although the reactant will be excited, driving the reaction forward, the product formed may also absorb the excitation light and simultaneously drive the back reaction. In this situation, an equilibrium will be set up, and achieving complete conversion to the forward reaction product will not be possible.

– Time-resolved optical (absorption/fluorescence) and vibrational (Raman/IR) spectroscopy will provide information on excited state lifetimes for fast pump–probe experiments.

– A comprehensive computational study of the reaction process may point to the formation of likely reaction products or identify side reactions that may occur.

2.2. Suitability of the crystals

For a single-crystal photocrystallographic experiment to be successful, it is essential that the quality of the crystal being studied is high. It should display a clean diffraction pattern to better than atomic resolution for the ground state structure. Preliminary crystallographic data collections across a range of temperatures are necessary to optimize the data collection parameters for the *photocrystallographic* experiments, and to highlight any unexpected effects, such as phase transitions. Other important factors to consider include:

– Crystal size: small crystals are preferred for *photocrystallography* studies to maximize light penetration, as mentioned previously.

– Crystal shape: for irradiation experiments involving lasers, illumination along specific crystal directions/normal to specific faces can be important. It is helpful to face-index the crystal to understand the crystal morphology prior to irradiation.

– Crystal system/space group: the crystal symmetry will affect the amount of unique data required and, thus, the speed of the experiment; this is especially important for stroboscopic pump–probe experiments.

– Diffraction power: small crystals often require high-flux X-rays (e.g. synchrotron radiation) to collect X-ray data in a reasonable time.

– Crystal stability: if the crystals are air or moisture sensitive precautions may have to be taken during the *photocrystallographic* experiment to avoid deterioration. If the crystals are sensitive to changes in temperature and undergo phase transitions or display hysteretic behaviour, the temperature range over which variable-temperature photocrystallographic studies can be carried out may be limited.

2.3. Factors involving the crystal structure

The way in which the molecules crystallize within the crystal may influence the path of the photoactivated process, and this is an additional constraint when compared to photochemical reactions in solution. Factors to consider include:

– Large changes in unit-cell parameters during the photoactivation may cause crystal deterioration to occur so that reversible single-crystal-to-single-crystal transformations are not possible. There are few examples of reversible photoactivation experiments where the unit-cell parameters change by more than 3%. Often, this problem can only be identified during the course of the photocrystallographic experiment, but the choice of chemical systems where there is flexibility within the crystal structure can prevent this problem, as highlighted by Ohashi with his reaction cavity concept (Ohashi, 2013). The use of metal–organic frameworks (MOFs) that act as cages to enclose the photoactivated species can be helpful (Blake *et al.*, 2010), or simply the use of bulky auxiliary ligands or the presence of bulky counter-ions in complex salts that create void space within the crystal structure.

– Intermolecular interactions within the crystal can either facilitate or block the progress of a solid-state reaction. It is hard to predict what the combined effect of a particular set of intermolecular interactions is, but there are several examples in the photocrystallographic literature where there are crystals with two crystallographically independent but chemically equivalent molecules in the crystallographic asymmetric unit that behave somewhat differently under photoactivation, and these differences are attributed to the presence of different intermolecular interactions (Coppens *et al.*, 2013; Hatcher, Bigos *et al.*, 2014).

Only after considering all of the points in the previous three sections and their implications is it sensible to proceed with a single-crystal *photocrystallographic* experiment. If at all possible, it is beneficial to simultaneously measure spectroscopic data from the crystal while the photocrystallographic measurements are being carried out so that the two forms of analysis can be correlated (Hasil *et al.*, 2024).

3. Case histories

Before discussing the details of `*how to carry out a molecular photocrystallographic experiment*', it is helpful to describe some of the *photocrystallographic* experiments that have been undertaken successfully to provide the reader with an idea of what can currently be achieved, how the methodology is continuing to develop and what the main challenges involved are. This is best achieved by describing a series of case histories.

Building on the results obtained for the irreversible solid-state photochemical reactions and taking into account the factors outlined above that determine whether or not a *photocrystallographic* experiment is likely to be successful, Coppens carried out the first studies on reversible molecular systems in the 1990s (Pressprich *et al.*, 1994). Using steady-state crystallographic methods, Coppens showed that the solid-state photoactivation of single crystals of iron–nitrosyl complexes resulted in the conversion of the molecule to a new *metastable* linkage isomer (Carducci *et al.*, 1997). In these crystallographic experiments, the term metastable is taken to mean that the structure of the molecule being studied does not change during the duration of the data collection; in this instance, each data collection took up to 20 h using a rotating-anode X-ray generator and an image-plate diffractometer. Crystals of sodium nitroprusside were irradiated with light from an Ar^{+} laser at λ = 488 nm and 50 K, until a *photostationary* state was reached. With irradiation, the nitrosyl coordination mode changed from a ground state (GS) η^1-NO isomer to an excited state (ES) isonitrosyl η^1-ON isomer with 37% population. The photoactivated crystal was then irradiated with 1064 nm laser light. With this irradiation, a second *metastable* linkage isomer was obtained, with the isonitrosyl isomer converting to a side-on-coordinated η^2-NO isomer, with 10% population (Fig. 1). As is common in *photocrystallographic* experiments, because the conversion from one form to another is not 100% complete, the various structural forms must be refined as components of a disordered structural model with variable atomic occupancies (summing to unity) for the multiple components. In this example, in the case of the ground state η^1-NO form and the isonitrosyl η^1-ON form, there is considerable overlap of the N and O atoms in the two isomers, and the occupancies are best determined by corroborating experimental techniques rather than by trying to refine the occupancies within the crystallographic model. The value of 37% for the conversion to the isonitrosyl η^1-ON isomer was obtained from supporting differential scanning calorimetry (DSC) studies (Woike *et al.*, 1993); however, because there is no atomic overlap between the η^1-NO and η^1-ON forms and the η^2-NO isomer, the occupancy of the η^2-NO group can be refined successfully within the crystallographic model, giving a value of 10% for this isomer.

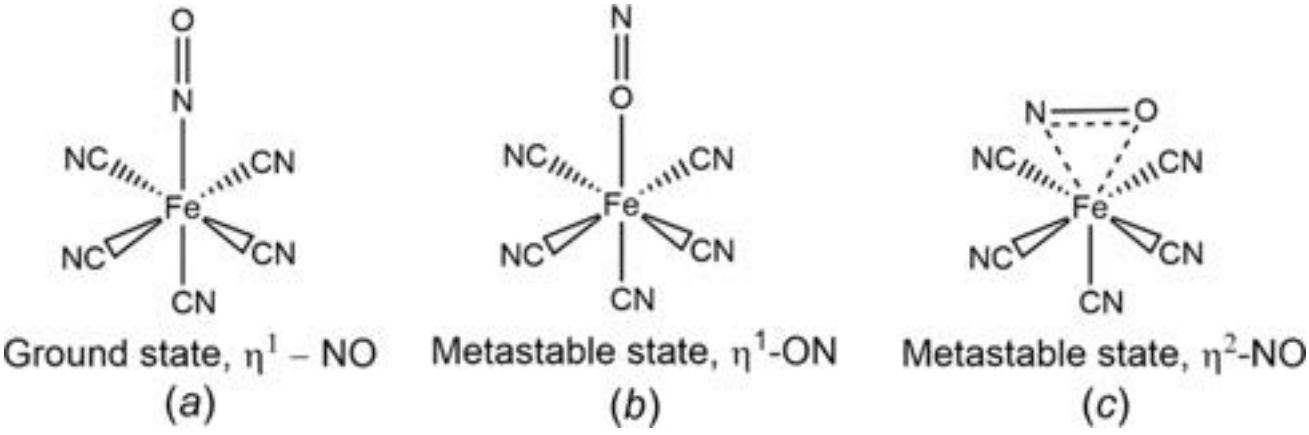


Figure 1. Structural diagram of the nitrosyl linkage isomers found in $Na[Fe(CN)_5(NO)]$ in the ground state and upon photoexcitation: (*a*) $[Fe(CN)_5(\eta^1\text{-NO})]^{-}$, (*b*) $[Fe(CN)_5(\eta^1\text{-ON})]^{-}$ and (*c*) $[Fe(CN)_5(\eta^2\text{-NO})]^{-}$.

In the photocrystallographic study, it was clear that it was not just the position of the nitrosyl group that changes upon excitation, but all the atoms in the structure. For example, for the $[Fe(CN)_5(\eta^2\text{-NO})]^{-}$ excited state isomer, the Fe atom and the *trans*-cyanide group are displaced towards the η^2-NO ligand. Additionally, the disorder present limits the accuracy of the bond parameters associated with the nitrosyl group, and restricts any assessment of the bonding within the unit. Generally, in refinements of disordered groups, it may be necessary to apply constraints or restraints to atomic positions or bond

parameters to obtain a stable refinement (see further discussion in Section 4.1 below). Clearly, if a bond parameter is restrained or constrained, nothing can be said about parameter changes upon excitation, and if the atoms are being refined freely, careful consideration needs to be given to the magnitude of the estimated standard deviations (e.s.d.'s) before changes in bond parameters can be evaluated meaningfully.

The use of DSC techniques to corroborate the metastable state occupancy in the example above reaffirms the importance of having a plethora of supporting information before undertaking even the most straightforward *photocrystallographic* experiments. In his 1997 article reporting the *photocrystallographic* study on sodium nitroprusside (Carducci *et al.*, 1997), Coppens also either reported or drew upon previously published Mössbauer, IR and Raman, and EPR spectroscopic studies, single-crystal X-ray and neutron diffraction studies of the ground state, and the observed colour change in the crystal when going from the ground to the metastable state supported by UV–visible (UV–Vis) spectroscopy, in order to plan the experiment and interpret the results. Quantum chemical calculations further underpinned the study. A subsequent neutron diffraction study also confirmed the nature of the two excited state nitrosyl isomers (Schaniel *et al.*, 2006). In much more recent studies on the nitrosyl linkage isomers of $[Ru(py)_4F(NO)](ClO_4)_2$, where the differences and similarities of using either continuous wave (CW) or pulsed lasers to photoactivate the crystal, *in-situ* UV–Vis absorption spectroscopy has been used to monitor the conversion of the ground state to the excited state structure. IR spectra of KBr pellets of the complex have also been recorded before, during and after laser irradiation under careful temperature control to monitor the nitrosyl stretching frequencies and correlate them with the simultaneous X-ray and UV experiments (Hasil *et al.*, 2024).

After the early groundbreaking work, there have been many *photocrystallographic* studies on the inter-conversion between linkage isomers in transition-metal complexes. The ligands studied include nitrosyls, nitrites, sulfur dioxide, dinitrogen and dimethyl sulfoxide (Fomitchev *et al.*, 2000; Coppens *et al.*, 2002; Casaretto *et al.*, 2015; Coppens, 2017; Schaniel *et al.*, 2018; Hatcher *et al.*, 2019; Cole, Gosztola, Velazquez-Garcia *et al.*, 2021; Borowski *et al.*, 2022; Cole *et al.*, 2022; Marr *et al.*, 2023; Mikhailov *et al.*, 2023; Potempa *et al.*, 2023). In most examples studied where photoactivated linkage isomerism occurs through a single-crystal-to-single-crystal transformation, there is no change in the crystallographic space group through the process, and the unit-cell volume alters by less than 3%. This observation reinforces the significance of the ideas relating to the *Topochemical Postulate* and the *reaction cavity* initially put forward by Cohen & Schmidt (1964) and Ohashi (2013), respectively, for solid-state processes. A recent *photocrystallographic* study on the *cis*-nitrosobenzene dimer shows that, under irradiation with a mercury lamp for 20 minutes at 100 K, it undergoes a transformation to a pair of monomers with an 8.6% monomer population and then reversibly recombines (Fig. 2) (Rodenbough *et al.*, 2018). The two N atoms move by a remarkable 2.97 (5) Å during this process. Despite this large change in the local environment about the nitroso moieties, there is still only a minimal change in the unit-cell volume before and after irradiation, and no change in the space group, which tends to indicate this study still conforms to aspects of the *Topochemical Postulate*. It is likely that the comparatively low excited state population may result from the limitation of maintaining crystal integrity, and if >10% of the molecules were to excite, this may result in the degradation of the single-crystal environment. However, this study is noteworthy as it suggests that it may be possible to extend photocrystallographic studies to processes involving more substantial movement of atoms.

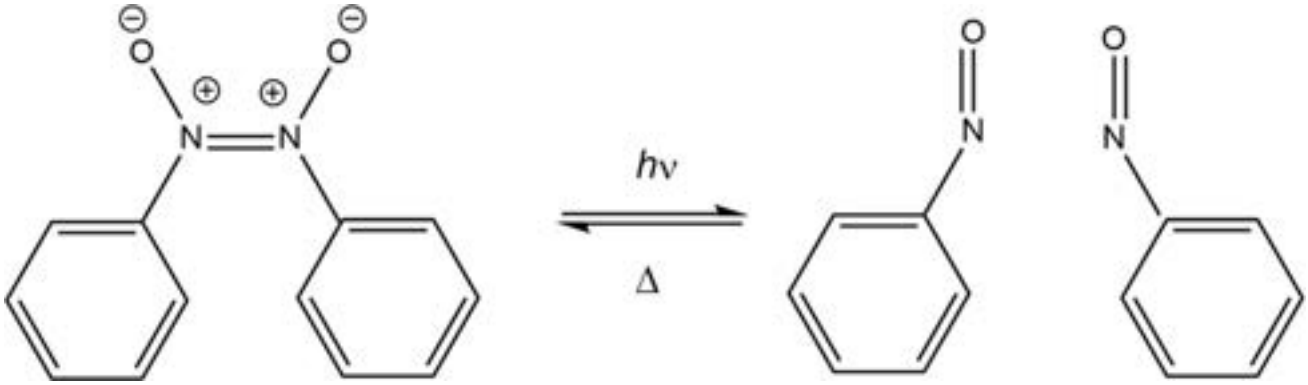


Figure 2. The *photocrystallographic* photolysis and redimerization of the *cis*-dimer of nitrosobenzene.

One of the driving forces for the investigation of molecular systems that switch between ground and *metastable* states under light irradiation in the solid state is their application as molecular switches in optoelectronic devices (Cole, 2011). To achieve this aim, it is helpful for the switching to be 100% efficient, with the crystalline product not containing any residual ground state structure or multiple isomeric *metastable* state structures, and for the switching process to occur near room temperature. During the last two decades, research efforts have focused on designing 100% efficient solid-state switching materials based on linkage isomers using the previously discussed photochemical and crystal engineering factors.

The first transition-metal nitro complex to display 100% efficient reversible linkage isomerism in the solid state under photoactivation was the square-planar nickel(II) complex [Ni(dppe)(η^1-NO_2)Cl] [dppe is 1,2-bis(diphenylphosphino)ethane], which was designed to contain the bulky dppe phosphine ligand that would control the crystal packing and provide adequate space within the crystal lattice for the nitro→nitrito interconversion to occur (Warren *et al.*, 2009). The complex was studied by Raman spectroscopy and *photocrystallography*. Irradiation of a crystal with 400 nm light from an LED, below 160 K, resulted in the structural change from the ground state nitro complex to the *endo*-nitrito form (Fig. 3). At temperatures above 160 K, the structure gradually reverted to the nitro form. This relaxation follows Arrhenius behaviour, with the lifetime of the *endo* form decreasing with increasing temperature, so that there is a specific temperature for a specific lifetime. This process was reversible without crystal degradation. Subsequent studies showed that the complexes*cis*-[Ni(dppe)(NO_2)$_2$] and *cis*-[Ni(dcpe)(NO_2)$_2$] both underwent complete reversible nitro→*endo*-nitrito conversion at 100 K, using 400 nm LED light, and that above 180 K the structures reverted to the nitro form (Warren *et al.*, 2014). The square-planar nickel(II) complex [Ni(3-{[2-(dimethylamino)ethyl]imino}-2-hydroxyimino-1-phenyl-propan-1-one)(NO_2)], with the bulky imino ligand, which shows traces of the presence of the *exo*- and *endo*-nitrito (η^1-ONO) forms in the ground state, undergoes 90% total conversion when irradiated with 405–530 nm LED light at temperatures up to 200 K, with the *exo*-nitrito isomer being the dominant form (Potempa *et al.*, 2023). The relative populations of the *endo* and *exo* forms are temperature dependent.

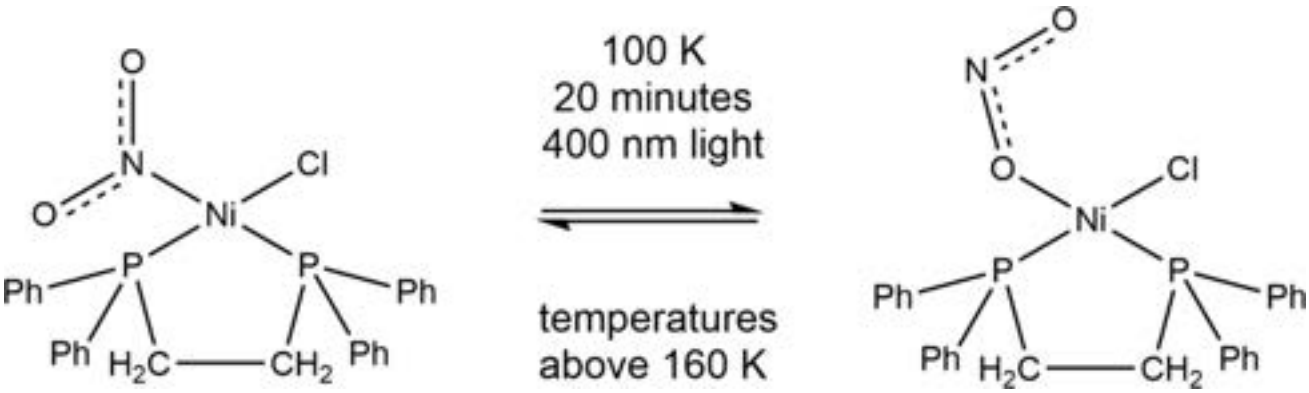


Figure 3. The reversible photoconversion of [Ni(dppe)(η^1-NO_2)Cl] into [Ni(dppe)(η^1-ONO)Cl].

Schaniel and Woike obtained 92% conversion from the η^1-NO-bound form to the η^1-ON-bound form of the nitrosyl ligand in crystals of $[RuCl(py)_4(NO)](PF_6)_2 \cdot 0.5H_2O$ using laser light of 473 nm at 80 K, which could then be converted to 48% of the η^2-NO form (Cormary *et al.*, 2009) (Fig. 4). The authors indicated that the conversion occurs *via* a metal-to-ligand charge-transfer process (MLCT) induced when the complex absorbs photons of the appropriate energy. This excitation must induce electron transfer between two orbitals to change the metal–nitrosyl bond, *e.g.* a $d \rightarrow \pi^*$(NO) transition. Also, for a *metastable* isomer to be generated, the potential energy surface for the excited state isomer must have a minimum point that directly overlaps with the maximum point of the ground state energy surface (Schaniel & Woike, 2009). The rate at which the excited state is populated must be greater than the rate of depopulation for the excited state to be identified. Since the ground and excited states will be in equilibrium, factors such as the temperature and illumination wavelength will influence the observed percentage conversion to the metastable state. These studies led to an extension of the work to include the spectroscopic and *photocrystallographic* investigation of a series of related complexes $[RuX(py)_4(NO)](Y)_2 \cdot nH_2O$ (*X* = halide and *Y* = counter-anion) (Cormary *et al.*, 2012). It was found that the shorter the distance between the NO ligand and the counter-ion in the ground state structure, the higher the population of the *metastable* state after irradiation. This implies that the intermolecular contacts in the *metastable* state are reduced, easing unfavourable packing constraints. Additionally, it was found that the lower the donating character of the ligand *trans* to the NO group in these octahedral complexes, the higher the photoconversion yield.

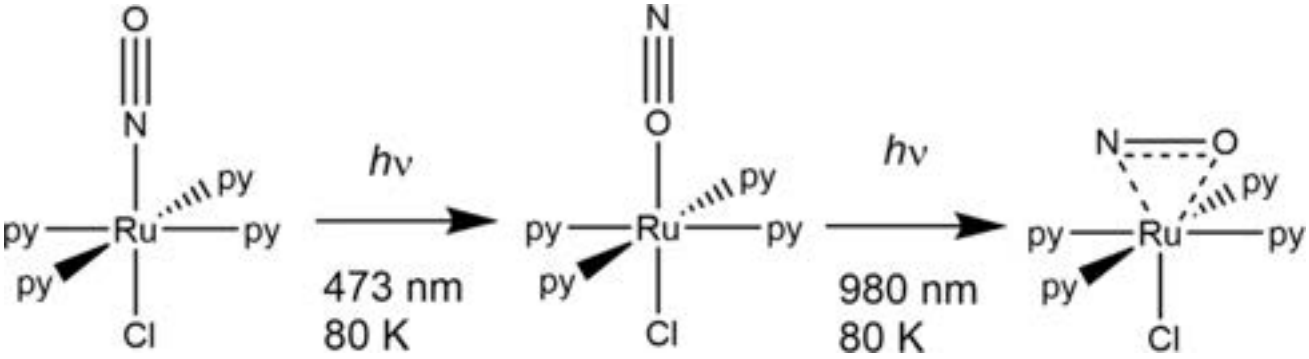


Figure 4. Photoactivated linkage isomerism in $[RuCl(py)_4(NO)](PF_6)_2 \cdot 0.5H_2O$, showing the two *metastable* forms.

The *trans*-$[Ru(SO_2)(NH_3)_4$(3-bromopyridine)$](tosylate)_2$ complex undergoes 100% conversion from the S-bound η^1-SO_2 isomer to the *O*-bound η^1-OSO photoisomer, which is metastable at 100 K (Fig. 5) (Cole, Gosztola & Velazquez-Garcia, 2021). The *photocrystallographic* experiments have been supported by single-crystal optical absorption and Raman spectroscopies that confirm the metal-to-ligand charge-transfer nature of the process. Notably, single crystals of this material act as nano-optomechanical transducers that have the potential to be used in light-driven molecular machinery, nanotechnology and quantum computing. The formation of the *metastable* η^1-OSO isomer is the stimulus for the transduction, with the MLCT modulations relaying through the ruthenium cation, causing a knock-on effect in the tosylate anion. The $Br^{\delta-}$ substituent on the cation interacts with the tosylate ring on the anion through anion$\cdots\pi$ interactions and the ring rotates to accommodate this interaction.

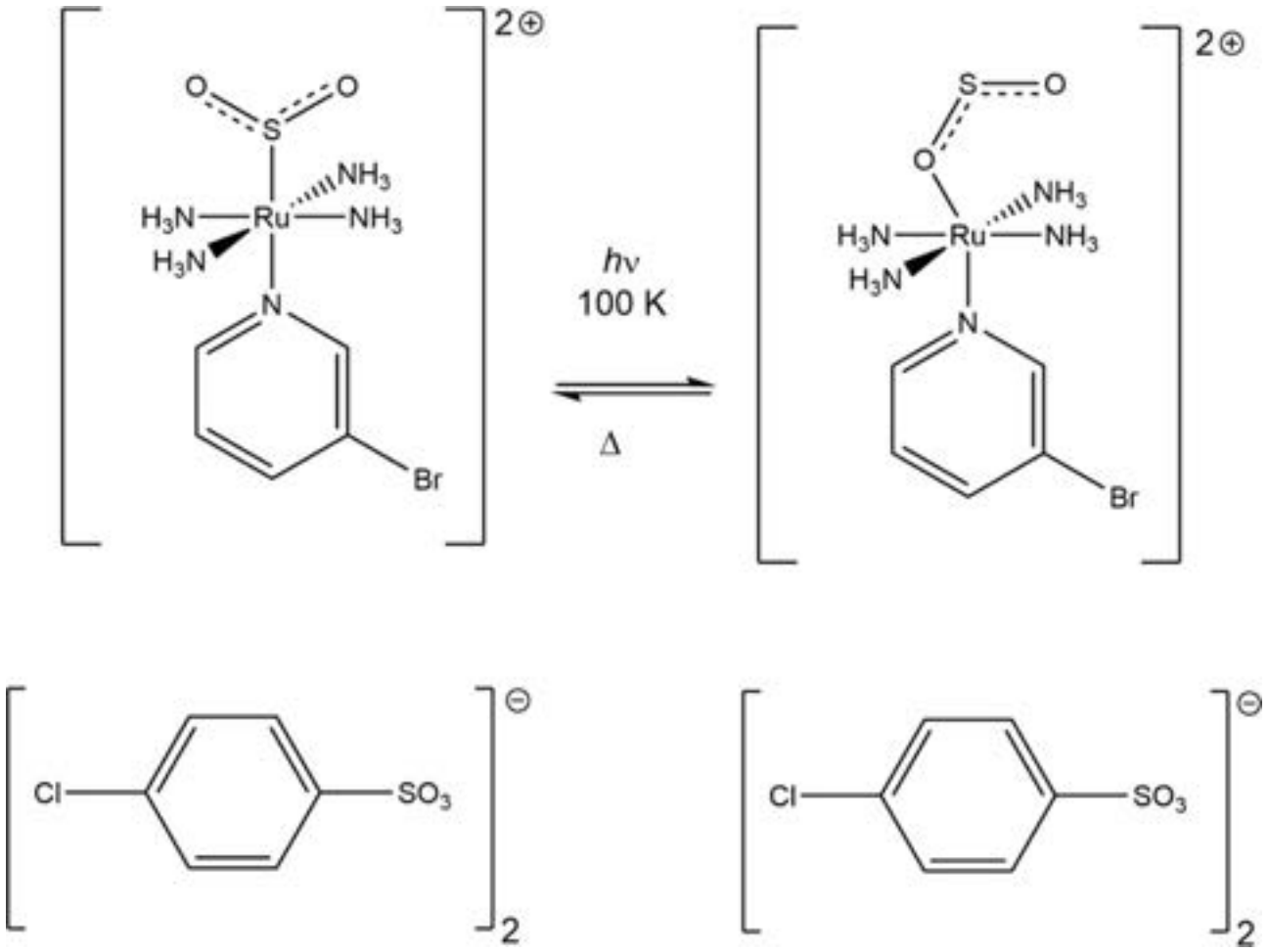


Figure 5. The η^1-SO_2 to η^1-OSO photoisomerization in *trans*-[Ru(SO_2)(NH_3)$_4$($_3$-bromopyridine)](tosylate)$_2$.

More recent experiments involving the nitro→nitrito interconversion have resulted in the investigation of the photoisomerization of the square-planar Pd complex [Pd(Bu_4dien)(η^1-NO_2)](BPh_4) (Bu_4dien = *N*,*N*′,*N*′-tetrabutyldiethylenetriamine and BPh_4− = tetraphenylborate), that contains a bulky tridentate amine ligand and also has a bulky counter-ion, both of which reduce the efficiency of the crystal packing and leave more void space in the crystalline lattice. This complex undergoes 100% conversion to the *metastable endo*-nitrito-(η^1-ONO) isomer in 15 minutes with irradiation by 400 nm LED light at a temperature of up to 240 K, while pseudo-steady-state *photocrystallographic* experiments, with continuous irradiation, showed that the excited state is retained at temperatures up to 260 K (Hatcher, 2016). This example shows the promise of linkage isomerism occurring under near-ambient conditions. A subsequent crystallographic kinetic study on the nitrito to nitro decay in this molecule confirms the Arrhenius-like decay behaviour, meaning that the excited state lifetimes can be tuned over several orders of magnitude through careful temperature control (Hatcher *et al.*, 2018). These results imply that it should be possible to `dial up' a specific excited state lifetime, through choice of temperature, to suit the parameters of a specific time-resolved experimental set-up.

Crystals of the *Pca*2_1 polymorph of the cobalt(III) complex [Co(Me-dpt)(NO_2)$_3$] (Me-dpt = 3,3′-diamino-*N*-methylpropanediamine) undergoes photoisomerization of one of the NO_2 groups at room temperature, with a maximum nitro-to-nitrito conversion of 55%, when irradiated with 470 nm light, and the transformation is reversible when the crystal is irradiated with 660 nm light (Fig. 6) (Deresz *et al.*, 2022). Since there are three NO_2 groups in the complex, and only one appears to undergo linkage isomerism, the reaction cavities for each NO_2 group were calculated. Interestingly, the cavity for the NO_2 ligand that does undergo isomerization is 7 and 5 Å^3 larger than for the other two NO_2 groups, respectively, with a volume of *ca* 30 Å^3, which provides a *topotatic* explanation for the observed site selectivity. Solid-state IR and UV–Vis spectroscopy also monitored the reversibility of the isomerization.

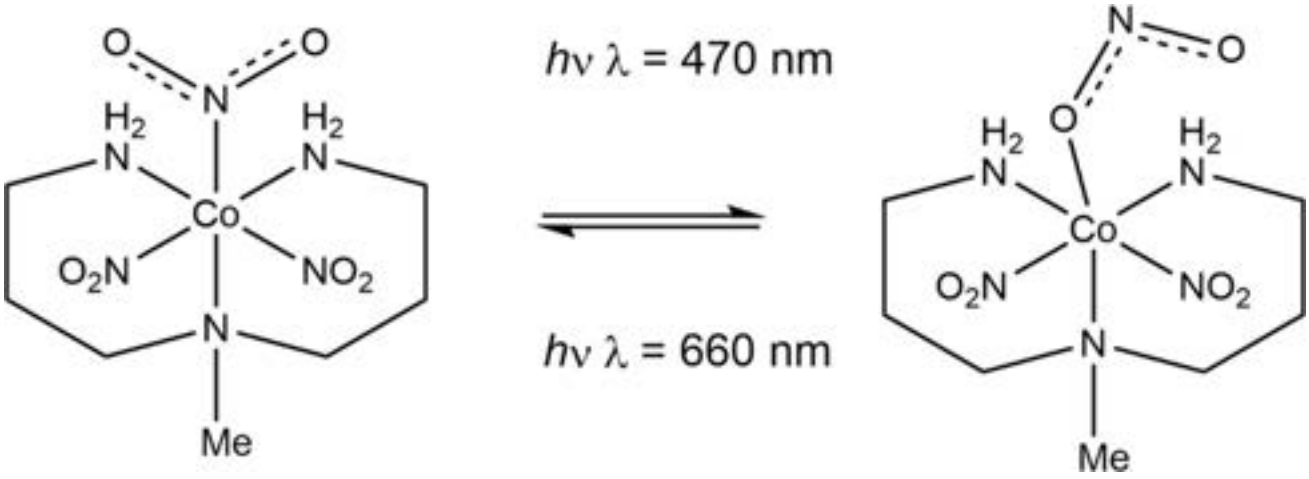


Figure 6. The light-induced transformation of [Co(Me-dpt)(NO_2)$_3$] between the nitro and nitrito forms.

The experiments discussed so far have been described as `steady state,' where the lifetime of the excited state exceeds the length of the experiment, providing certain experimental conditions, such as temperature, are maintained and no further irradiation is required, or `pseudo-steady state', where the excited state persists providing that the sample is continuously irradiated. However, obtaining the structures of species with shorter excited state lifetimes is possible using *stroboscopic* or *pump–probe photocrystallographic* techniques. In these experiments, short-duration pulses of light are used, which are synchronized with X-ray pulses that are synchronized to arrive at the crystalline sample in a specific time sequence (Fullagar *et al.*, 2000), so that the X-ray data is only measured when the crystal is photoactivated. Usually, a laser is used that generates nanosecond or picosecond pulses, although pulsed LED sources have been used successfully on the millisecond to microsecond timescale (Hatcher *et al.*, 2022). The laser or LED light acts as the *pump*, while the X-ray pulses function as the *probe*.

Coppens was among the first molecular crystallographers to use the higher intensity X-ray flux available at synchrotrons to conduct *photocrystallographic* experiments on molecules with microsecond lifetimes. In 2002, he conducted pump–probe experiments on salts of the tetraanion $[Pt_2(pop)_4]^{4-}$ (pop = $[H_2P_2O_5]^{2-}$) (Fig. 7) using monochromatic X-ray radiation. In the case of the tetraethylammonium salt, the anion showed structural distortions when photoactivated by 355 nm laser light, producing a triplet excited state with a microsecond lifetime (Kim *et al.*, 2002). The anion showed a 2% conversion to the excited state, at 17 K, using 33 µs wide light pulses from a Nd/YAG laser with a repetition rate of 5100 Hz. The refinement of the excited state focused on changes in the Pt···Pt separation, while the remainder of the structure was treated as a rigid group. The Pt···Pt distance was found to shorten by 0.28 (9) Å, with an accompanying rotation of 3° about the Pt···Pt vector. In a subsequent diffraction study on $[(n\text{-}Bu_4N)_2H_2][Pt_2(pop)_4]$, Ohashi showed a decrease in the Pt···Pt distance of 0.23 Å upon photoactivation (Ozawa *et al.*, 2003).

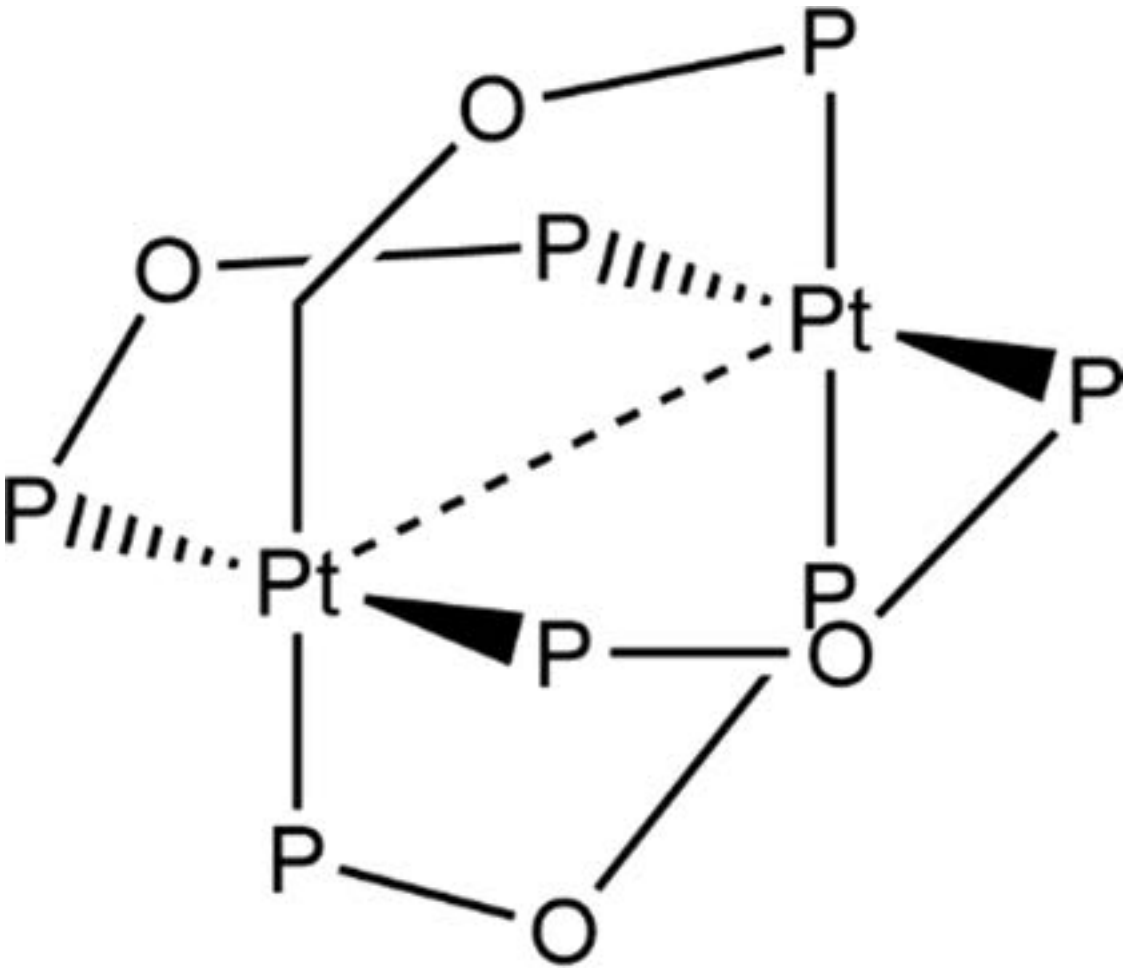


Figure 7. The core of the $[Pt_2(pop)_4]^{4-}$ tetraanion. The Pt···Pt separation reduces by 0.28 (9) Å upon photoactivation.

The dimetallic complex $[Rh_2(dimen)_4](PF_6)_2$·MeCN (dimen = 1,8-diisocyanomethane) also shows a reduction of 0.86 Å in the Rh—Rh bond and a bond rotation of 13° upon photoactivation with 335 nm laser light at 23 K (Coppens *et al.*, 2004). The maximum level of excitation reached was 2.5%, with an excited state lifetime of 11.7 µs. Two copper complexes have also been studied using pump–probe methods with monochromatic radiation, *i.e.* $[Cu_3\{3,5\text{-}(CF_3)pyrazolate\}_3]$ (Vorontsov *et al.*, 2005) and $[Cu(dmp)(dppe)](PF_6)$ (dmp = 2,9-dimethyl-1,10-phenanthroline) (Vorontsov *et al.*, 2009). In the former case, photoactivation with 355 nm laser light at 17 K causes a rearrangement of adjacent Cu_3 triangular units into pairs such that one interplanar Cu···Cu intermolecular distance is reduced by 0.65 Å, and the separation to the next pair of Cu_3 triangles is increased by 0.30 Å. In $[Cu(dmp)(dppe)](PF_6)$, there are two independent molecules in the asymmetric crystallographic unit. Upon excitation, one of the pseudo-tetrahedral molecules flattens out more than the other, with a concomitant increase in the Cu—P distances. This difference is attributed to the slightly different crystalline environments of the two molecules. The population of the excited state was estimated to be in the range 7–10%.

An alternative approach to using monochromatic X-ray radiation in time-resolved crystallographic experiments is to use Laue diffraction techniques while pumping the crystalline material with laser or LED-generated light. In Laue experiments, a `white beam' including a range of X-ray wavelengths is used, which provides a much wider energy range of X-ray photons (Moffat, 2019). This technique vastly increases the number of X-ray reflections measured per diffraction frame recorded, thus speeding up the experiment, reducing the risk of crystal damage and potentially allowing systems with shorter excited state lifetimes to be probed. The complication is that each diffraction spot recorded must be matched with the X-ray wavelength that generated it.

In 2011, Coppens first used Laue diffraction methods to attempt a `single-shot' experiment on the molecular dirhodium complex $[Rh_2(\mu\text{-}pnp)_2(pnp)_2](BPh_4)$ [pnp = *N*,*N*-bis(dimethoxyphosphanyl)methanamine] (Benedict *et al.*, 2011; Makal *et al.*, 2011). The polychromatic X-ray source was used at

the 14-ID BioCARS Station at the APS. A small single crystal of the sample was cooled to 225 K and irradiated with a 35 ps-wide laser pulse with a wavelength of 337 nm and then exposed to a single 100 ps X-ray pulse after a 100 ps delay. This excitation populated the triplet state and resulted in the transient shortening of the Rh—Rh bond distance, similar to that observed previously for $[Rh_2(dimen)_4](PF_6)_2$·MeCN when monochromatic X-ray radiation had been used (Coppens *et al.*, 2004).

A copper(I) complex, [Cu(1,10-phenanthroline)$(PPh_3)_2$](BPh_4), has also been studied using Laue techniques (Makal *et al.*, 2012), and the results compared with those obtained for the similar complex [Cu(dmp)(dppe)](PF_6), whose excited state structure had been obtained using monochromatic X-ray radiation in a time-resolved crystallographic experiment (Vorontsov *et al.*, 2009). As in the previous case, [Cu(1,10-phenanthroline)$(PPh_3)_2$](BPh_4) crystallizes with two independent cations in the asymmetric unit, and from analysis of the intermolecular contacts in the ground state structure, one of the cations exhibits a more sterically constrained crystalline environment than the other. Photoexcitation with 390 nm light at 90 K induces an MLCT transition, but the two independent molecules undergo different structural changes. X-ray data were recorded using the single-pulse Laue method (Kalinowski *et al.*, 2012). The analysis showed that the less sterically crowded cation exhibited a considerable distortion, but no significant changes in the more constrained cation.

A `pink-beam' Laue diffraction study, in which a restricted range of X-ray wavelengths are employed, has been carried out on a tetranuclear Cu^I–Ag^I complex, $[Ag_2Cu_2$(2-diphenylphosphino-3-methylindole)$_4]$ (Fig. 8) (Jarzembska *et al.*, 2014). The triplet excited state, which has a 1 µs lifetime at 90 K, is activated by 390 nm light pulses and probed with 80 ps resolution. The `zigzag' arrangement of the two Cu and two Ag centres shows a reduction in the Ag···Cu distance of 0.59 (3) Å and a shortening of the Ag···Ag distance by 0.38 (3) Å, suggesting a strengthening of the d^{10}···d^{10} interactions. An accompanying quantum chemical study confirms that the strengthening of the Ag···Ag interaction is the result of ligand-to-metal charge transfer (LMCT).

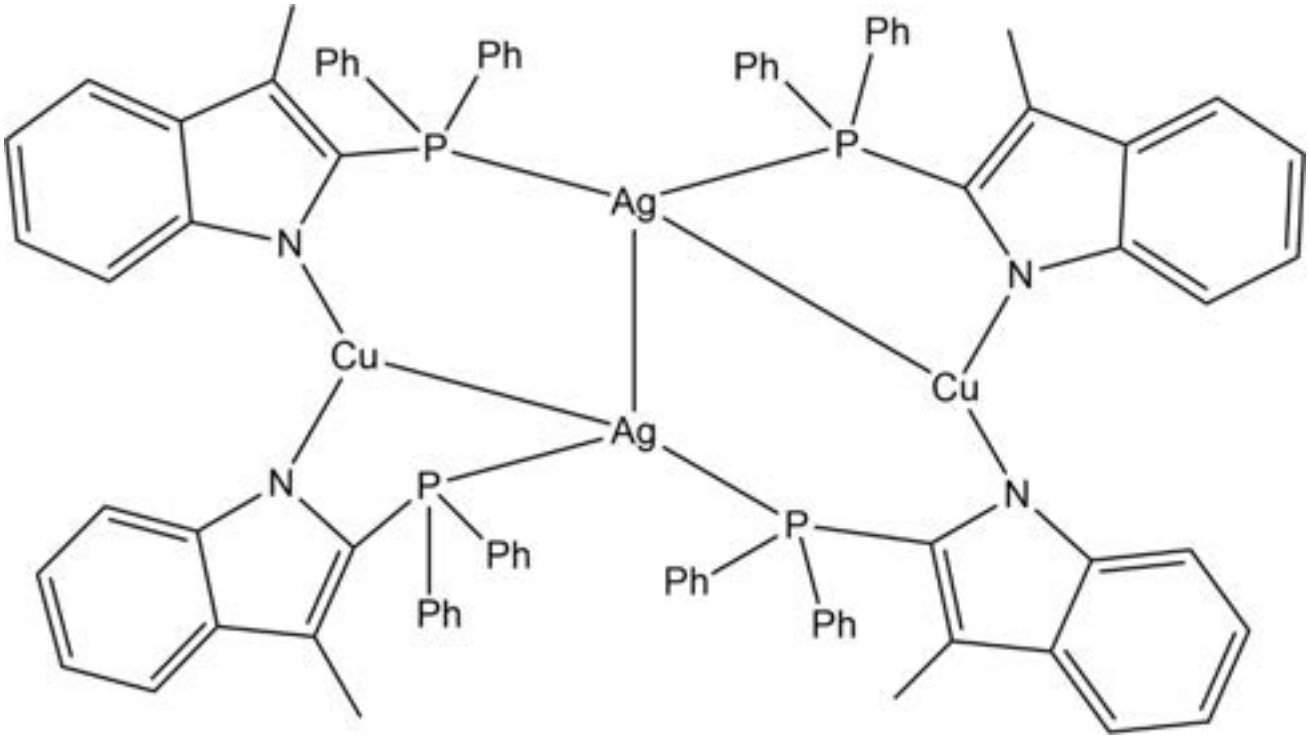


Figure 8. The molecular structure of $[Ag_2Cu_2$(2-diphenylphosphino-3-methylindole)$_4]$.

The copper(I) benzoate complex $[Cu_4(PhCO_2)_4]$ (Fig. 9) has been studied using time-resolved Laue diffraction techniques at 90 and 225 K, using 355 and 360 nm light, and this shows an expected Cu···Cu contraction in the solid state (Jarzembska *et al.*, 2019). As in previous examples, the asymmetric unit contains two independent molecules, each displaying slightly different distortions. The complex shows luminescent thermochromism at 90 K, and the low-energy triplet state has been assigned to the Cu_4

core. The emission from this state matches the red band at 660–715 nm.

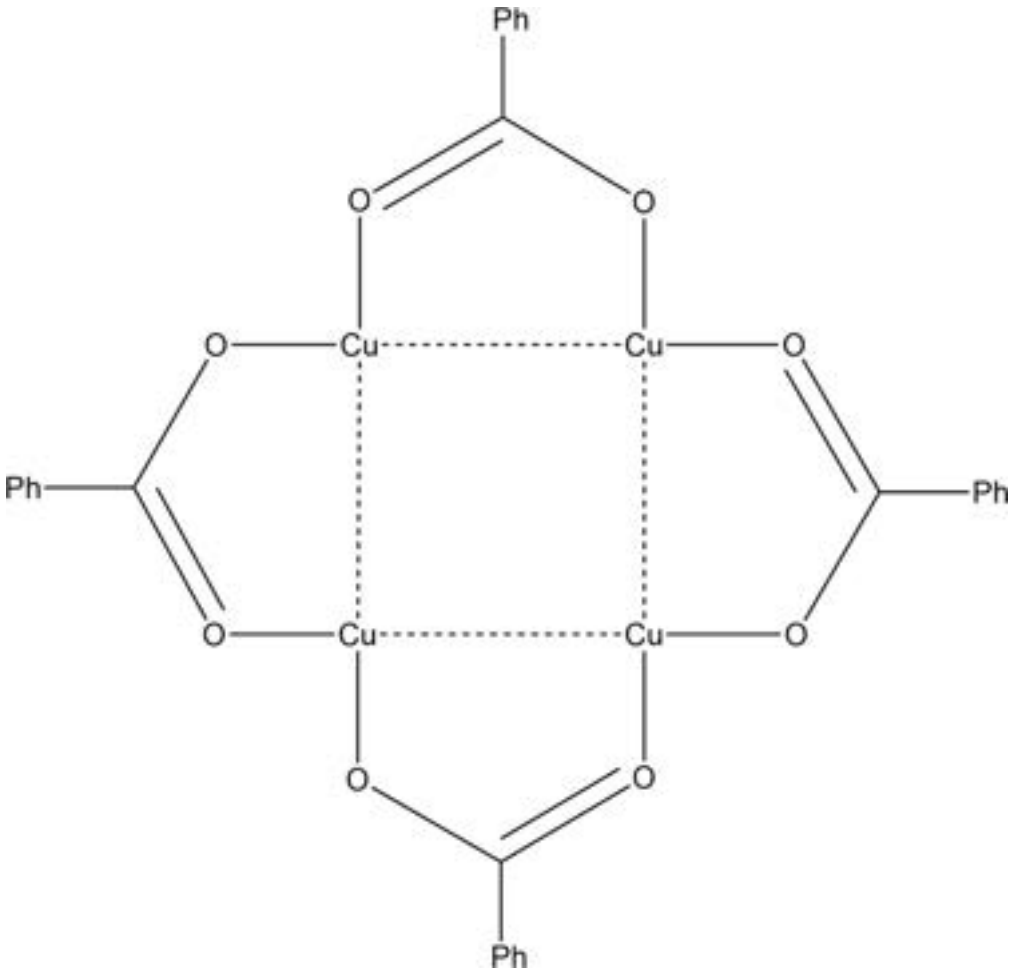


Figure 9. The molecular structure of $[Cu_4(PhCO_2)_4]$.

4. Timescales

Photochemical processes can occur on timescales ranging from femtoseconds to years, and distinct aspects of a reaction occur on quite different timescales (Fig. 10). Some processes are irreversible, and the reaction pathway occurs only in the forward direction, although, depending on the reaction conditions, it may take periods of hours or days to reach 100% conversion to the reaction product, such as in the case of some [2 + 2] cycloaddition reactions (Allen *et al.*, 2005; Mahon *et al.*, 2008). Other processes are reversible, and it is for these systems that photocrystallography can be used to monitor the forward and backward reactions, covering a whole range of timescales. The timescale of a particular process is susceptible to a variety of external factors, perhaps most commonly changes in temperature, so, for example, an isomer may be metastable under irradiation at one temperature, but at a higher temperature, it may have a lifetime of microseconds. Generally, electron-transfer processes within a molecule can occur in picoseconds, whereas the population dynamics of excited state formation throughout a crystal can vary over timescales of several minutes. If the processes are to be monitored or snapshots taken along a reaction pathway, thought needs to be given to the methodology to be used to pick out the feature of the reaction that is of interest. When using crystallographic techniques, the shorter the timescale of the process, the more complicated and challenging the crystallographic experiment required (Pillet, 2018; Raithby, 2020).

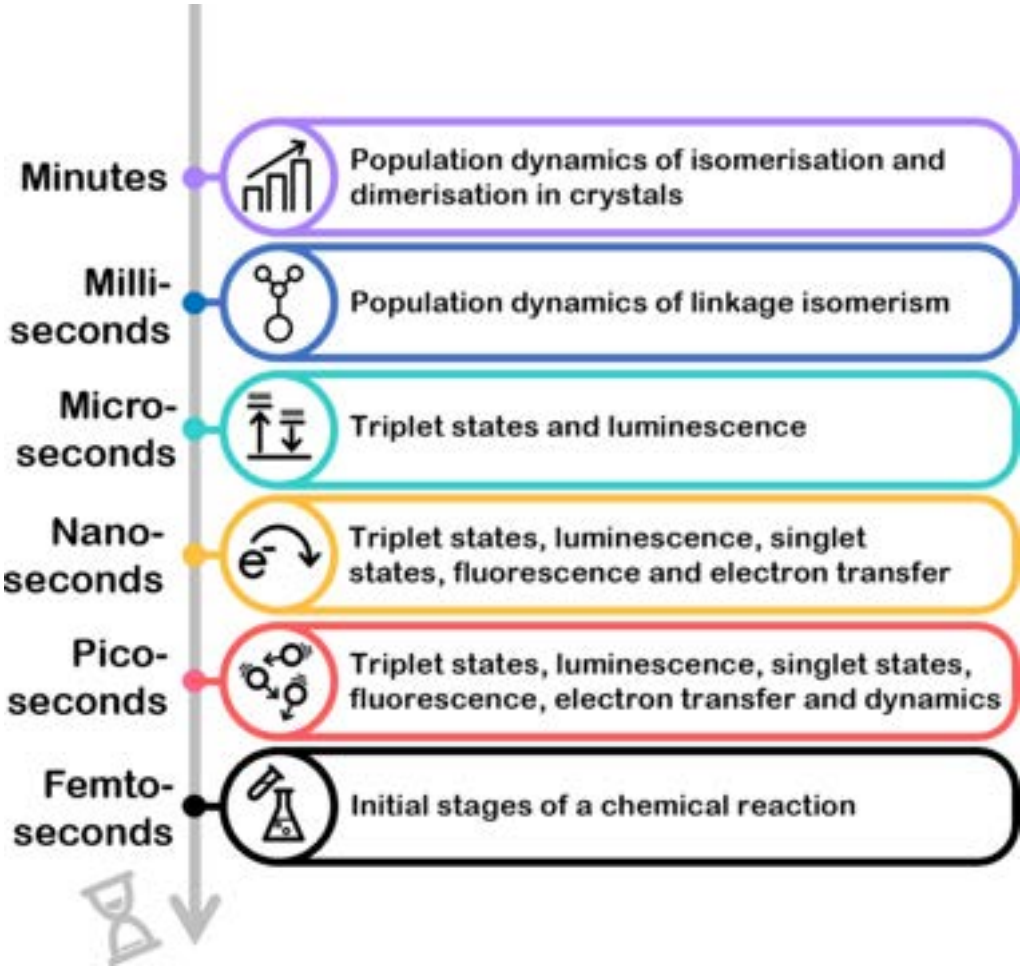


Figure 10. The timescales of dynamic processes that occur in chemistry.

Given the caveats mentioned above, Fig. 10 contains a summary of common light-induced processes and the timescales on which they may occur.

4.1. `Steady-state' experiments

In *photocrystallographic* experiments where the excited state or metastable state lifetime of the system is measured in hours and is longer than the duration of the diffraction experiment, conventional single-crystal X-ray diffraction techniques are used to determine the structures of the ground and excited states. They are described as `steady-state' experiments. A laboratory-based diffractometer with an area detector can be used, although using a diffractometer at a synchrotron facility will substantially speed up the experiments, particularly if multiple data sets are collected over a range of temperatures and under different illumination conditions. The flux of the synchrotron X-ray source is several orders of magnitude higher than that from a conventional laboratory instrument. The diffractometer should be equipped with a crystal-cooling apparatus capable of maintaining temperatures between 100 and 500 K, and the ability to reach down to temperatures of a few degrees K is necessary for some experiments. Most importantly, for *photocrystallographic* experiments, the diffractometer must be equipped with a light source to illuminate the crystal. The light source may be a lamp, a laser or a ring of LEDs, depending on the requirements of the study to be conducted (Fig. 11). Attempting to irradiate the crystal during a diffraction experiment when the diffractometer is moving position to record data can be challenging and several ingenious set-ups have been devised to achieve this using either a laser (Thompson *et al.*, 2004; Kamiński *et al.*, 2016) or LEDs (Brayshaw *et al.*, 2010).

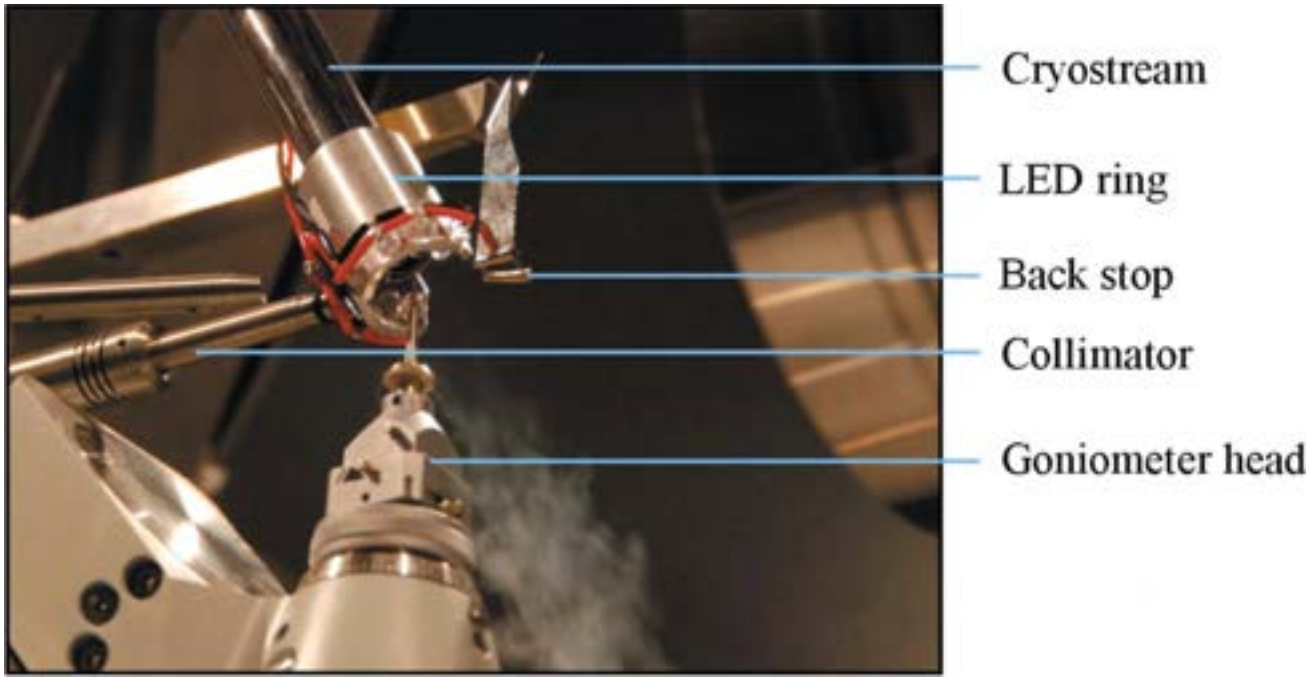


Figure 11. An Oxford Diffraction Gemini A Ultra diffractometer equipped with an Oxford Cryostream crystal-cooling device and a ring of LEDs to illuminate the crystal. [Reproduced from Brayshaw *et al.* (2010) with permission from the International Union of Crystallography.]

In a typical single-crystal *photocrystallographic* experiment to study the structure of a complex that exhibits a long-lived metastable state under light irradiation using the set-up described above, the crystal is first cooled in the dark to a low temperature to obtain the ground state structure with minimum risk of contamination from the metastable state. A conventional high-resolution data set is then collected in the dark at the low temperature selected. The crystal is then illuminated for a set period, usually ranging from minutes to hours, depending on the knowledge obtained from preliminary spectroscopic and photochemical studies. The metastable state is kinetically trapped at low temperatures, and a significant steady-state population builds during irradiation. Depending on the system, the selected temperature is usually from a few degrees K to around 150 K. A second conventional high-resolution data set is then collected to obtain the metastable state structure. In fortuitous and rare cases, complete conversion from the ground state structure to 100% of the metastable structure has occurred. More commonly, the resultant structure contains a mixture of ground and metastable states, resulting in a disordered picture. To resolve this disorder, the crystal is usually irradiated for a further period, and then subsequent data are collected. This cycle is repeated until the maximum photostationary state population is reached. Once the maximum population has been identified, the crystal is often maintained in the dark, and a series of data collections at different temperatures are conducted to establish the temperature range over which the metastable state is maintained and at what rate it will decay at a given temperature. The structures of many of the metastable nitrosyl, nitrite and sulfur dioxide complexes have been determined using this methodology (Bowes *et al.*, 2006; Hatcher *et al.*, 2019).

Processing of the ground and excited state data sets and comparing them can be challenging, particularly if 100% conversion to the excited state structure does not occur. There will be small changes in the unit-cell dimensions between the clean ground state structure and the structures that contain components of the ground and excited states, and indeed of the 100% excited state structure if photoactivation occurs within the single crystal. In order to accommodate these changes, the coordinates of the ground state crystal need to be normalized relative to the changes associated with the unit-cell dimensions of the photoactivated data set. The resulting coordinates can then be used to represent the ground state component of the model as a fixed rigid body in the refinement of the photoactived data. Examination of the photoelectron density difference maps can then be used to show the disorder components of the excited state structures within the crystal, which can be refined in the disorder model. Once the disorder components have settled, the coordinates for all the other atoms not involved in the

photoexcitation process can be released from their rigid-body constraints, and the atomic positions and displacement parameters are allowed to refine freely, all with occupancies set to unity (Bowes *et al.*, 2006). An example of a photoelectron density difference map for the structure of the cation in the $[Ru(NH_3)_4(H_2O)(\eta^1\text{-}SO_2)](MeC_6H_4SO_3)_2$ salt is shown in Fig. 12. Upon excitation with a tungsten lamp at 13 K, for 75 minutes, the (η^1-SO_2) isomer was formed with a population of *ca* 35% (disordered over two orientations). In the difference map, the two orientations of the (η^1-SO_2) linkage isomer are shown in green (Bowes *et al.*, 2006).

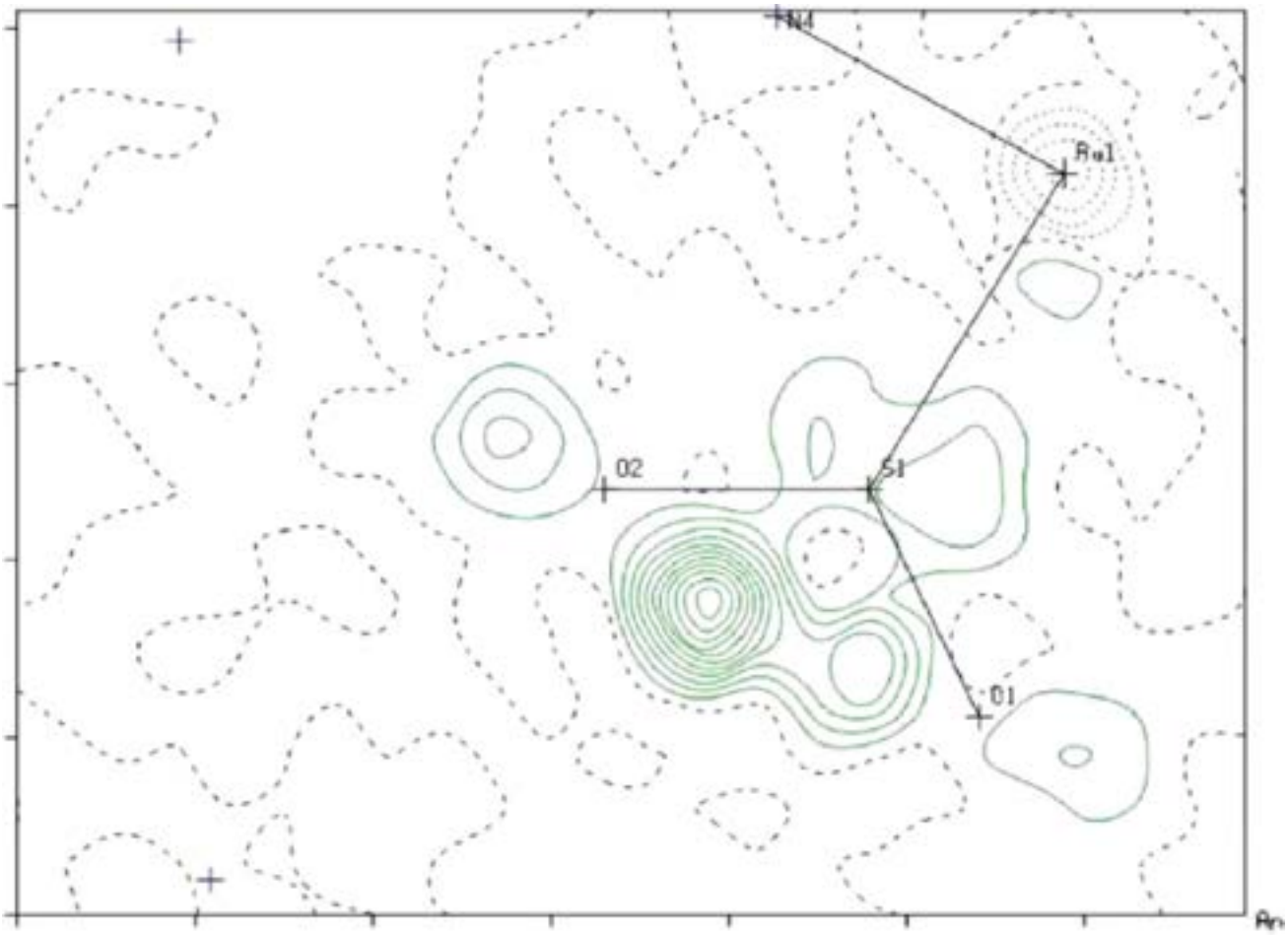


Figure 12. The electron-density difference map drawn through the ground state Ru1/S1/O1/O2 plane calculated using the rigid-body ground state structure and the X-ray data set recorded after photoactivation. The highest residual electron density in the map (green) shows the positions of the two disordered components of the (η^1-SO_2) linkage isomer. [Reproduced from Bowes *et al.* (2006) with permission from the Royal Society of Chemistry.]

In some cases, it may not be possible to obtain a stable refinement of the mixed ground state and excited state disorder model, and then constraints or restraints on some bond parameters may have to be retained in the final refinement cycles. The values to be used in any constraints or restraints should be chemically sensible and may be taken from either a fully-ordered structure of the same material (*e.g.* a `clean' 100% ground state or 100% excited state structure, where available), or else from another suitable experimental source (*e.g.* by identifying the average values for that bond type though analysis of similar crystal structures in the Cambridge Structural Database; Groom *et al.*, 2016). Under those circumstances, while it is possible to identify the presence of different isomers from changes in the positions of the atoms involved, it may not be possible to comment quantitatively on changes in the bond parameters of the isomers present, and certainly not if the bond lengths or angles are constrained in the refinement. This is particularly true if the level of excitation to produce the excited state isomer is not high. For example, in a detailed study of the $[Ru(py)_4Cl(NO)](PF_6)_2$ salt, Schaniel and Woike showed that for nitrosyl isomers with less than 50% excited state populations, only a qualitative assessment of the bonding could be given (Cormary*et al.*, 2009). In cases where it may be possible to compare the bond parameters in different isomers, the estimated standard deviations should be analysed carefully before

any qualitative comparisons can be made.

4.2. `Pseudo-steady-state' experiments

As mentioned in the *Introduction*, an alternative to the `steady-state' experiment is a `pseudo-steady-state' experiment. In a `steady-state' experiment, the excitation and decay processes can be considered to be independent. In a `pseudo-steady-state' experiment, the crystal is continuously irradiated throughout the data collection, the excitation and decay are competitive, and an equilibrium between the two processes will be reached.

There are slight differences in the methodology of the experiment depending on whether a continuous or a pulsed radiation source is used. Both lasers and LEDs can either provide a constant stream of illumination, or the illumination can be pulsed with short pulses of illumination with precise time intervals between them. The two situations are shown in Fig. 13 (Hatcher *et al.*, 2020).

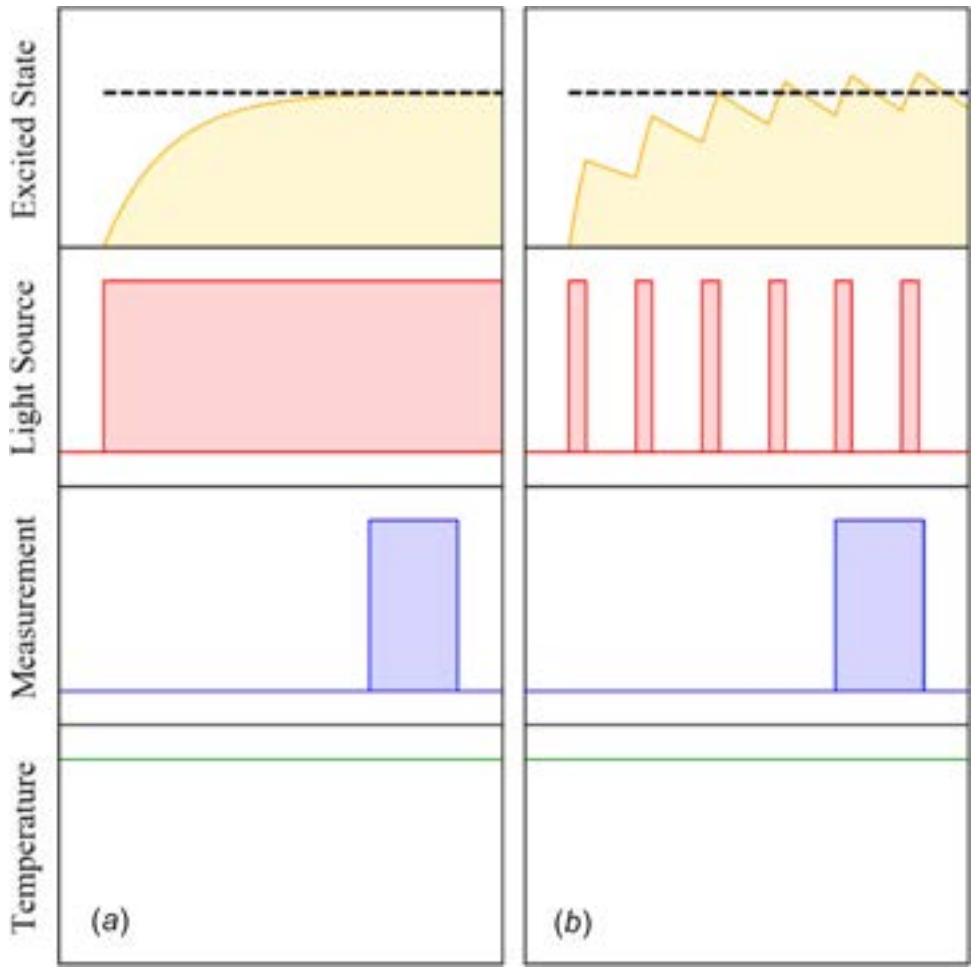


Figure 13. Schematic of a typical (*a*) `steady state' and a (*b*) `pseudo-steady-state' experiment. In part (*a*), the sample is illuminated continuously, and the excited state population builds to a steady-state value. This equilibrium population, marked by a dashed black line, is then measured after a pre-determined equilibration time. In part (*b*), the sample is illuminated with a pulsed laser or LED, resulting in the excited state population oscillating about an equilibrium value. If the measurement time is slower than the pulse frequency, the average population, again denoted by the dashed black line, is measured. [Reproduced from Hatcher *et al.* (2020) with permission.]

The `pseudo-steady-state' method has been used to advantage in several instances, highlighting features of the structural dynamics of the linkage isomerization process that are not apparent when using `steady-state' methods. For example, using a `steady-state' methodology, single crystals of [Ni(Et_4dien)(η^2-O,ON)(η^1-NO_2)] (Et_4dien = *N*,*N*,*N*′,*N*′-tetraethyldiethylenetriamine) can be irradiated with 500 nm light at temperatures below 150 K to generate the *endo*-nitrito isomer [Ni(Et_4dien)(η^2-O,ON)(η^1-ONO)] in 100% yield. However, when the crystal is continuously pumped with the 500 nm light source during the data collection, a previously unobserved *exo*-nitrito (η^1-ONO) linkage isomer is detected (Hatcher, Christensen *et al.*, 2014). The use of `pseudo-steady-state' methods is also

helpful in studying the decay of metastable isomers above their metastable limit. Since the decay rate generally increases with temperature while the excitation rate remains relatively constant, the `steady-state' excited state population falls from its maximum as the temperature increases. For crystals of the salt [Pd(Bu_4dien)(η^1-NO_2)](BPh_4), under irradiation, the decay of the excited state *endo*-(η^1-ONO) isomer to the ground state (η^1-NO_2) becomes competitive at around 230 K, and between 230 and 290 K the observable excited state population drops to zero (Hatcher *et al.*, 2018) as the decay process swamps the excitation.

4.3. Pump–probe experiments

As the lifetimes of the excited state species become shorter, more complicated methodologies are required to monitor the time evolution of the excited state structure during the X-ray experiment. Ideally, complete X-ray data sets could be collected within the duration of one excitation pulse or, more realistically, an excited state equilibrium needs to be set up with a repetitive pump–probe methodology, where the crystalline species is repeatedly pumped up into an excited state, and the resultant structure is probed by an X-ray pulse only when it is excited. Hence, these techniques are described as pump–probe methods or stroboscopic methods. These methods are suitable for studying species with lifetimes of milliseconds and shorter. The technique is called Time-Resolved Single-Crystal X-ray Diffraction (TR-SCXRD), which is in part to differentiate it from the studies of metastable and long lifetime systems (Raithby, 2020).

For these experiments, the light pump pulse has to be synchronized with the X-ray probe pulse so that the X-ray pulse records the diffraction pattern when the crystal is in the excited state and not when the excited state has decayed back to the ground state. In the early pump–probe experiments, the X-ray source was interrupted by a mechanical chopper (Fullagar *et al.*, 2000; Husheer *et al.*, 2010), so that the X-rays were blocked when the crystal had decayed to the ground state. More recently, mechanical choppers have been replaced by electronically time-gated pixel detectors (Casaretto *et al.*, 2017).

Pump–probe experiments are most commonly run at synchrotron sources, where the probe synchrotron beam has a time structure and is essentially pulsed. However, depending on the lifetime of the species to be investigated, mechanical choppers or time-gated detectors are often used. The short-duration light pulses and the monochromatic X-ray pulses are synchronized to arrive at the crystal in a specific time sequence (Fullagar *et al.*, 2000). A repeating sequence is set up in which the crystal is excited by the light pulse at time $t = 0$ and is allowed to decay to the ground state before the next pulse arrives. The X-ray probe pulse is synchronized with the light pulse so that the diffraction pattern is collected after a fixed time delay Δt. The pump pulse generates an excited state population, and the probe pulse measures the population over a brief time consistent with the time resolution of the experiment. The pump–probe sequence for a typical TR-SCXRD experiment is illustrated in Fig. 14(*a*). The technique has been used successfully by several research groups (Deresz *et al.*, 2021), most notably by Coppens (2017) to determine the photoactivated structures of molecular complexes with lifetimes in the microsecond range. However, many pump–probe cycles are required per data collection frame to build up a strong diffraction image, and many frames are necessary to obtain a complete X-ray data set so that a single experiment may take many hours. Additional drawbacks to the method are that the repeated pumping and probing with high-intensity beams causes crystal damage, and there may also be heating effects that are detrimental to the crystal.

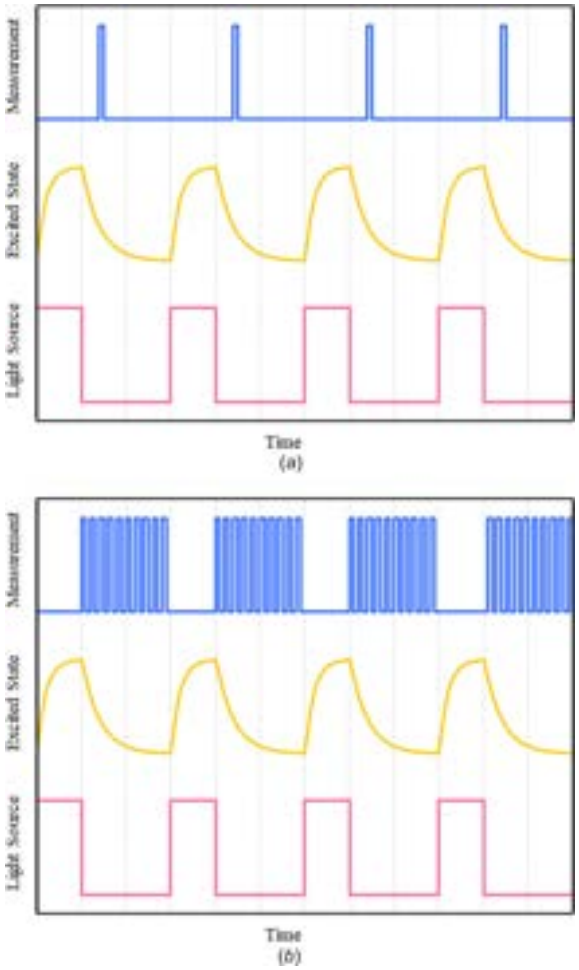


Figure 14. (*a*) In a pump–probe experiment, a single X-ray probe pulse is timed to measure the excited state population at a specific time delay Δt after excitation by the pump light source. The complete experiment is repeated for each Δt to be measured. (*b*) In the pump–multiprobe method, a series of probe pulses are generated after each pulse to measure multiple time delays in a single experiment. [Reproduced from Hatcher *et al.* (2020) with permission.]

4.4. Pump–multiprobe experiments

Pump–multiprobe techniques have been designed to overcome some of these disadvantages and speed up the X-ray data collection. The ability to perform pump–multiprobe experiments has been enhanced by the development of electronically time-gated pixel detectors with fast readout times that make it possible to record the output from multiple probe pulses at different time delays, Δt, following a single pump pulse, with the total signal from each probe sequence being recorded as a single measurement, as illustrated in Fig. 14(*b*). With time-gated or pixel detectors, the photon-counting statistics determine the quality of the X-ray data recorded, and there is no dark current or read-out noise to interfere with the signal recorded as occurs with conventional CCD detectors. The concept of pump–multiprobe experiments was developed initially by macromolecular crystallographers using the Hadamard transformation (Yorke *et al.*, 2014). The sensitivity of the experiment is defined by the number of photons in the whole probe sequence, with the time resolution being defined by the complete length of the probe sequence divided by the number of pulses. Application of the method means that the time resolution is no longer limited to X-ray flux by summing the time points across the probe sequence. The signal-to-noise ratio is also improved because of the increased number of photons recorded during the experiment.

Over the last five years, time-gated detectors have been supplied with new laboratory-based diffractometers. So, with appropriate laser or LED equipment, the synchronization of light and X-ray pulses is possible across a wide range of timescales by electronically gating the detector so that the X-ray diffraction pattern is only measured when the crystal is activated (Casaretto *et al.*, 2017). Building on these advances, a bank of pulsed LEDs has been combined with a time-gated Timepix 3 detector, at

the Diamond Light Source, to conduct pump–multiprobe analysis of the linkage isomerism in [Pd(Bu_4dien)(η^1-NO_2)](BPh_4), at close to room temperature, and this produced a time-resolved `molecular movie' with a 400 millisecond time resolution (Hatcher *et al.*, 2022).

4.5. Laue diffraction experiments

As mentioned earlier in the discussion, an alternative approach to using monochromatic X-ray radiation for TR-SCXRD experiments is to employ polychromatic or Laue X-ray radiation (Schmøkel *et al.*, 2010; Makal *et al.*, 2011). With the broader range of energies used, the flux of the X-ray beam is higher than from a monochromatic source, meaning that time-resolved X-ray data can be collected more quickly. Generally, a pink Laue beam is used rather than a white beam. Here `pink' means a beam containing a small range of wavelengths rather than a white beam with all wavelengths. Because of the higher X-ray intensity, the number of pump–probe cycles in a pump–probe data collection can be significantly reduced (Coppens, Vorontsov *et al.*, 2005) and, as a consequence, crystal decay and crystal heating problems may be reduced. However, because the diffraction pattern obtained contains diffraction spots with different wavelengths, it is more difficult to process and interpret the data. A wavelength dependence correction has to be applied. Additionally, because molecular crystal structures have relatively small unit cells, there are relatively few diffraction spots on any given frame of data, and the scaling of intensities can be challenging. To meet this challenge, Coppens developed the RATIO method (Coppens *et al.*, 2009), in which the intensity difference for each reflection is identified by using *on*/*off* ratios as the observables in the refinement of the excited state structure using the *LASER* software (Vorontsov *et al.*, 2010). For this method to be successful, the laser-*on* and laser-*off* intensities for each reflection must be measured immediately after one another. This approach eliminates the effect of any slow crystal deterioration, and scaling is not required since the paired data frames are collected under the same conditions.

Once the Laue data have been collected and processed, Fourier difference maps can be computed to analyse the structural changes that occur upon excitation of the crystal (Fournier & Coppens, 2014). As the RATIO method has been used in data processing, the computed photodifference map is based on the difference between the observed laser-*on* and laser-*off* structure factors. The method has been shown to be useful in dynamic spin-state photoswitching crystallographic studies (Collet *et al.*, 2012) and in the excited state structural analyses of several coordination complexes displaying microsecond lifetimes (Makal *et al.*, 2012; Coppens, 2017).

4.6. Picosecond and XFEL experiments

For excited state species with lifetimes in the picosecond range and below, the time structure of the synchrotron beam itself can be used to provide very short probe pulses of X-rays. A schematic of a synchrotron is illustrated in Fig. 15 (Clegg, 2000). The bunch structure of the synchrotron originates from the linear accelerator (Linac). Electrons produced by an electron gun are fired into a Linac and accelerated to nearly the speed of light by a series of oscillating electric potentials along a linear path. The synchronized electric field in the cavities accelerates the electrons each time they pass through, causing them to group into bunches.

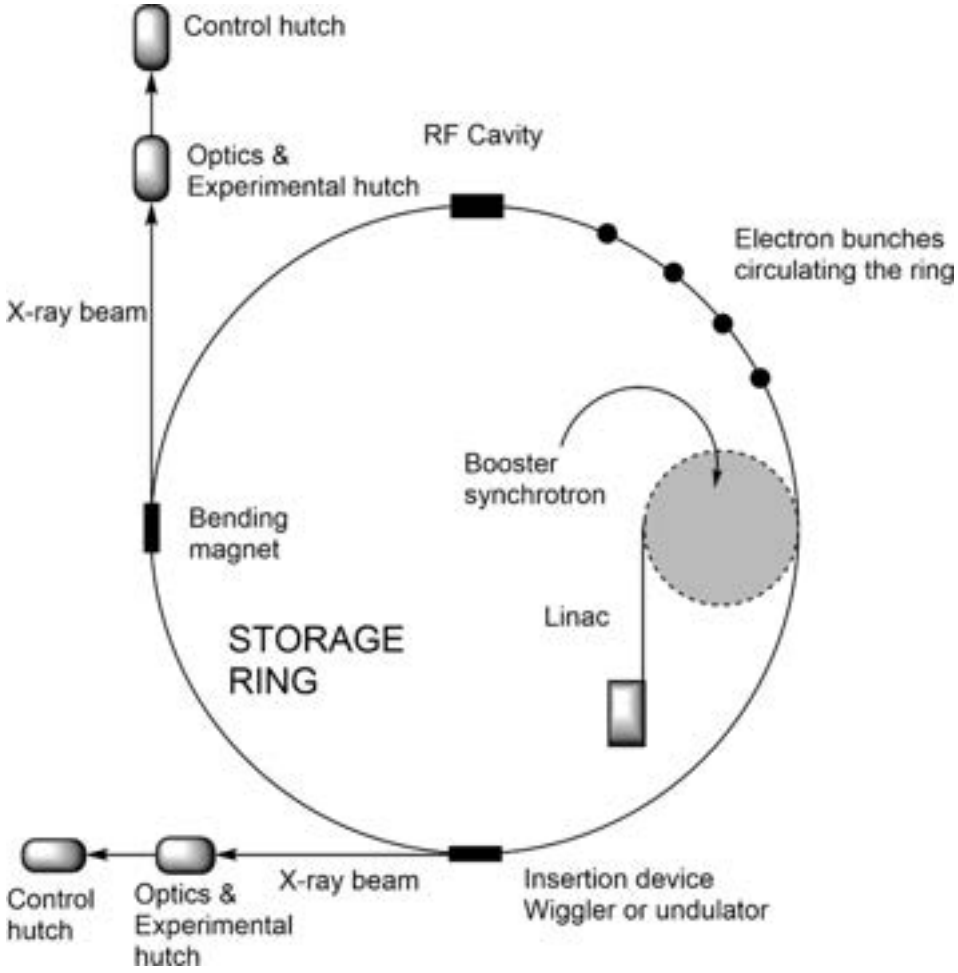


Figure 15. A schematic diagram of a synchrotron showing the various components.

The electrons then pass into the booster ring, an `athletics track' containing radio frequency (RF) cavities in the straight sections and bending magnets in the curved sections to keep the electrons circulating. The main purpose of the booster ring is to further accelerate the electrons to the required energy. The megahertz (MHz) oscillating electric field in the RF cavities further enhances the bunches with a separation equal to the frequency of oscillation.

The electron bunches are injected into the main storage ring, which is used to generate electromagnetic radiation for the beamline end stations. Electromagnetic radiation is generated when a charged particle, such as an electron bunch, travelling at relativistic speeds is deflected from its original path, resulting in an acceleration when passing through a magnetic field. This acceleration causes the electron bunch to radiate electromagnetic waves (synchrotron light) tangentially to the arc of motion.

The storage ring is a multi-sided polygon with bending magnets at each corner, curving the electron bunches and producing electromagnetic radiation. In the straight sections, insertion devices, arrays of magnets with alternating polarity, force the electron bunches into a sinusoidal path, generating intense electromagnetic radiation.

RF cavities are placed at regular intervals around the ring to replenish the energy lost by the generation of electromagnetic radiation. The bunches are synchronized to arrive slightly after the peak of the oscillating electric field, on the downslope of the wave. Electrons within the bunch that have less energy and are, therefore, slightly slower, will arrive later and receive a larger boost, while those with higher energy moving faster will arrive earlier and get a smaller boost. This ensures that bunches remain compact and uniformly spaced.

In the storage ring, the time separation between the bunches is determined by the RF cavity frequency. For example, a 500 MHz frequency results in a 2 ns separation between bunches. The orbit time for a single bunch traveling at relativistic speed depends on the ring circumference. At Diamond Light Source

(DLS), with a 562 m ring, the orbit time is 1.872 µs, while at Advanced Photon Source (APS), with a 1104 m ring, the orbit time is 3.68 µs. At DLS, with a 500 MHz RF cavity and 2 ns separation, there are 936 available bunch slots. For stability, 900 slots are filled, followed by 36 empty slots, creating a 72 ns gap between the end and start of the main bunch train. For time-resolved experiments, the storage ring can be filled with an arbitrary bunch pattern. One common pattern is the single bunch mode, where only one RF `bucket' is filled. The repetition rate is determined by the storage ring size and the orbit period. At DLS and APS, the repetition rates are 1.871 and 3.68 µs, respectively. APS uses 24 single bunches, giving a 153 ns repetition rate.

The minimum experimental time resolution is determined by the overlap between the X-ray and laser pulses. Intense pulsed lasers used in time-resolved experiments have pulse widths in the femtosecond range. At synchrotrons, X-rays produced by single bunches have pulse widths of a few tens of picoseconds (20–40 ps at DLS and 20–50 ps at APS).

Most synchrotrons can perform pump–probe experiments within the picosecond to nanosecond timeframe without electronic time-gating. The laser pump repetition rate is synchronized with the storage ring repetition rate (Coppens, Iversen & Larsen, 2005). However, the X-ray flux from a single bunch is much lower than that from a standard fill pattern. At DLS, a single bunch with a charge of 3 nC is compared to 900 bunches with a charge of 0.62 nC each. Thus, a single time point would take 186 times longer if the laser repetition rate matches the ring, making these experiments often flux-limited and not feasible for many systems.

To study chemical processes that occur on the femtosecond timescale, more complicated experiments need to be designed. For macromolecules, the ultimate approach is the `single-shot' experiment, where the complete diffraction pattern from the crystal can be obtained in one X-ray pulse. This is not really feasible for the study of molecular systems because there are only a small number of X-ray reflections on each frame and indexing to obtain a crystallographic unit cell and crystal orientation is difficult. In particular, establishing the intensity of partially recorded diffraction spots relies heavily on the accurate determination of the crystal orientation, which is particularly difficult if there are only a few reflections on a frame, as is the case for molecular crystals with small unit-cell dimensions. The serial femtosecond crystallographic (SFX) approach is employed instead (Barends *et al.*, 2022), where it is possible to obtain an indexable number of reflections on each frame and then data from many crystals are merged to obtain a complete diffraction pattern. Recently, Iversen and co-workers (Støckler *et al.*, 2023) have developed a data-reduction pipeline approach that automatically handles all the steps in the data-reduction process from spot harvesting to the merging of structure factors. The pipeline uses a sparse indexing approach, based on previously known unit-cell parameters, seed-skewness integration and overlap-based intensity corrections, which can be dynamically adjusted after the initial refinement.

X-ray Free Electron Lasers (XFELs) produce several orders of magnitude higher flux than the most powerful synchrotron and are ideal for studies at the shortest required timescales. However, the experiments are extremely challenging. XFELs have been used to study the dynamic structures of several macromolecular systems using the `diffract-and-destroy' approach, where the crystal is destroyed by the highly intense X-ray pulse, but a diffraction pattern is recorded in a few picoseconds before its destruction (Spence, 2017; Schmidt, 2019). In these experiments, repeat measurements are possible if a stream of crystals is passed through the X-ray beam (Nam, 2019), the serial femtosecond crystallography (SFX) approach (Barends *et al.*, 2022). In these experiments, a single diffraction image is recorded from an individual crystal with, ideally, enough reflections to allow indexing of the diffraction pattern and, thereby, determination of that crystal's orientation. The full diffraction pattern is then obtained by merging the data from many tens, if not hundreds, of individual crystals. Interest in SFX and other serial crystallography approaches is growing considerably, both in the macromolecular and small molecule disciplines, in line with the continued push to brighter X-ray sources as current `third generation' synchrotron sources are being upgraded (Raimondi *et al.*, 2023; Watanabe & Tanaka, 2023), new `fourth generation' synchrotrons are being developed (Chapman, 2023) and the crystallographic use of XFEL instruments increases. However, SFX experiments are not without significant challenges: scaling

between crystals is difficult and it has not been possible to obtain data down to atomic resolution. Furthermore, as mentioned above, the need to obtain enough reflections from a single X-ray shot to enable indexing of the diffraction pattern from a single image is a particular challenge for molecular crystal systems, with typically smaller unit cells and fewer reflections per image. However, the situation changed recently, and Ivsesen and co-workers (Støckler *et al.*, 2023) have applied their pipeline approach to the previously studied structure of the potassium salt of $[Pt_2(pop)_4]^{4-}$ and, using known unit-cell parameters, refined its structure to an R_1 value of *ca* 9.1%. Ihee and co-workers (Kang *et al.*, 2024) have published a report on the dynamic structure of a molecular metal–organic framework (MOF) molecule using time-resolved serial femtosecond crystallography at the Pohang Accelerator Laboratory X-ray free-electron laser facility. The MOF structure, PCN-224(Fe), consists of a porous coordination network of iron porphyrin units linked with hexazirconium nodes, Zr_6. The iron centres can bind to carbon monoxide molecules to give the complex PCN-224(Fe)-CO, which then undergoes CO loss under photoactivation. The electron-density maps from the study slow loss of the CO ligand after 0.1 ps, together with movement of the iron centre, and these features become more evident after 1.1 ps. Importantly, the atomic resolution of the structures is better than 1 Å, a level of precision that is appropriate for molecular crystallography. Rather than using an injector-style crystal delivery system usually used in macromolecular XFEL studies, Ihee and co-workers chose to employ a fixed-target sample holder, where crystals were placed on a thin film and the film moved between measurements to allow fresh single crystals to be exposed to the pump and probe pulses. This experiment has shown that, with suitable modifications, dynamics within molecular crystals can be studied at very short timescales and sets a benchmark for future studies.

5. Conclusions

Since the mid-1990s, with advances in technology and methodology, it is now possible to monitor chemical processes in the crystalline state in real time and obtain structural information on photoactivated molecules with excited state lifetimes from hours to picoseconds using single-crystal X-ray crystallography. Generally, the shorter the lifetime of the molecule whose structure is to be determined, the more complex is the Time-Resolved Single-Crystal X-ray Diffraction (TR-SCXRD) experiment. However, with a modern laboratory-based single-crystal X-ray diffractometer fitted with a high-flux microfocus X-ray source and equipped with electronically time-gated pixel detectors, a crystal-cooling apparatus and either a pulsed laser or pulsed LEDs, it is now possible to conduct quite sophisticated TR-SCXRD experiments on molecules that are metastable under the experimental conditions and those with lifetimes down to milliseconds in the home laboratory. For time-resolved studies on molecules with excited state lifetimes in the microsecond to nanosecond range, the use of synchrotron facilities remains the better option since it must be remembered that all TR-SCXRD experiments remain flux-limited, and the lower the X-ray flux, the longer the experiment will take. Pump–probe or pump–multiprobe experiments can be successfully completed using either the time structure of the synchrotron or an electronically time-gated detector to control the probe pulses, and either a pulsed laser or pulsed LEDs to provide the pump pulses. For molecular structures with excited states in the picosecond to femtosecond domain, highly sophisticated XFEL experiments are required. Femtosecond pulsed lasers provide the pump pulses, and the XFEL generates femto- or picosecond X-ray pulses. It is only very recently that XFEL studies on photoactivated molecular materials, with a resolution suitable for an accurate molecular structure determination, have been achieved (Kang *et al.*, 2024).

Whatever the lifetime of the molecular species being investigated, it is essential to meticulously plan the photocrystallographic experiment before proceeding. If pitfalls in the time-resolved experiment are to be avoided, as much additional information on the reaction as possible needs to be obtained, with a full set of spectroscopic data, thermal analysis, crystal degradation pathways, *etc.* A computational analysis of the chemical process is also very helpful, as this information may support the interpretation of data from electron-density maps, for example.

What is certain is that the future of TR-SCXRD is exciting. With the recent developments in XFEL studies for molecular materials, serial femtosecond studies will become commonplace (Coppens, 2017) and

transformative new science will result. For the slower timescale processes, in the microsecond to minute lifetime regimes, the development of faster, more efficient, time-gated X-ray detectors and their implementation on laboratory-based X-ray diffractometers will mean that many more `routine' time-resolved experiments will be carried out, without the need to bid for scarce synchrotron time (Coppens, 2015). The use of multiple techniques to simultaneously monitor solid-state time-resolved processes will become more prominent (Konieczny *et al.*, 2022; Hasil *et al.*, 2024) and will assist in the design of new advanced functional materials. For example, the combination of TR-SCXRD with Raman spectroscopy and emission spectroscopy will permit the exploration of molecular processes and transformations within the crystalline environment in ways that have not been possible previously.

Acknowledgements

We are grateful to the Engineering and Physical Sciences Research Council (EPSRC) for funding the photocrystallographic research. LEH is supported by a Royal Society University Research Fellowship.

Funding information

Funding for this research was provided by: Engineering and Physical Sciences Research Council (grant Nos. EP/P001548/1, EP/M010481/1, EP/K004956/1 and EP/I01974X/1); Royal Society University Research Fellowship (grant No. URF\R1\191104 to L. E. Hatcher).

References

Allen, F., Mahon, M., Raithby, P., Shields, G. & Sparkes, H. (2005). *New J. Chem.* **29**, 182–187.

Barends, T. R. M., Stauch, B., Cherezov, V. & Schlichting, I. (2022). *Nat. Rev. Methods Primers*, **2**, 59.

Benedict, J. B., Makal, A., Sokolow, J. D., Trzop, E., Scheins, S., Henning, R., Graber, T. & Coppens, P. (2011). *Chem. Commun.* **47**, 1704–1706.

Blake, A. J., Champness, N. R., Easun, T. L., Allan, D. R., Nowell, H., George, M. W., Jia, J. & Sun, X. Z. (2010). *Nat. Chem.* **2**, 688–694.

Borowski, P., Kutniewska, S. E., Kamiński, R., Krówczyński, A., Schaniel, D. & Jarzembska, K. N. (2022). *Inorg. Chem.* **61**, 6624–6640.

Bowes, K., Cole, J., Husheer, S., Raithby, P., Savarese, T., Sparkes, H., Teat, S. & Warren, J. (2006). *Chem. Commun.* pp. 2448–2450.

Brayshaw, S. K., Knight, J. W., Raithby, P. R., Savarese, T. L., Schiffers, S., Teat, S. J., Warren, J. E. & Warren, M. R. (2010). *J. Appl. Cryst.* **43**, 337–340.

Carducci, M. D., Pressprich, M. R. & Coppens, P. (1997). *J. Am. Chem. Soc.* **119**, 2669–2678.

Casaretto, N., Pillet, S., Bendeif, E. E., Schaniel, D., Gallien, A. K. E., Klüfers, P. & Woike, T. (2015). *IUCrJ*, **2**, 35–44.

Casaretto, N., Schaniel, D., Alle, P., Wenger, E., Parois, P., Fournier, B., Bendeif, E.-E., Palin, C. & Pillet, S. (2017). *Acta Cryst.* B**73**, 696–707.

Chapman, H. N. (2019). *Annu. Rev. Biochem.* **88**, 35–58.

Chapman, H. N. (2023). *IUCrJ*, **10**, 246–247.

Clegg, W. (2000). *J. Chem. Soc. Dalton Trans.* pp. 3223–3232.

Cohen, M. D. (1975). *Angew. Chem. Int. Ed. Engl.* **14**, 386–393.

Cohen, M. D. & Schmidt, G. M. J. (1964). *J. Chem. Soc.* p. 1996.

Cohen, M. D., Schmidt, G. M. J. & Sonntag, F. I. (1964). *J. Chem. Soc.* p. 2000.

Cole, J. M. (2008). *Acta Cryst.* A**64**, 259–271.

Cole, J. M. (2011). *Analyst*, **136**, 448–455.

Cole, J. M., Gosztola, D. J., Velazquez-Garcia, J., Grass Wang, S. & Chen, Y. (2021). *Chem. Commun.* **57**, 1320–1323.

Cole, J. M., Gosztola, D. J. & Velazquez-Garcia, J. D. (2021). *J. Phys. Chem. C*, **125**, 8907–8915.

Cole, J. M., Gosztola, D. J. & Velazquez-Garcia, J. D. (2022). *J. Phys. Chem. C*, **126**, 6047–6059.

Collet, E., Moisan, N., Baldé, C., Bertoni, R., Trzop, E., Laulhé, C., Lorenc, M., Servol, M., Cailleau, H., Tissot, A., Boillot, M. L., Graber, T., Henning, R., Coppens, P. & Buron-Le Cointe, M. (2012). *Phys. Chem. Chem. Phys.* **14**, 6192–6199.

Coppens, P. (2015). *Struct. Dyn.* **2**, 020901.

Coppens, P. (2017). *Struct. Dyn.* **4**, 032102.

Coppens, P., Gerlits, O., Vorontsov, I. I., Kovalevsky, A. Y., Chen, Y. S., Graber, T., Gembicky, M. & Novozhilova, I. V. (2004). *Chem. Commun.* pp. 2144–2145.

Coppens, P., Iversen, B. & Larsen, F. K. (2005). *Coord. Chem. Rev.* **249**, 179–195.

Coppens, P., Novozhilova, I. & Kovalevsky, A. (2002). *Chem. Rev.* **102**, 861–884.

Coppens, P., Pitak, M., Gembicky, M., Messerschmidt, M., Scheins, S., Benedict, J., Adachi, S., Sato, T., Nozawa, S., Ichiyanagi, K., Chollet, M. & Koshihara, S. (2009). *J. Synchrotron Rad.* **16**, 226–230.

Coppens, P., Sokolow, J., Trzop, E., Makal, A. & Chen, Y. (2013). *J. Phys. Chem. Lett.* **4**, 579–582.

Coppens, P., Vorontsov, I. I., Graber, T., Gembicky, M. & Kovalevsky, A. Y. (2005). *Acta Cryst.* A**61**, 162–172.

Cormary, B., Ladeira, S., Jacob, K., Lacroix, P. G., Woike, T., Schaniel, D. & Malfant, I. (2012). *Inorg. Chem.* **51**, 7492–7501.

Cormary, B., Malfant, I., Valade, L., Buron-Le Cointe, M., Toupet, L., Todorova, T., Delley, B., Schaniel, D., Mockus, N., Woike, T., Fejfarová, K., Petříček, V. & Dušek, M. (2009). *Acta Cryst.* B**65**, 787–787.

Deresz, K. A., Kamiński, R., Kutniewska, S. E., Krówczyński, A., Schaniel, D. & Jarzembska, K. N. (2022). *Chem. Commun.* **58**, 13439–13442.

Deresz, K. A., Łaski, P., Kamiński, R. & Jarzembska, K. N. (2021). *Crystals*, **11**, 1345.

Drenth, J. (2007). In *Principles of Protein X-Ray Crystallography*, 3rd ed. Berlin: Springer.

Enkelmann, V., Wegner, G., Novak, K. & Wagener, K. B. (1993). *J. Am. Chem. Soc.* **115**, 10390–10391.

Fomitchev, D. V., Novozhilova, I. & Coppens, P. (2000). *Tetrahedron*, **56**, 6813–6820.

Fournier, B. & Coppens, P. (2014). *Acta Cryst.* A**70**, 291–299.

Fullagar, W. K., Wu, G., Kim, C., Ribaud, L., Sagerman, G. & Coppens, P. (2000). *J. Synchrotron Rad.* **7**, 229–235.

Groom, C. R., Bruno, I. J., Lightfoot, M. P. & Ward, S. C. (2016). *Acta Cryst.* B**72**, 171–179.

Hasil, A., Konieczny, K. A., Mikhailov, A., Pillet, S. & Schaniel, D. (2024). *ChemPhotoChem*, **8**, e202300149.

Hatcher, L. E. (2016). *CrystEngComm*, **18**, 4180–4187.

Hatcher, L. E., Bigos, E. J., Bryant, M. J., MacCready, E. M., Robinson, T. P., Saunders, L. K., Thomas, L. H., Beavers, C. M., Teat, S. J., Christensen, J. & Raithby, P. R. (2014). *CrystEngComm*, **16**, 8263–8271.

Hatcher, L. E., Christensen, J., Hamilton, M. L., Trincao, J., Allan, D. R., Warren, M. R., Clarke, I. P., Towrie, M., Fuertes, D. S., Wilson, C. C., Woodall, C. H. & Raithby, P. R. (2014). *Chem. A Eur. J.* **20**, 3128–3134.

Hatcher, L. E., Saunders, L. K. & Coulson, B. A. (2023). *Faraday Discuss.* **244**, 370–390.

Hatcher, L. E., Skelton, J. M., Warren, M. R. & Raithby, P. R. (2019). *Acc. Chem. Res.* **52**, 1079–1088.

Hatcher, L. E., Skelton, J. M., Warren, M. R., Stubbs, C., da Silva, E. L. & Raithby, P. R. (2018). *Phys. Chem. Chem. Phys.* **20**, 5874–5886.

Hatcher, L. E., Warren, M. R., Pallipurath, A. R., Saunders, L. K. & Skelton, J. M. (2020). *Watching Photochemistry Happen: Recent Developments in Dynamic Single-Crystal X-Ray Diffraction Studies*, in *21st Century Challenges in Chemical Crystallography I: History and Technical Developments*, edited by D. M. P. Mingos & P. R. Raithby, pp. 199–238, Vol. 185 of the series *Structure and Bonding*. Berlin: Springer.

Hatcher, L. E., Warren, M. R., Skelton, J. M., Pallipurath, A. R., Saunders, L. K., Allan, D. R., Hathaway, P., Crevatin, G., Omar, D., Williams, B., Coulson, B., Wilson, C. C. & Raithby, P. R. (2022). *Commun. Chem.* **5**, 102.

Husheer, S. L. G., Cole, J. M., d'Almeida, T. & Teat, S. J. (2010). *Rev. Sci. Instrum.* **81**, 043905.

Jarzembska, K. N., Hapka, M., Kaminski, R., Bury, W., Kutniewska, S. E., Szarejko, D. & Szczesniak, M. M. (2019). *Crystals*, **9**, 9010036.

Jarzembska, K. N., Kamiński, R., Fournier, B., Trzop, E., Sokolow, J. D., Henning, R., Chen, Y. & Coppens, P. (2014). *Inorg. Chem.* **53**, 10594–10601.

Kalinowski, J. A., Fournier, B., Makal, A. & Coppens, P. (2012). *J. Synchrotron Rad.* **19**, 637–646.

Kamiński, R., Jarzembska, K. N., Kutyła, S. E. & Kamiński, M. (2016). *J. Appl. Cryst.* **49**, 1383–1387.

Kang, J., Lee, Y., Lee, S., Ki, H., Kim, J., Gu, J., Cha, Y., Heo, J., Lee, K. W., Kim, S. O., Park, J., Park, S. Y., Kim, S., Ma, R., Eom, I., Kim, M., Kim, J., Lee, J. H. & Ihee, H. (2024). *Nat. Chem.* **16**, 693–699.

Kim, C. D., Pillet, S., Wu, G., Fullagar, W. K. & Coppens, P. (2002). *Acta Cryst.* A**58**, 133–137.

Konieczny, K., Hasil, A., Schaniel, D. & Pillet, S. (2022). *Acta Cryst.* A**78**, e764–e765.

Levantino, M., Kong, Q. Y., Cammarata, M., Khakhulin, D., Schotte, F., Anfinrud, P., Kabanova, V., Ihee, H., Plech, A., Bratos, S. & Wulff, M. (2021). *C. R. Phys.* **22**, 75–94.

Lim, M., Jackson, T. A. & Anfinrud, P. A. (1995). *Science*, **269**, 962–966.

Mahon, M. F., Raithby, P. R. & Sparkes, H. A. (2008). *CrystEngComm*, **10**, 573–576.

Makal, A., Benedict, J., Trzop, E., Sokolow, J., Fournier, B., Chen, Y., Kalinowski, J. A., Graber, T., Henning, R. & Coppens, P. (2012). *J. Phys. Chem. A*, **116**, 3359–3365.

Makal, A., Trzop, E., Sokolow, J., Kalinowski, J., Benedict, J. & Coppens, P. (2011). *Acta Cryst.* A**67**, 319–326.

Marr, Z. Y., Thapa Magar, R., Fournier, B., Benedict, J. B. & Rack, J. J. (2023). *Chem. Sci.* **14**, 7279–7284.

Mikhailov, A., Konieczny, K. A., Gladysheva, M., Plyusnin, P., Pillet, S. & Schaniel, D. (2023). *Inorg. Chem.* **62**, 5531–5542.

Moffat, K. (2019). *Phil. Trans. R. Soc. A.* **377**, 20180243.

Nam, K. H. (2019). *Int. J. Mol. Sci.* **20**, 1094.

Natarajan, A. & Bhogala, B. R. (2011). *Bimolecular Photoreactions in the Crystalline State*, in *Supramolecular Photochemistry*, edited by V. Ramamurty & Y. Inoue, pp. 175–228. New York: Wiley & Sons, Inc.

Naumov, P. (2012). *Chemical X-Ray Photodiffraction: Principles, Examples, and Perspectives*, in *Advanced X-Ray Crystallography*, edited by K. Rissanen, Vol. 315, pp. 111–131. Berlin: Springer.

Naumov, P., Karothu, D. P., Ahmed, E., Catalano, L., Commins, P., Mahmoud Halabi, J., Al-Handawi, M. B. & Li, L. (2020). *J. Am. Chem. Soc.* **142**, 13256–13272.

Ohashi, Y. (2013). *Crystallogr. Rev.* **19**, 2–146.

Ohashi, Y., Yanagi, K., Kurihara, T., Sasada, Y. & Ohgo, Y. (1981). *J. Am. Chem. Soc.* **103**, 5805–5812.

Ozawa, Y., Terashima, M., Mitsumi, M., Toriumi, K., Yasuda, N., Uekusa, H. & Ohashi, Y. (2003). *Chem. Lett.* **32**, 62–63.

Pillet, S. (2018). *Time-resolved structural analysis: probing condensed matter in motion*, in *Structures on Different Time Scales*, edited by W. Theo & S. Dominik, pp. 143–220. Berlin, Boston: De Gruyter.

Potempa, K., Deresz, K. A., Jankowska, J., Jarzembska, K. N., Krówczyński, A., Mikhailov, A., Schaniel, D. & Kamiński, R. (2023). *Chem. A Eur. J.* **29**, e202302629.

Pressprich, M. R., White, M. A., Vekhter, Y. & Coppens, P. (1994). *J. Am. Chem. Soc.* **116**, 5233–5238.

Raimondi, P., Benabderrahmane, C., Berkvens, P., Biasci, J. C., Borowiec, P., Bouteille, J. F., Brochard, T., Brookes, N. B., Carmignani, N., Carver, L. R., Chaize, J. M., Chavanne, J., Checchia, S., Chushkin, Y., Cianciosi, F., Di Michiel, M., Dimper, R., D'Elia, A., Einfeld, D., Ewald, F., Farvacque, L., Goirand, L., Hardy, L., Jacob, J., Jolly, L., Krisch, M., Le Bec, G., Leconte, I., Liuzzo, S. M., Maccarrone, C., Marchial, T., Martin, D., Mezouar, M., Nevo, C., Perron, T., Plouviez, E., Reichert, H., Renaud, P., Revol, J. L., Roche, B., Scheidt, K. B., Serriere, V., Sette, F., Susini, J., Torino, L., Versteegen, R., White, S. & Zontone, F. (2023). *Commun. Phys.* **6**, 82.

Raithby, P. R. (2007). *Crystallogr. Rev.* **13**, 121–142.

Raithby, P. R. (2020). *Time-Resolved Single-Crystal X-Ray Crystallography*, in *21st Century Challenges in Chemical Crystallography I: History and Technical Developments*, edited by D. M. P. Mingos & P. R. Raithby, pp. 239–271, Vol. 185 of the series *Structure and Bonding*. Berlin: Springer.

Rodenbough, P. P., Karothu, D. P., Gjorgjieva, T., Commins, P., Hara, H. & Naumov, P. (2018). *Cryst. Growth Des.* **18**, 1293–1296.

Schaniel, D., Bendeif, E. E., Woike, T., Böttcher, H. C. & Pillet, S. (2018). *CrystEngComm*, **20**, 7100–7108.

Schaniel, D. & Woike, T. (2009). *Phys. Chem. Chem. Phys.* **11**, 4391–4395.

Schaniel, D., Woike, T., Schefer, J., Petricek, V., Kramer, K. W. & Gudel, H. U. (2006). *Phys. Rev. B*, **73**, 5.

Schmidt, G. M. J. (1964). *J. Chem. Soc.* p. 2014.

Schmidt, M. (2019). *Int. J. Mol. Sci.* **20**, 1401.

Schmøkel, M. S., Kamiński, R., Benedict, J. B. & Coppens, P. (2010). *Acta Cryst.* A**66**, 632–636.

Spence, J. C. H. (2017). *IUCrJ*, **4**, 322–339.

Spence, J. C. H., Weierstall, U. & Chapman, H. N. (2012). *Rep. Prog. Phys.* **75**, 10.

Srajer, V., Ren, Z., Teng, T. Y., Schmidt, M., Ursby, T., Bourgeois, D., Pradervand, C., Schildkamp, W., Wulff, M. & Moffat, K. (2001). *Biochemistry*, **40**, 13802–13815.

Šrajer, V., Teng, T. Y., Ursby, T., Pradervand, C., Ren, Z., Adachi, S., Schildkamp, W., Bourgeois, D., Wulff, M. & Moffat, K. (1996). *Science*, **274**, 1726–1729.

Støckler, L. J., Krause, L., Svane, B., Tolborg, K., Richter, B., Takahashi, S., Fujita, T., Kasai, H., Sugahara, M., Inoue, I., Nishibori, E. & Iversen, B. B. (2023). *IUCrJ*, **10**, 103–117.

Thompson, A. L., Beeby, A. & Goeta, A. E. (2004). *J. Appl. Cryst.* **37**, 652–653.

Vorontsov, I., Pillet, S., Kamiński, R., Schmøkel, M. S. & Coppens, P. (2010). *J. Appl. Cryst.* **43**, 1129–1130.

Vorontsov, I. I., Graber, T., Kovalevsky, A. Y., Novozhilova, I. V., Gembicky, M., Chen, Y. S. & Coppens, P. (2009). *J. Am. Chem. Soc.* **131**, 6566–6573.

Vorontsov, I. I., Kovalevsky, A. Y., Chen, Y. S., Graber, T., Gembicky, M., Novozhilova, I. V., Omary, M. A. & Coppens, P. (2005). *Phys. Rev. Lett.* **94**, 4.

Warren, M. R., Brayshaw, S. K., Johnson, A. L., Schiffers, S., Raithby, P. R., Easun, T. L., George, M. W., Warren, J. E. & Teat, S. J. (2009). *Angew. Chem. Int. Ed.* **48**, 5711–5714.

Warren, M. R., Easun, T. L., Brayshaw, S. K., Deeth, R. J., George, M. W., Johnson, A. L., Schiffers, S., Teat, S. J., Warren, A. J., Warren, J. E., Wilson, C. C., Woodall, C. H. & Raithby, P. R. (2014). *Chem. A Eur. J.* **20**, 5468–5477.

Watanabe, T. & Tanaka, H. (2023). *Synchrotron Rad. News*, **36**, 3–6.

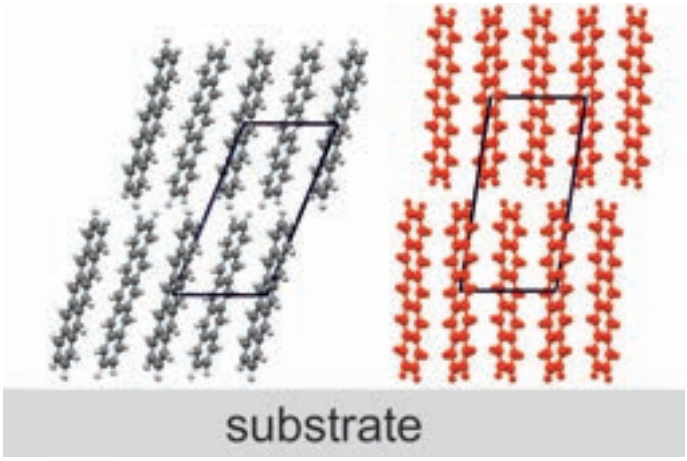
Woike, T., Krasser, W., Zöllner, H., Kirchner, W. & Haussühl, S. (1993). *Z. Phys. D. Atoms Mol. Clusters*, **25**, 351–356.

Yorke, B. A., Beddard, G. S., Owen, R. L. & Pearson, A. R. (2014). *Nat. Methods*, **11**, 1131–1134.

This article was originally published in *Acta Cryst.* (2024). C**80**, 585–600.

FEATURE ARTICLE

On the importance of crystal structures for organic thin film transistors



Guillaume Schweicher, Susobhan Das, Roland Resel, Yves Geerts

This article is part of the collection Best practice in crystallography.

Historically, knowledge of the molecular packing within the crystal structures of organic semiconductors has been instrumental in understanding their solid-state electronic properties. Nowadays, crystal structures are thus becoming increasingly important for enabling engineering properties, understanding polymorphism in bulk and in thin films, exploring dynamics and elucidating phase-transition mechanisms. This review article introduces the most salient and recent results of the field.

1. Introduction

The field of organic electronics relies on the use of organic compounds as semiconducting materials for the transport of either electrons (e^-) or holes (h^+) to perform logic operations and to convert light into electrical current or *vice versa*. Organic semiconductors are π-conjugated systems that are often flat and rigid. Two classes of organic semiconductors exist: polymers and low-molecular-weight compounds (Ostroverkhova, 2016). Macromolecules provide a fast lane for charge transport along their π-conjugated backbone, but charge hopping between chains is much slower which limits charge carrier mobility μ (cm^2 V^{-1} s^{-1}). The latter is defined as the drift velocity of the charge carrier (cm s^{-1}) per unit applied electric field (V cm^{-1}) and serves as the figure of merit for benchmarking semiconductor performance. π-Conjugated polymers are only semicrystalline, meaning that some ordered and amorphous regions co-exist within the same sample, but also within the same macromolecular chain (Ding *et al.*, 2023). Crystalline order is essential for efficient charge transport; for example, single-crystal silicon (μ = 1200 cm^2 V^{-1} s^{-1}) exhibits a charge carrier mobility three times greater than amorphous films (μ = 1 cm^2 V^{-1} s^{-1}) (Schweicher *et al.*, 2020). Low-molecular-weight organic semiconductors generally show higher charge carrier mobility values than π-conjugated polymers, which is a result of their crystallinity (Sawatzki-Park *et al.*, 2023). The fact that molecular semiconductors can completely crystallize paves the way to comprehensive studies on the role of molecular structure, crystal packing and crystal–lattice dynamics in charge transport (Fratini *et al.*, 2020; Giannini & Blumberger, 2022). Notably, charge-transport studies on single crystals are particularly instructive for establishing reliable structure–property relationships (Gershenson*et al.*, 2006; Liu *et al.*, 2011; Takimiya *et al.*, 2014; Iino *et al.*, 2015; Fraboni *et al.*, 2016; Tsurumi *et al.*, 2017; Onwubiko *et al.*, 2018; Wang *et al.*, 2018; Yamamura *et al.*, 2018; Zhang *et al.*, 2018; He *et al.*, 2018). As can be seen in Fig. 1, which presents a selection of good-performing organic semiconductors, solubilizing side groups are often linked to π-conjugated cores. However, side groups do much more than just confer solubility in common organic solvents. They are also essential for engineering crystal structures that majorly impact the transfer integrals *J* (meV), which quantify the extent of wave function overlap between adjacent π-systems (Anthony, 2006, 2008; Coropceanu *et al.*, 2007; Liu *et al.*, 2011; Mas-Torrent & Rovira, 2011; Mitsui *et al.*, 2014; Schweicher *et al.*, 2014, 2020; Yu *et al.*, 2019; Jiang & Hu, 2020; Okamoto *et al.*, 2020; Takimiya *et al.*, 2024). In principle, the higher the value of *J*, the larger the value of μ. However, it is a necessary, but not sole, condition since lattice dynamics and the dimensionality of transport [one- (1D), two- (2D) or three-dimensional (3D)] also play major roles in the performance of semiconductors (Sundar *et al.*, 2004; Schweicher *et al.*, 2015; Illig *et al.*, 2016). Static and dynamic disorder force charges to localize which substantially decreases charge carrier mobility (Fratini *et al.*, 2016; Tsutsui *et al.*, 2016; Schweicher *et al.*, 2019; Banks *et al.*, 2023). Finally, it is worth mentioning that thermal expansion coefficients along different crystallographic directions are instrumental for studying and understanding the temperature dependence of charge-transport properties (Li *et al.*, 2012, 2013; van der Lee *et al.*, 2018; Jouclas *et al.*, 2022). This review focuses on the link between the crystal structures of molecular semiconductors and their charge-transport properties. It is not the ambition to be comprehensive due to the many types of molecules and crystal structures in this field. However, it highlights the importance of crystallographic information for characterizing and understanding solid-state properties using some representative examples, mostly, but not exclusively, from our research groups (Rivnay *et al.*, 2012).

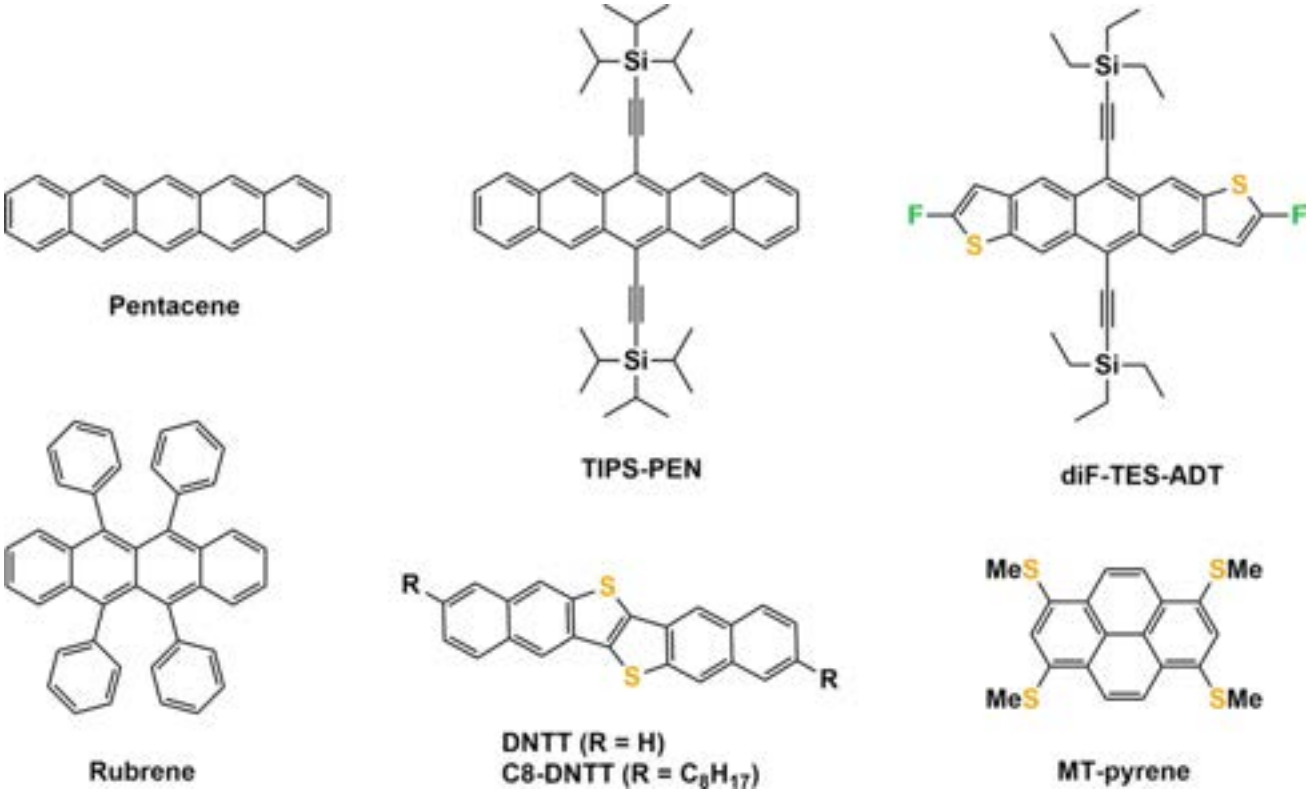


Figure 1. A selection of some good-performing and historically important molecular semiconductors: pentacene (Mas-Torrent & Rovira, 2011), rubrene (Menard *et al.*, 2004; Sundar *et al.*, 2004), 6,13-bis(triisopropylsilylethynyl)pentacene (TIPS-PEN) (Anthony *et al.*, 2001), 2,8-difluoro-5,11-bis(triethylsilylethynyl)anthradithiophene (diF-TES-ADT) (Subramanian *et al.*, 2008), dinaphtho[2,3-*b*:2′,3′-*f*]thieno[3,2-*b*]thiophene (DNTT) (Takimiya *et al.*, 2014), dioctyldinaphtho[2,3-*b*:2′,3′-*f*]thieno[3,2-*b*]thiophene (C8-DNTT) (Kang *et al.*, 2011) and 1,3,6,8-tetrakis(methylthio)pyrene (MT-pyrene) (Takimiya *et al.*, 2021).

2. Molecular structure assessment

Materials chemists synthesizing organic semiconductors rely heavily on proton and carbon nuclear magnetic resonance (^{1}H and ^{13}C NMR) and on UV–visible (UV–Vis) spectroscopy for assessing molecular structures (Takimiya *et al.*, 2014; Anthony, 2008). These methods require, however, a minimum solubility in common organic solvents that nonsubstituted extended π-systems rarely possess. Mass spectrometry, which can be performed on powders, provides valuable information on parent ions and fragmentation fingerprints that give hints to the molecular structures, but which cannot be considered as sufficient proof itself. Despite the fact that nonsubstituted extended π-systems are rather insoluble, their high thermal stability allows their sublimation under high vacuum (Jiang & Kloc, 2013). In many cases, these π-systems form, from the vapour phase, high-quality crystals that are ideal for crystal structure determination by X-ray diffraction (Zhang *et al.*, 2018). On the other hand, extended π-systems substituted by alkyl chains or other side groups allow the production of single-crystal domains through conventional or advanced solution-processing methods in the event of decent solubility in conventional solvents (Diao *et al.*, 2014*b*; Yamamura *et al.*, 2018). Single crystals obtained from solution are equally suitable for structure solution by X-ray diffraction. Poor solubility combined with poor thermal stability will lead to a more challenging crystal structure determination. In some cases, the electron diffraction (ED) analysis of micron-sized or even submicron-sized crystals can help in solving a structure (Altoe *et al.*, 2012; Gruene *et al.*, 2021; Brázda *et al.*, 2019). ED also provides information on crystal disorder and dynamics (Illig *et al.*, 2016). In general, crystal structures offer the ultimate evidence of molecular identity when solution characterization methods are inoperative, as illustrated for DN4T in Fig. 2(*a*) (Jouclas *et al.*, 2022). Importantly, this also holds true for assessing stereochemistry at the molecular and supramolecular levels. Fig. 2(*b*) shows the chiral supramolecular packing of the achiral DNTT core due to the presence of chiral alkyl side chains (Volpi *et al.*, 2023).

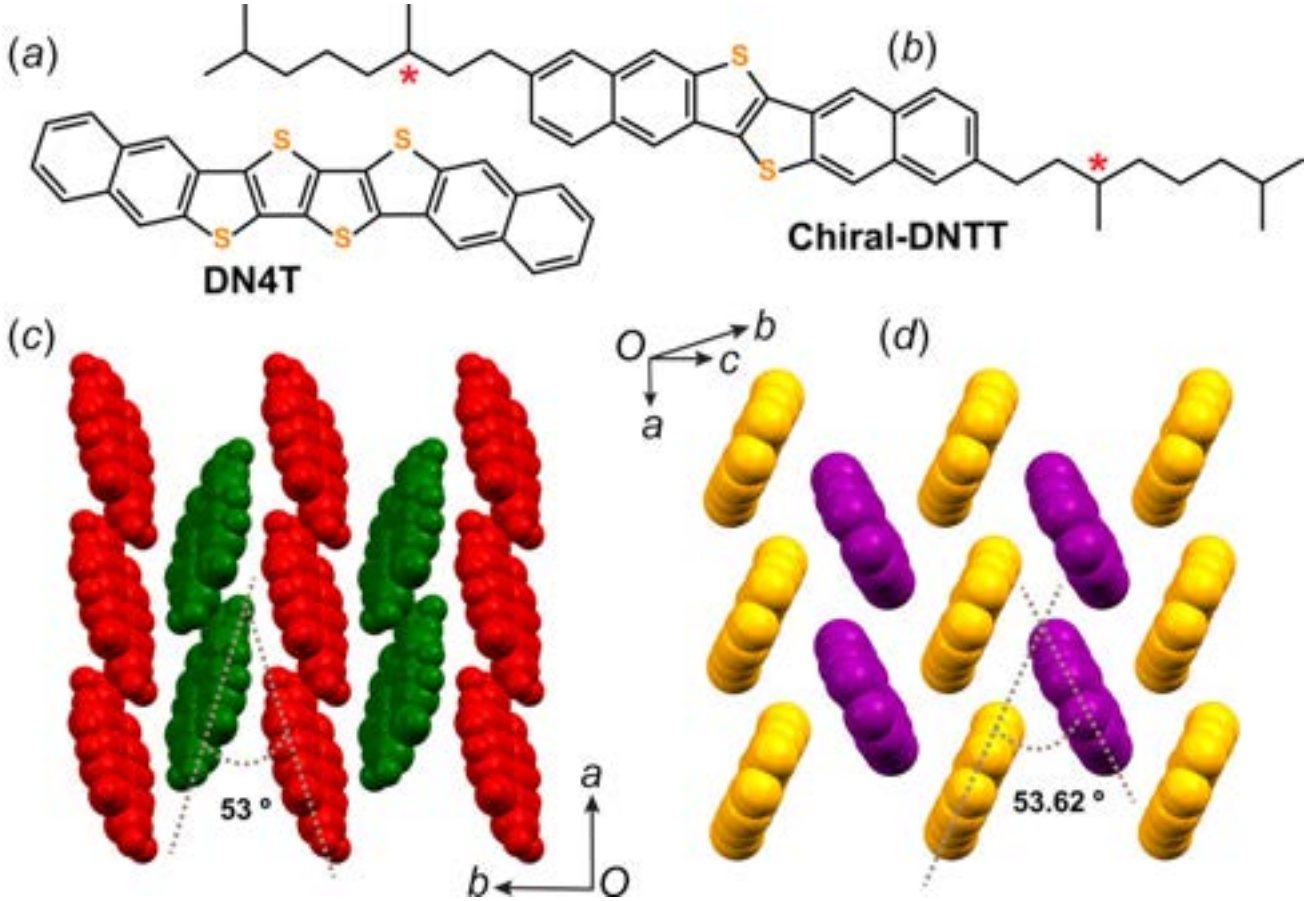


Figure 2. The molecular structure of (*a*) DN4T and (*b*) chiral DNTT. (*c*)/(*d*) The corresponding crystallographic herringbone packing, defining the change in the dihedral angle, ultimately determined by solving the crystal structures. The chiral supramolecular arrangement of the achiral DNTT core induced by the chiral alkyl side chains is indicated (marked by red asterisks) (Volpi *et al.*, 2023).

3. Intermolecular and electronic interactions

Crystal structures contain a wealth of information that is particularly valuable for assessing the intermolecular interactions between adjacent molecules. The relative positions of π-systems, the intermolecular distances, the molecular volume and the number of crystallographically different molecules per unit cell originate from the delicate balance between attractive and repulsive intermolecular interactions (Sutton *et al.*, 2016). Various types of attractive electrostatic intermolecular interactions are at play, such as hydrogen bonding, van der Waals forces and quadrupolar interactions. Intermolecular repulsion, explained by the Pauli exclusion principle, is far from being negligible as it accounts for molecular shape (Israelachvili, 2011). To deal with the complexity and the amount of information on intermolecular interactions within crystal structures, computing tools, such as fingerprint plots and Hirshfeld surfaces, are nowadays used routinely (Spackman & McKinnon, 2002; Spackman & Jayatilaka, 2009; Spackman, 2013; Niebel *et al.*, 2015). Crystal structures are also exploited to calculate the above-mentioned transfer integrals (Coropceanu *et al.*, 2007; Fratini *et al.*, 2020). There exists, however, no general correlation between the relative positions and the intermolecular distances of π-systems with *J* values since the latter are determined by the extent of wave function overlap between adjacent molecules (Fratini *et al.*, 2017). Transfer integrals assume values in the range 0–100 meV, while significantly larger values of up to 800 meV are encountered in disk-like molecules such as phthalocyanines (Tant *et al.*, 2005). Transfer integral patterns are orbital specific. Notably, *J* value patterns for highest occupied molecular orbitals (HOMOs) and lowest unoccupied molecular orbitals (LUMOs) differ considerably (Brédas *et al.*, 2002). Crystal structures also allow the calculation of intramolecular (local) and intermolecular (nonlocal) phonon modes that are essential for understanding the lattice dynamics within crystals (Bedoya-Martínez *et al.*, 2017; Schweicher *et al.*, 2019; Jouclas *et al.*, 2022; Banks *et al.*, 2023). Slow intermolecular vibrations, corresponding to 10–150 cm^{-1} phonon modes, limit charge transport by inducing a fluctuating structural disorder causing the transfer integrals to adopt a wide distribution of values at room temperature (Fratini *et al.*, 2016). Consequently, charge carriers get transiently localized over clusters of π-systems, resulting in charge carrier mobility values on the order of 10 $cm^2\ V^{-1}\ s^{-1}$ over long time and length scales. The situation differs radically at short time and length scales, *i.e.* 10^{-10} s and 100 nm, respectively. Under these conditions, the charge carrier mobility exceeds 100 $cm^2\ V^{-1}\ s^{-1}$ (Tsutsui *et al.*, 2016; Giannini *et al.*, 2023). The resulting localization length is determined by the crystal structure, phonon modes and temperature (Giannini *et al.*, 2023). Crystal dynamics and, in particular, some specific intermolecular phonon modes, also trigger crystal-to-crystal phase transitions (*vide infra*) (Chung *et al.*, 2018*a*; Asher *et al.*, 2022, 2023; Ferrari *et al.*, 2023). In any case, crystal structures are the essential inputs for many further studies. Note, however, that crystal structures do not provide all information regarding charge transport. Notably, crystal twisting, *i.e.* the formation of helical ribbons, with repetitive optical textures in the 1–100 μm range, also impacts charge transport (Yang *et al.*, 2022, 2024; Whittaker *et al.*, 2023).

4. Crystal structure engineering

As the performance of molecular semiconductors depends jointly on their molecular identity and packing, chemists have engineered crystal structures that are categorized into four main groups, as shown in Fig. 3 (no sharp borders separate them). Note that other structural arrangements, such as sandwich herringbone packing, also exist, but they are less often encountered (Desiraju & Gavezzotti, 1989). The key design concept for crystal structures is to maximize the dimensionality of charge transport. One-dimensional (1D) semiconductors,*i.e.* when charge transport is efficient only along one specific crystallographic orientation, perform less well than two-dimensional (2D) semiconductors, which are more resilient to defects and allow the delocalization of charge carriers over a larger number of molecules (Skabara *et al.*, 2013). Another important feature of the performance of organic devices is the thin film quality (Virkar *et al.*, 2010). In general, brick-wall and herringbone arrangements tend to yield better thin films made of plate-like crystals (Wang *et al.*, 2018). Materials chemists have mostly played with the size, shape and volume of electronically inert side groups for reaching the desired 2D charge transport inherent in herringbone and brick-wall arrangements, as illustrated in Figs. 3(*a*) and 3(*d*), respectively (Wang *et al.*, 2018; Takimiya *et al.*, 2021). This is probably best illustrated by the TIPS-PEN and diF-TES-ADT cases (see Fig. 1). Both molecules form p-type semiconductors because they preferentially transport h^+ over e^-. The steric demand of the inert triisopropylsilylethynyl side groups of TIPS-PEN allows the positioning of the pentacene core in a brick-wall arrangement that is the most favourable for charge transport because h^+ can move along several pathways. Smaller or larger side groups fail to provide the necessary bulkiness for reaching the desired brick-wall arrangement (Anthony *et al.*, 2001). The molecular design is even more elaborate for diF-TES-ADT, for which the best packing is reached through the steric demand of the triethylsilylethynyl side groups, *i.e.* slightly less than for TIPS-PEN, because the antradithiophene core has a lower volume than the pentacene core, but also *via* attractive interactions between the F and S atoms. Such precise molecular engineering work would have simply been impossible without the wealth of information provided by the solution of crystal structures (Subramanian *et al.*, 2008). The same concept of optimizing crystal packing by side groups also applies to C8-DNTT and MT-Pyrene (Takimiya *et al.*, 2011, 2021). A slightly different approach consists in varying the position and number of substituents on π-conjugated cores, as illustrated in Fig. 4 for TCNQ, F2-TCNQ and F4-TCNQ. For these compounds also, the crystal structures have been essential in understanding why F2-TCNQ stands out as an exceptional n-type semiconductor, preferentially transporting e^- over h^+, whereas TCNQ and F4-TCNQ perform rather poorly (Krupskaya*et al.*, 2015; Shukla *et al.*, 2019). The F2-TCNQ case shows that crystal structure elucidation enables much more than simply a discussion of packing. It allows an investigation of the physics of charge transport in organic semiconductors (Chernyshov *et al.*, 2017; Sosorev, 2017; Ji *et al.*, 2018). The next two sections with discuss polymorphism, which is the rival of crystal structure engineering.

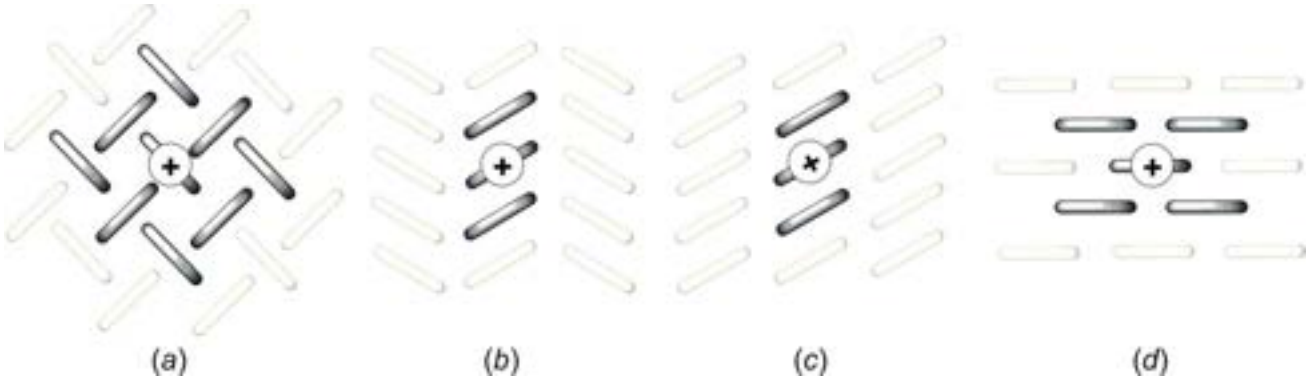


Figure 3. Schematic illustration of the most encountered crystalline packing motifs of molecular semiconductors. The molecules bearing a plus (+) sign and their first neighbours are strongly connected electronically and are represented in dark grey. (*a*) The herringbone arrangement with charge transport dominated by edge-to-face interactions, (*b*) slipped π-stacking, (*c*) slipped-stack packing and (*d*) a brick-wall arrangement.

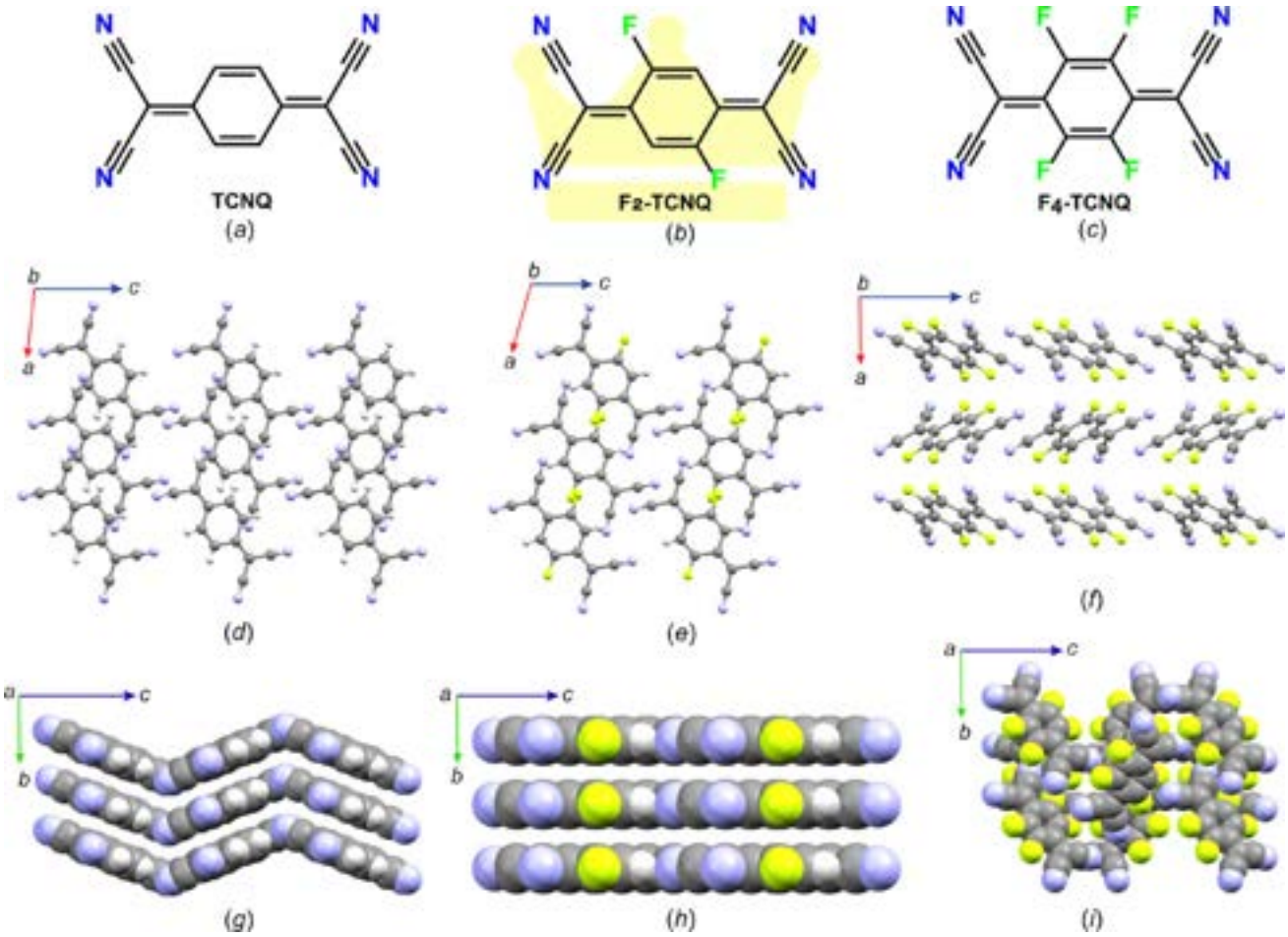
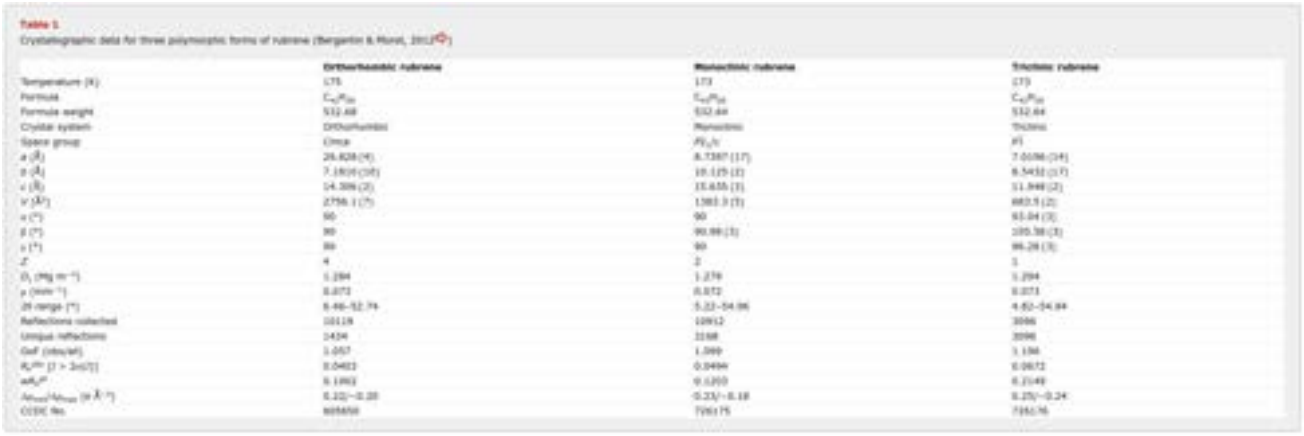


Figure 4. The molecular structures and a comparison of the crystallographic packing in the TCNQ family for (*a*) TCNQ, (*b*) F2-TCNQ and (*c*) F4-TCNQ. The molecular packing viewed along different crystallographic directions for (*d*)/(*g*) TCNQ, (*e*)/(*h*) F2-TCNQ and (*f*)/(*i*) F4-TCNQ. Note that F2-TCNQ has the superior transporting nature [highlighted by a coloured crown in the background in part (*b*)] within the family.

5. Polymorphism and charge transport

Polymorphism, defined as the occurrence of more than one crystal structure for a given molecule, is very common among organic compounds (Braga *et al.*, 2010; Lecomte, 2021); organic semiconductors are no exception. Polymorphism offers the opportunity to study the influence of molecular packing in a crystal on charge transport for exactly the same organic semiconductor (Chung & Diao, 2016; Riera-Galindo *et al.*, 2018; Gentili *et al.*, 2019). In any case, crystal structures are of the upmost importance, as illustrated for the emblematic case of rubrene, for which three crystallographic forms are known (see Table 1). Only one of the three, *i.e.* orthorhombic rubrene, gives rise to a substantial charge carrier mobility value, on the order of 20 $cm^2\ V^{-1}\ s^{-1}$, illustrating once more the crucial importance of crystal structures on charge transport (da Silva Filho *et al.*, 2005; Jurchescu *et al.*, 2006; Bergantin & Moret, 2012; McGarry *et al.*, 2013; Hathwar *et al.*, 2015; Ren *et al.*, 2017*b*). Interestingly, the crystal structures and charge-transport properties have also been determined for the isotopically substituted rubrene-d_{28} and the fully substituted ^{13}C-rubrene (Xie *et al.*, 2013; Ren *et al.*, 2017*a*). Polymorphism impacts also the properties of numerous other semiconductors, notably TIPS-PEN (Diao *et al.*, 2014*a*) and is widely considered as a phenomenon occurring in bulk. However, the presence of a substrate surface during the crystallization process has to be taken into account, as discussed below.



6. Polymorphism at surfaces and interfaces

One peculiarity of charge transport in organic semiconductors is that it takes place at the interface with a flat and impenetrable dielectric layer in the case of thin film transistors (Schweicher *et al.*, 2020). Such a rigid wall positions the centre of mass of the molecules at a given distance and, consequently, molecules adopt crystal motifs that differ from their bulk crystal structures (Jones *et al.*, 2016). A 2D confinement of the molecular packing with the substrate surface contributes to the formation of polymorphs (Diao *et al.*, 2014*a*; Giri *et al.*, 2014; Jiang & Ward, 2014; Meldrum & O'Shaughnessy, 2020; de Oliveira Martins *et al.*, 2022; Fellah *et al.*, 2022). Importantly, substrate-induced polymorphism is not caused by epitaxy because it occurs on flat and unstructured substrates (Schweicher *et al.*, 2020).

Substrate-induced polymorphism is not restricted to organic semiconductors but tends to occur more for them than for other molecules (*e.g.* pharmaceutical compounds) (Simões *et al.*, 2018; Braun *et al.*, 2019). Two reasons can be invoked to explain this observation. On the one hand, organic semiconductors are often high aspect ratio molecules forming rather elongated unit cells for which one lattice parameter is greater than the other two. Consequently, one face of the unit cell has a considerably smaller area than the others and thus a lower surface tension than the others (Drummy & Martin, 2005). The inter-facial tension with the dielectric layer is therefore considerably decreased if the unit cell stands on its smaller area face, causing a preferential orientation that constitutes a second structural constraint ruling substrate-induced polymorphism. Molecules which exhibit a more globular shape, resulting in unit cells for which the faces have rather comparable areas, present less often a preferential orientation. On the other hand, organic semiconductors, by virtue of their conjugated π-systems, are generally more rigid and more symmetrical than general molecules. Another reason is that organic semiconductor molecules have less directional bonds since they are generally devoid of hydrogen bonds and strong dipoles (Sutton *et al.*, 2016). The geometrical requirement to position their molecular centre at a given distance from the rigid wall (*e.g.* the substrate surface) can thus more easily relax by adopting other conformations (Aliaga-Gosalvez *et al.*, 2019; Simbrunner *et al.*, 2021). A further feature is that the molecular packing is restricted by the rigid wall, which also induces polymorphism within thin films (Resel *et al.*, 2018; Bedoya-Martínez *et al.*, 2017). Considerable system-to-system variations are observed, which holds generally true for crystalline molecular systems. In most cases, the substrate-induced phases are observed as being metastable (Wedl *et al.*, 2012; Jones *et al.*, 2016).

A quite illustrative example is given by pentacene (Fig. 5). A new polymorph was observed within thin films prepared for transistor applications (Dimitrakopoulos *et al.*, 1996). It took more than a decade until the crystal structure of the substrate-induced phase could be solved (Nabok *et al.*, 2007; Schiefer *et al.*, 2007; Yoshida *et al.*, 2007). In the meantime, crystal structure solution protocols have been developed for substrate-induced polymorphs, a combined experimental/theoretical approach is used based on grazing incidence X-ray diffraction (GIXD) and on molecular dynamics (MD) calculations and density functional theory (DFT) (Werzer *et al.*, 2024; Lercher *et al.*, 2015; Jones *et al.*, 2017). It is also worth discussing the consequences of substrate-induced polymorphism on nucleation that extends well beyond the restricted case of organic semiconductors. It is generally admitted that homogeneous nucleation

(high energy barrier) is rare and that heterogeneous nucleation (low energy barrier) is definitively more common. This is evidenced by the ratio of crystallization to melting temperature (T_c/T_m), which is close to unity, as routinely determined by differential scanning calorimetry (DSC) (Jackson, 1965). When substrate-induced polymorphs are present, the simple picture of the decreased energy barrier of the bulk phase due to the catalytic role of the substrate breaks down. In a first stage, heterogeneous nucleation implies the substrate-induced polymorphs and not the bulk phase. In a second stage, the latter undergoes cross-nucleation on the former. The twofold nucleation process involves two energy barriers instead of one. Two competing interactions are important at the initial state of crystallization: the molecule–substrate interaction and the molecule–molecule interaction (Winkler, 2016). A strong molecule–substrate interaction can force the molecules into a different orientation relative to the substrate surface, which is not the case when molecule–molecule interactions dominate (Resel, 2008). Detailed thin film growth studies have been performed on pentacene deposited at various dielectrics (Pratontep *et al.*, 2004; Ruiz *et al.*, 2004; Luo *et al.*, 2003; Gundlach *et al.*, 1997, 1999; Dickey *et al.*, 2006; Lee *et al.*, 2007; Dinelli *et al.*, 2004; Mannsfeld *et al.*, 2009). The nucleation is associated with the formation of monolayers which are assembled by upright standing molecules; subsequently, the first monolayer acts as a crystalline template for subsequent thin film growth (Pratontep *et al.*, 2004; Mannsfeld *et al.*, 2009). In the multilayer regime, the formation of islands is observed, so that layer-plus-island (Stranski–Krastanov) is present for the pentacene thin film crystallization (Ruiz *et al.*, 2004; Luo *et al.*, 2003). Please note that considerable differences can be observed between the crystallographic order of the first molecular layer at the substrate surface and the packing of the molecules in the subsequent layer grown upon this first layer (Novák *et al.*, 2011; Hofer *et al.*, 2021).

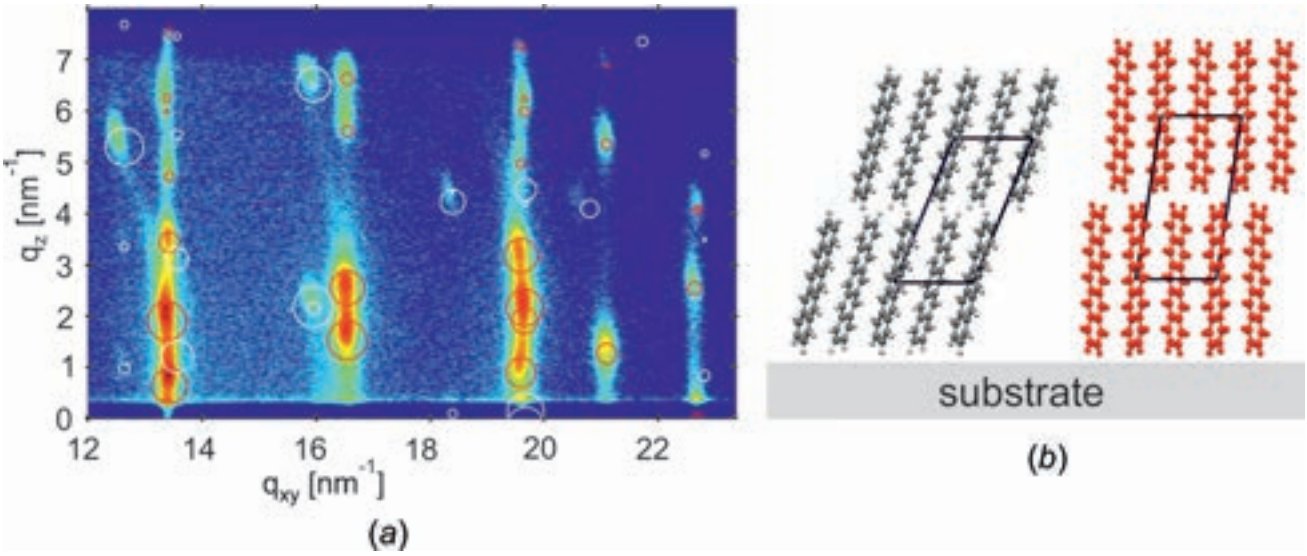


Figure 5. (*a*) X-ray diffraction pattern represented in a reciprocal space map of a 50 nm thick pentacene thin film with two concomitant polymorphs. The substrate-induced (or thin film) phase and the Campbell phase are identified by red and white circles, respectively, representing the peak patterns calculated on the basis of their crystal structures. (Reproduced with permission by Springer Nature.) (*b*) Orientations of the pentacene molecules relative to the substrate surface for the Campbell phase (gray atoms) and for the substrate-induced phase (red atoms).

For the sake of completeness, one must mention crystal structure predictions by advanced computational methods. They constitute a formidable tool to guide the search for polymorphs, but also to rationalize the stability order of crystal forms from first principles (Woodley & Catlow, 2008; Price, 2014; Hoja *et al.*, 2019; Firaha *et al.*, 2023; Beran, 2023). Most studies have been dedicated to active pharmaceutical ingredients (APIs), although there are some reports on organic semiconductors (Sánchez-Carrera *et al.*, 2010; Sokolov *et al.*, 2011; Obata *et al.*, 2013; Della Valle *et al.*, 2008). The field has recently been reviewed but evolves rapidly (Bhat *et al.*, 2023*a*). A hierarchy of machine-learning approaches are currently used to accelerate the development of organic semiconductors by predicting their structures and properties (Bhat *et al.*, 2023*b*). However, transport properties are not only ruled by crystal structures, but also by the presence of defects and impurities that it is not possible to compute.

7. Lattice dynamics

Crystals of organic semiconductors not only have a large variety of structures but also some rich phonon dynamics that relate to structure and symmetry. Local (intramolecular) and nonlocal (intermolecular) phonon modes must be differentiated (Coropceanu *et al.*, 2007). Intramolecular phonon modes, observed above 150 cm^{-1}, contribute to the reorganization energy (λ) associated with electron transfer and ranges from 100 to 800 meV (Tant *et al.*, 2005). Intermolecular phonon modes appear in the 10 to 150 cm^{-1} spectral window (Asher *et al.*, 2022; Ferrari *et al.*, 2023; Salzillo & Brillante, 2022). They cause the localization of charge carriers (so-called electron phonon couplings) over one to several molecules, thus reducing drastically the charge carrier mobility values. It is only recently that thermal fluctuations have been recognized as the bottleneck limiting the performance of organic semiconductors due to the resulting dynamic disorder (Fratini *et al.*, 2016, 2017; Giannini *et al.*, 2023; Giannini & Blumberger, 2022). But not all phonon modes are equally important. Some `killer' modes, those presenting a large amplitude coupled with a large electron–phonon coupling value, occurring at low frequency, give rise to larger fluctuations of transfer integrals than others, as illustrated in Fig. 6 in the case of DNTT and C8-DNTT-C8 (Schweicher *et al.*, 2019; Stoeckel *et al.*, 2021; Banks *et al.*, 2023). Intermolecular phonon modes are essentially probed by inelastic neutron scattering or by any low-frequency vibrational spectroscopy technique (Raman, THz). Data analysis implies knowledge of the crystal structure to fit the vibrational spectra and extract phonon modes. Recent results on a series of organic semiconductors show that the harmonic vibration potential hypothesis breaks down and that intermolecular phonon modes interact (Asher *et al.*, 2022; Benshalom *et al.*, 2023). This brief discussion of crystal dynamics illustrates that crystal structure elucidation is again an enabling step for further physical studies. Intra- and intermolecular vibrations not only shape charge-transport physics, but also trigger phase transitions, as will be discussed in the next section.

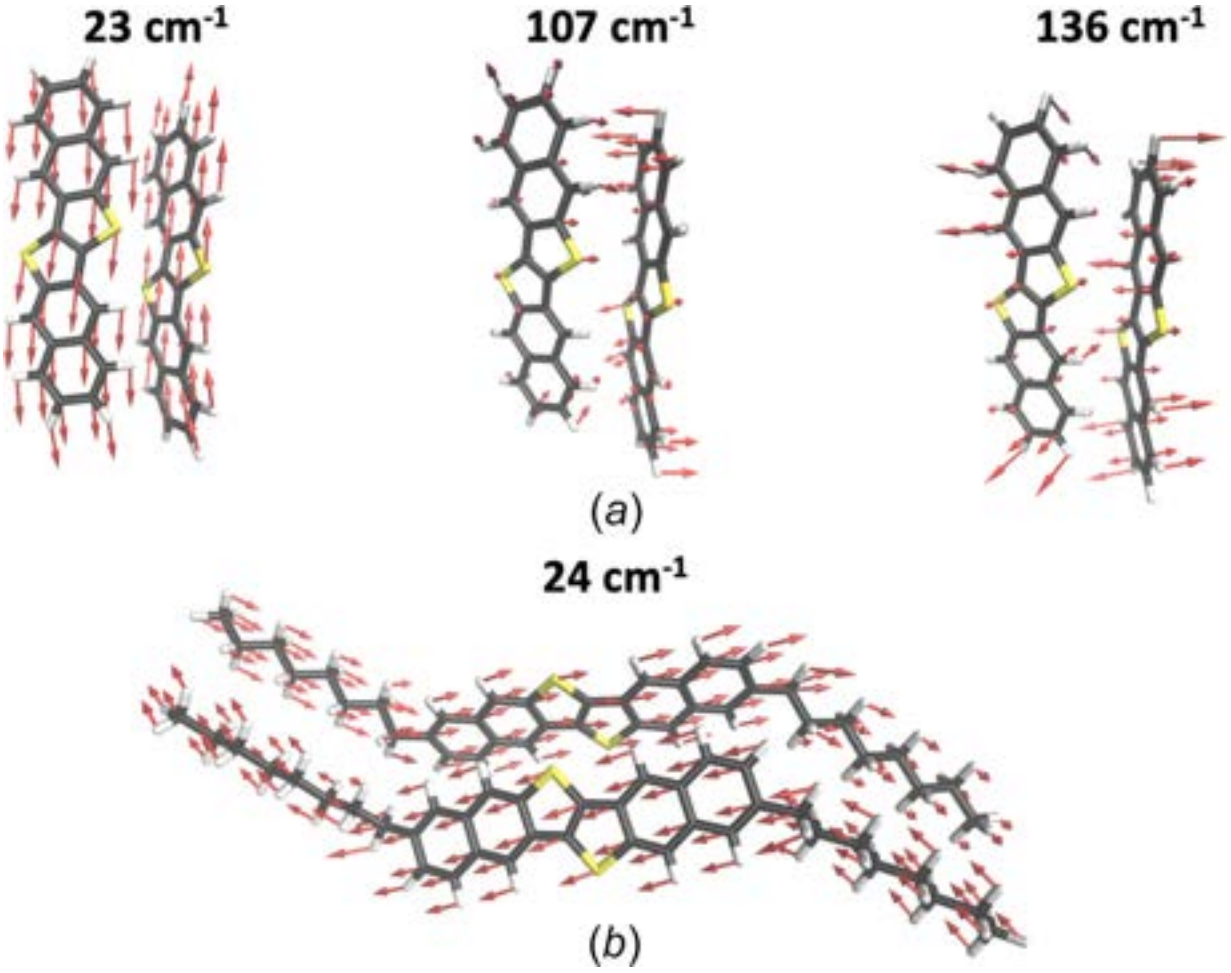


Figure 6. Relative displacements of neighbouring molecules associated with the most detrimental phonon modes in (*a*) DNTT (23, 107 and 136 cm^{-1}) and (*b*) C8-DNTT-C8 (24 cm^{-1}). [Adapted from Schweicher *et al.* (2019).]

8. Crystal-to-crystal transitions

Polymorphs are most often obtained from an amorphous phase, either a gas phase, a solution or a melt state. But polymorphs transform also into each other by crystal-to-crystal phase transitions, that can be either reversible or irreversible, and that are strongly kinetically hindered. In most cases, the crystal structures of two polymorphs are structurally too different to allow a direct interconversion without passing through an intermediate disordered phase (Chung *et al.*, 2019, 2020). A few exceptions exist, notably the case of ditBu-BTBT, which exhibits both a low- and a high-temperature form that interconvert between 340 and 350 K by a concerted mechanism reminiscent of Martensitic transitions. When inspecting both crystal structures, one immediately notices their structural similarity, except for the *tert*-butyl side groups that present some disorder (Fig. 7) (Chung *et al.*, 2018*a*,*b*; Park & Diao, 2020). Compelling Raman spectroscopic evidence corroborates that the phase transition is triggered by partial rotation of the *tert*-butyl side groups and that this specific phonon mode drives the phase (Asher *et al.*, 2022, 2023). In some cases, solvent vapour annealing (SVA) – a post deposition treatment of thin films – is used to trigger phase changes and, in most cases, transition towards the thermodynamic equilibrium state is initiated (Jones *et al.*, 2015). But solvent vapour annealing can also induce a substantial improvement of structural order in terms of thin film morphology and crystalline properties (Lee *et al.*, 2007; Dickey *et al.*, 2006). Crystal-to-crystal phase transitions are much more than laboratory curiosities because they allow the identification of the phase-transition mechanisms that cause them, thanks to the availability of the crystal structures. This conclusion can be extended to the most ordered liquid crystal phases, such as the smectic E phase (Ferrari *et al.*, 2023). The dynamics of crystals is gaining an increasing importance because it contributes to the mechanical and electronic properties, probably as much as the structures (Davies *et al.*, 2023; Awad *et al.*, 2023; Das *et al.*, 2020).

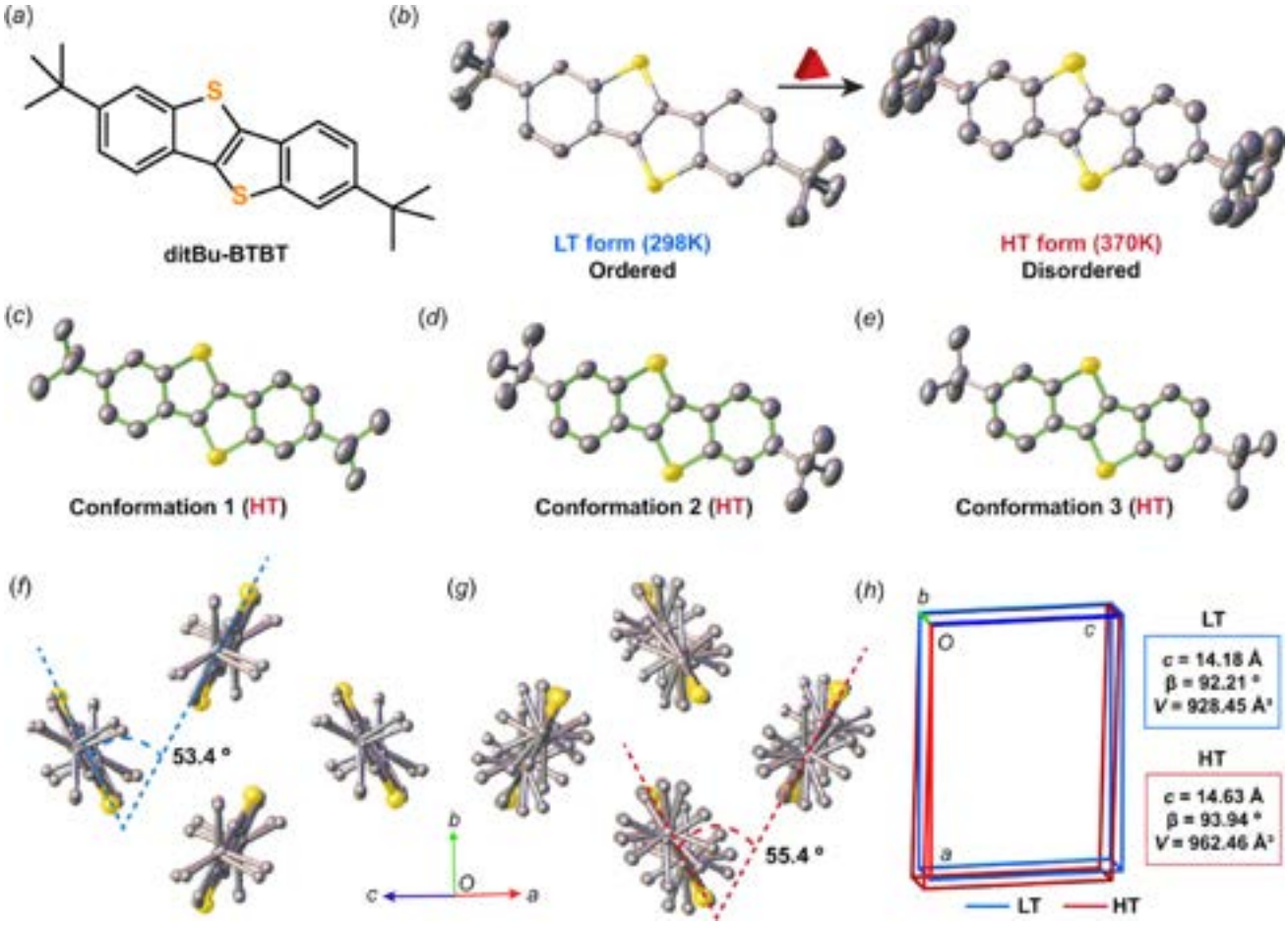


Figure 7. Single-crystal-to-single-crystal polymorphic transition in ditBu-BTBT from the LT to the HT form, showing (*a*) the molecular structure of ditBu-BTBT, (*b*) the order-to-disorder transition of the side –ditBu groups and (*b*)/(*d*)/(*e*) the three isolated conformations of the HT disordered phase. (*f*) The change in the herringbone dihedral angle in the (*f*) LT and (*g*) HT forms. H atoms have been omitted for clarity and better presentation. (*h*) Overlay of the unit cells and significant changes of the unit-cell parameters before and after the polymorphic phase transition (Chung *et al.*, 2018*a*).

9. Conclusions and perspectives

This review presents a large portfolio of research activities that would not have been possible without initial crystal structure elucidation. Novel molecular materials design, supramolecular interaction studies, crystal engineering, polymorphism studies, spectroscopic analysis, lattice dynamics studies and charge-transport physics heavily rely on crystal structures, in bulk, but also at the interface with a substrate that acts as a rigid wall imposing geometrical constraints causing the occurrence of some substrate-induced phases. The latter requires the development of new crystal structure elucidation methods based on GIXD data obtained at synchrotron facilities. One future challenge deals with the control of nucleation and growth through better-defined crystallization conditions, implying also time-resolved structural elucidation to monitor the formation of transient phases. Structural elucidation from bulk single crystals is and will continue to play a pivotal role, but there is also a demand for the development of time- and space-resolved X-ray diffraction methods.

Acknowledgements

The authors thank the Belgian National Fund for Scientific Research (FNRS) for financial support. Financial support from ULB and the French Community of Belgium through the concerted research action ARC SADI (No. 20061) is also gratefully acknowledged. GS is an FNRS Research Associate and acknowledges financial support from the FNRS, Francqui Foundation (Francqui Start-Up Grant) and Wiener-Anspach Foundation (FWA, ZT1 research project).

Funding information

Funding for this research was provided by: Fonds De La Recherche Scientifique – FNRS (project Nos. PHASETRANS BTBT PDR 2.4565.11, PDR T.0058.14, Pi-Fast PDR T.0072.18, PICHIR PDR T.0094.2, DIFFRA GEQ U.G001.19, POLYP EQP U.N032.21F, POLYP2 EQP U.N03323F, CHIRI CDR J. 0088.24, CISSCA WEAVE T.W.023.23, WEL-T-CR-2023 A-04, 2Dto3D EOS 30489208 and CHISUB EOS 40007495; COHERENCE2 project No. F.4536.23 to G. Schweicher).

References

Aliaga–Gosalvez, M. J., Demitri, N., Dohr, M., Roldao, J. C., Park, S. K., Oh, S., Varghese, S., Park, S. Y., Olivier, Y., Milián–Medina, B., Resel, R. & Gierschner, J. (2019). *Adv. Opt. Mater.* **7**, 1900749.

Altoe, V., Martin, F., Katan, A., Salmeron, M. & Aloni, S. (2012). *Nano Lett.* **12**, 1295–1299.

Anthony, J. E. (2006). *Chem. Rev.* **106**, 5028–5048.

Anthony, J. E. (2008). *Angew. Chem. Int. Ed.* **47**, 452–483.

Anthony, J. E., Brooks, J. S., Eaton, D. L. & Parkin, S. R. (2001). *J. Am. Chem. Soc.* **123**, 9482–9483.

Asher, M., Bardini, M., Catalano, L., Jouclas, R., Schweicher, G., Liu, J., Korobko, R., Cohen, A., Geerts, Y., Beljonne, D. & Yaffe, O. (2023). *J. Phys. Chem. Lett.* **14**, 1570–1577.

Asher, M., Jouclas, R., Bardini, M., Diskin-Posner, Y., Kahn, N., Korobko, R., Kennedy, A. R., Silva de Moraes, L., Schweicher, G. & Liu, J. (2022). *ACS Mater. Au*, **2**, 699–708.

Awad, W. M., Davies, D. W., Kitagawa, D., Mahmoud Halabi, J., Al-Handawi, M. B., Tahir, I., Tong, F., Campillo-Alvarado, G., Shtukenberg, A. G., Alkhidir, T., Hagiwara, Y., Almehairbi, M., Lan, L., Hasebe, S., Karothu, D. P., Mohamed, S., Koshima, H., Kobatake, S., Diao, Y., Chandrasekar, R., Zhang, H., Sun, C. C., Bardeen, C., Al-Kaysi, R. O., Kahr, B. & Naumov, P. (2023). *Chem. Soc. Rev.* **52**, 3098–3169.

Banks, P. A., D'Avino, G., Schweicher, G., Armstrong, J., Ruzié, C., Chung, J. W., Park, J. I., Sawabe, C., Okamoto, T., Takeya, J., Sirringhaus, H. & Ruggiero, M. T. (2023). *Adv. Funct. Mater.* **33**, 2303701.

Bedoya-Martínez, N., Schrode, B., Jones, A. O., Salzillo, T., Ruzié, C., Demitri, N., Geerts, Y. H., Venuti, E., Della Valle, R. G., Zojer, E. & Resel, R. (2017). *J. Phys. Chem. Lett.* **8**, 3690–3695.

Benshalom, N., Asher, M., Jouclas, R., Korobko, R., Schweicher, G., Liu, J., Geerts, Y., Hellman, O. & Yaffe, O. (2023). *J. Phys. Chem. C*, **127**, 18099–18106.

Beran, G. J. (2023). *Chem. Sci.* **14**, 13290–13312.

Bergantin, S. & Moret, M. (2012). *Cryst. Growth Des.* **12**, 6035–6041.

Bhat, V., Callaway, C. P. & Risko, C. (2023*a*). *Chem. Rev.* **123**, 7498–7547.

Bhat, V., Sornberger, P., Pokuri, B. S. S., Duke, R., Ganapathysubramanian, B. & Risko, C. (2023*b*). *Chem. Sci.* **14**, 203–213.

Braga, D., Grepioni, F. & Maini, L. (2010). *Chem. Commun.* **46**, 6232–6242.

Braun, D. E., Rivalta, A., Giunchi, A., Bedoya-Martinez, N., Schrode, B., Venuti, E., Della Valle, R. G. & Werzer, O. (2019). *Cryst. Growth Des.* **19**, 6058–6066.

Brázda, P., Palatinus, L. & Babor, M. (2019). *Science*, **364**, 667–669.

Brédas, J. L., Calbert, J. P., da Silva Filho, D. & Cornil, J. (2002). *Proc. Natl Acad. Sci. USA*, **99**, 5804–5809.

Chernyshov, I. Y., Vener, M. V., Feldman, E. V., Paraschuk, D. Y. & Sosorev, A. Y. (2017). *J. Phys. Chem. Lett.* **8**, 2875–2880.

Chung, H., Chen, S., Patel, B., Garbay, G., Geerts, Y. H. & Diao, Y. (2020). *Cryst. Growth Des.* **20**, 1646–1654.

Chung, H., Chen, S., Sengar, N., Davies, D. W., Garbay, G., Geerts, Y. H., Clancy, P. & Diao, Y. (2019). *Chem. Mater.* **31**, 9115–9126.

Chung, H. & Diao, Y. (2016). *J. Mater. Chem. C.* **4**, 3915–3933.

Chung, H., Dudenko, D., Zhang, F., D'Avino, G., Ruzié, C., Richard, A., Schweicher, G., Cornil, J., Beljonne, D., Geerts, Y. & Diao, Y. (2018*a*). *Nat. Commun.* **9**, 278.

Chung, H., Ruzié, C., Geerts, Y. & Diao, Y. (2018*b*). *Cryst. Growth Des.* **18**, 4245–4251.

Coropceanu, V., Cornil, J., da Silva Filho, D. A., Olivier, Y., Silbey, R. & Brédas, J. L. (2007). *Chem. Rev.* **107**, 926–952.

Das, S., Mondal, A. & Reddy, C. M. (2020). *Chem. Soc. Rev.* **49**, 8878–8896.

Davies, D. W., Seo, B., Park, S. K., Shiring, S. B., Chung, H., Kafle, P., Yuan, D., Strzalka, J. W., Weber, R., Zhu, X., Savoie, B. M. & Diao, Y. (2023). *Nat. Commun.* **14**, 1304.

Della Valle, R. G., Venuti, E., Brillante, A. & Girlando, A. (2008). *J. Phys. Chem. A*, **112**, 1085–1089.

Desiraju, G. R. & Gavezzotti, A. (1989). *Acta Cryst.* B**45**, 473–482.

Diao, Y., Lenn, K. M., Lee, W.-Y., Blood-Forsythe, M. A., Xu, J., Mao, Y., Kim, Y., Reinspach, J. A., Park, S., Aspuru-Guzik, A., Xue, G., Clancy, P., Bao, Z. & Mannsfeld, S. C. B. (2014*a*). *J. Am. Chem. Soc.* **136**, 17046–17057.

Diao, Y., Shaw, L., Bao, Z. & Mannsfeld, S. C. (2014*b*). *Energy Environ. Sci.* **7**, 2145–2159.

Dickey, K. C., Anthony, J. E. & Loo, Y. L. (2006). *Adv. Mater.* **18**, 1721–1726.

Dimitrakopoulos, C. D., Brown, A. R. & Pomp, A. (1996). *J. Appl. Phys.* **80**, 2501–2508.

Dinelli, F., Murgia, M., Levy, P., Cavallini, M., Biscarini, F. & de Leeuw, D. M. (2004). *Phys. Rev. Lett.* **92**, 116802.

Ding, L., Yu, Z.-D., Wang, X.-Y., Yao, Z.-F., Lu, Y., Yang, C.-Y., Wang, J.-Y. & Pei, J. (2023). *Chem. Rev.* **123**, 7421–7497.

Drummy, L. F. & Martin, D. C. (2005). *Adv. Mater.* **17**, 903–907.

Fellah, N., Tahsin, L., Zhang, C. J., Kahr, B., Ward, M. D. & Shtukenberg, A. G. (2022). *Cryst. Growth Des.* **22**, 7527–7543.

Ferrari, E., Pandolfi, L., Schweicher, G., Geerts, Y., Salzillo, T., Masino, M. & Venuti, E. (2023). *Chem. Mater.* **35**, 5777–5783.

Firaha, D., Liu, Y. M., van de Streek, J., Sasikumar, K., Dietrich, H., Helfferich, J., Aerts, L., Braun, D. E., Broo, A., DiPasquale, A. G., Lee, A. Y., Le Meur, S., Nilsson Lill, S. O., Lunsmann, W. J., Mattei, A., Muglia, P., Putra, O. D., Raoui, M., Reutzel-Edens, S. M., Rome, S., Sheikh, A. Y., Tkatchenko, A., Woollam, G. R. & Neumann, M. A. (2023). *Nature*, **623**, 324–328.

Fraboni, B., Fraleoni–Morgera, A., Geerts, Y., Morpurgo, A. & Podzorov, V. (2016). *Adv. Funct. Mater.* **26**, 2229–2232.

Fratini, S., Ciuchi, S., Mayou, D., de Laissardière, G. T. & Troisi, A. (2017). *Nat. Mater.* **16**, 998–1002.

Fratini, S., Mayou, D. & Ciuchi, S. (2016). *Adv. Funct. Mater.* **26**, 2292–2315.

Fratini, S., Nikolka, M., Salleo, A., Schweicher, G. & Sirringhaus, H. (2020). *Nat. Mater.* **19**, 491–502.

Gentili, D., Gazzano, M., Melucci, M., Jones, D. & Cavallini, M. (2019). *Chem. Soc. Rev.* **48**, 2502–2517.

Gershenson, M., Podzorov, V. & Morpurgo, A. (2006). *Rev. Mod. Phys.* **78**, 973–989.

Giannini, S. & Blumberger, J. (2022). *Acc. Chem. Res.* **55**, 819–830.

Giannini, S., Di Virgilio, L., Bardini, M., Hausch, J., Geuchies, J. J., Zheng, W., Volpi, M., Elsner, J., Broch, K., Geerts, Y. H., Schreiber, F., Schweicher, G., Wang, H. I., Blumberger, J., Bonn, M. & Beljonne, D. (2023). *Nat. Mater.* **22**, 1361–1369.

Giri, G., Li, R., Smilgies, D.-M., Li, E. Q., Diao, Y., Lenn, K. M., Chiu, M., Lin, D. W., Allen, R., Reinspach, J., Mannsfeld, S. C. B., Thoroddsen, S. T., Clancy, P., Bao, Z. & Amassian, A. (2014). *Nat. Commun.* **5**, 3573.

Gruene, T., Holstein, J. J., Clever, G. H. & Keppler, B. (2021). *Nat. Rev. Chem.* **5**, 660–668.

Gundlach, D., Jackson, T., Schlom, D. & Nelson, S. (1999). *Appl. Phys. Lett.* **74**, 3302–3304.

Gundlach, D. J., Lin, Y.-Y., Jackson, T. N., Nelson, S. & Schlom, D. (1997). *IEEE Electron Device Lett.* **18**, 87–89.

Hathwar, V. R., Sist, M., Jørgensen, M. R. V., Mamakhel, A. H., Wang, X., Hoffmann, C. M., Sugimoto, K., Overgaard, J. & Iversen, B. B. (2015). *IUCrJ*, **2**, 563–574.

He, T., Wu, Y., D'Avino, G., Schmidt, E., Stolte, M., Cornil, J., Beljonne, D., Ruden, P. P., Würthner, F. & Frisbie, C. D. (2018). *Nat. Commun.* **9**, 2141.

Hofer, S., Hofer, A., Simbrunner, J., Ramsey, M., Sterrer, M., Sanzone, A., Beverina, L., Geerts, Y. & Resel, R. (2021). *J. Phys. Chem. C*, **125**, 28039–28047.

Hoja, J., Ko, H.-Y., Neumann, M. A., Car, R., DiStasio, R. A. Jr & Tkatchenko, A. (2019). *Sci. Adv.* **5**, eaau3338.

Iino, H., Usui, T. & Hanna, J. (2015). *Nat. Commun.* **6**, 6828.

Illig, S., Eggeman, A. S., Troisi, A., Jiang, L., Warwick, C., Nikolka, M., Schweicher, G., Yeates, S. G., Henri Geerts, Y., Anthony, J. E. & Sirringhaus, H. (2016). *Nat. Commun.* **7**, 10736.

Israelachvili, J. N. (2011). In *Intermolecular and Surface Forces*. Cambridge, MA: Academic Press.

Jackson, K. A. (1965). *Ind. Eng. Chem.* **57**, 28–32.

Ji, L.-F., Fan, J.-X., Zhang, S.-F. & Ren, A.-M. (2018). *Phys. Chem. Chem. Phys.* **20**, 3784–3794.

Jiang, H. & Hu, W. (2020). *Angew. Chem. Int. Ed.* **59**, 1408–1428.

Jiang, H. & Kloc, C. (2013). *MRS Bull.* **38**, 28–33.

Jiang, Q. & Ward, M. D. (2014). *Chem. Soc. Rev.* **43**, 2066–2079.

Jones, A. O., Geerts, Y. H., Karpinska, J., Kennedy, A. R., Resel, R., Röthel, C., Ruzié, C., Werzer, O. & Sferrazza, M. (2015). *Appl. Mater. Interfaces*, **7**, 1868–1873.

Jones, A. O. F., Chattopadhyay, B., Geerts, Y. H. & Resel, R. (2016). *Adv. Funct. Mater.* **26**, 2233–2255.

Jones, A. O. F., Röthel, C., Lassnig, R., Bedoya-Martínez, O. N., Christian, P., Salzmann, I., Kunert, B., Winkler, A. & Resel, R. (2017). *CrystEngComm*, **19**, 1902–1911.

Jouclas, R., Liu, J., Volpi, M., Silva de Moraes, L., Garbay, G., McIntosh, N., Bardini, M., Lemaur, V., Vercouter, A., Gatsios, C., Modesti, F., Turetta, N., Beljonne, D., Cornil, J., Kennedy, A. R., Koch, N., Erk, P., Samorì, P., Schweicher, G. & Geerts, Y. H. (2022). *Adv. Sci.* **9**, 2105674.

Jurchescu, O. D., Meetsma, A. & Palstra, T. T. M. (2006). *Acta Cryst.* B**62**, 330–334.

Kang, M. J., Doi, I., Mori, H., Miyazaki, E., Takimiya, K., Ikeda, M. & Kuwabara, H. (2011). *Adv. Mater.* **23**, 1222–1225.

Krupskaya, Y., Gibertini, M., Marzari, N. & Morpurgo, A. F. (2015). *Adv. Mater.* **27**, 2453–2458.

Lecomte, C. (2021). *Acta Cryst.* B**77**, 184–185.

Lee, W. H., Kim, D. H., Cho, J. H., Jang, Y., Lim, J. A., Kwak, D. & Cho, K. (2007). *Appl. Phys. Lett.* **91**, 092105.

Lee, A. van der, Roche, G. H., Wantz, G., Moreau, J. J., Dautel, O. J. & Filhol, J.-S. (2018). *Chem. Sci.* **9**, 3948–3956.

Lercher, C., Röthel, C., Roscioni, O. M., Geerts, Y. H., Shen, Q., Teichert, C., Fischer, R., Leising, G., Sferrazza, M., Gbabode, G. & Resel, R. (2015). *Chem. Phys. Lett.* **630**, 12–17.

Li, Y., Coropceanu, V. & Brédas, J. (2012). *J. Phys. Chem. Lett.* **3**, 3325–3329.

Li, Y., Coropceanu, V. & Brédas, J. L. (2013). *J. Phys. Chem. Lett.* **4**, 950.

Liu, C., Minari, T., Lu, X., Kumatani, A., Takimiya, K. & Tsukagoshi, K. (2011). *Adv. Mater.* **23**, 523–526.

Luo, Y., Wang, G., Theobald, J. A. & Beton, P. H. (2003). *Surf. Sci.* **537**, 241–246.

Mannsfeld, S. C., Virkar, A., Reese, C., Toney, M. F. & Bao, Z. (2009). *Adv. Mater.* **21**, 2294–2298.

Mas-Torrent, M. & Rovira, C. (2011). *Chem. Rev.* **111**, 4833–4856.

McGarry, K. A., Xie, W., Sutton, C., Risko, C., Wu, Y., Young, V. G. Jr, Brédas, J., Frisbie, C. D. & Douglas, C. J. (2013). *Chem. Mater.* **25**, 2254–2263.

Meldrum, F. C. & O'Shaughnessy, C. (2020). *Adv. Mater.* **32**, 2001068.

Menard, E., Podzorov, V., Hur, S. H., Gaur, A., Gershenson, M. E. & Rogers, J. A. (2004). *Adv. Mater.* **16**, 2097–2101.

Mitsui, C., Okamoto, T., Yamagishi, M., Tsurumi, J., Yoshimoto, K., Nakahara, K., Soeda, J., Hirose, Y., Sato, H., Yamano, A., Uemura, T. & Takeya, J. (2014). *Adv. Mater.* **26**, 4546–4551.

Nabok, D., Puschnig, P., Ambrosch-Draxl, C., Werzer, O., Resel, R. & Smilgies, D.-M. (2007). *Phys. Rev. B*, **76**, 235322.

Niebel, C., Kim, Y., Ruzié, C., Karpinska, J., Chattopadhyay, B., Schweicher, G., Richard, A., Lemaur, V., Olivier, Y., Cornil, J., Kennedy, A. R., Diao, Y., Lee, W., Mannsfeld, S., Bao, Z. & Geerts, Y. H. (2015). *J. Mater. Chem. C.* **3**, 674–685.

Novák, J., Oehzelt, M., Berkebile, S., Koini, M., Ules, T., Koller, G., Haber, T., Resel, R. & Ramsey, M. G. (2011). *Phys. Chem. Chem. Phys.* **13**, 14675–14684.

Obata, S., Miura, T. & Shimoi, Y. (2013). *Jpn J. Appl. Phys.* **53**, 01AD02.

Okamoto, T., Kumagai, S., Fukuzaki, E., Ishii, H., Watanabe, G., Niitsu, N., Annaka, T., Yamagishi, M., Tani, Y. & Sugiura, H. (2020). *Sci. Adv.* **6**, eaaz0632.

Oliveira Martins, I. de, Marin, F., Modena, E. & Maini, L. (2022). *Faraday Discuss.* **235**, 490–507.

Onwubiko, A., Yue, W., Jellett, C., Xiao, M., Chen, H.-Y., Ravva, M. K., Hanifi, D. A., Knall, A.-C., Purushothaman, B., Nikolka, M., Flores, J. C., Salleo, A., Bredas, J. L., Sirringhaus, H., Hayoz, P. & McCulloch, I. (2018). *Nat. Commun.* **9**, 416.

Ostroverkhova, O. (2016). *Chem. Rev.* **116**, 13279–13412.

Park, S. K. & Diao, Y. (2020). *Chem. Soc. Rev.* **49**, 8287–8314.

Pratontep, S., Brinkmann, M., Nüesch, F. & Zuppiroli, L. (2004). *Phys. Rev. B*, **69**, 165201.

Price, S. L. (2014). *Chem. Soc. Rev.* **43**, 2098–2111.

Ren, X., Bruzek, M. J., Hanifi, D. A., Schulzetenberg, A., Wu, Y., Kim, C.-H., Zhang, Z., Johns, J. E., Salleo, A., Fratini, S., Troisi, A., Douglas, C. J. & Frisbie, C. D. (2017*a*). *Adv. Elect Mater.* **3**, 1700018–1700024.

Ren, X., Schmidt, E., Walter, J., Ganguly, K., Leighton, C. & Frisbie, C. D. (2017*b*). *J. Phys. Chem. C*, **121**, 6540–6545.

Resel, R. (2008). *J. Phys. Condens. Matter*, **20**, 184009.

Resel, R., Jones, A. O. F., Schweicher, G., Fischer, R., Demitri, N. & Geerts, Y. H. (2018). *IUCrJ*, **5**, 304–308.

Riera-Galindo, S., Tamayo, A. & Mas-Torrent, M. (2018). *ACS Omega*, **3**, 2329–2339.

Rivnay, J., Mannsfeld, S. C., Miller, C. E., Salleo, A. & Toney, M. F. (2012). *Chem. Rev.* **112**, 5488–5519.

Ruiz, R., Choudhary, D., Nickel, B., Toccoli, T., Chang, K.-C., Mayer, A. C., Clancy, P., Blakely, J. M., Headrick, R. L., Iannotta, S. & Malliaras, G. G. (2004). *Chem. Mater.* **16**, 4497–4508.

Salzillo, T. & Brillante, A. (2022). *Adv. Mater. Interfaces*, **9**, 2200815.

Sánchez-Carrera, R. S., Atahan, S., Schrier, J. & Aspuru-Guzik, A. (2010). *J. Phys. Chem. C*, **114**, 2334–2340.

Sawatzki-Park, M., Wang, S.-J., Kleemann, H. & Leo, K. (2023). *Chem. Rev.* **123**, 8232–8250.

Schiefer, S., Huth, M., Dobrinevski, A. & Nickel, B. (2007). *J. Am. Chem. Soc.* **129**, 10316–10317.

Schweicher, G., D'Avino, G., Ruggiero, M. T., Harkin, D. J., Broch, K., Venkateshvaran, D., Liu, G., Richard, A., Ruzié, C., Armstrong, J., Kennedy, A. R., Shankland, K., Takimiya, K., Geerts, Y. H., Zeitler, J. A., Fratini, S. & Sirringhaus, H. (2019). *Adv. Mater.* **31**, 1902407.

Schweicher, G., Garbay, G., Jouclas, R., Vibert, F., Devaux, F. & Geerts, Y. H. (2020). *Adv. Mater.* **32**, 1905909.

Schweicher, G., Lemaur, V., Niebel, C., Ruzié, C., Diao, Y., Goto, O., Lee, W. Y., Kim, Y., Arlin, J. B., Karpinska, J., Kennedy, A. R., Parkin, S. R., Olivier, Y., Mannsfeld, S. C., Cornil, J., Geerts, Y. H. & Bao, Z. (2015). *Adv. Mater.* **27**, 3066–3072.

Schweicher, G., Olivier, Y., Lemaur, V. & Geerts, Y. H. (2014). *Isr. J. Chem.* **54**, 595–620.

Shukla, R., Ruzié, C., Schweicher, G., Kennedy, A. R., Geerts, Y. H., Chopra, D. & Chattopadhyay, B. (2019). *Acta Cryst.* B**75**, 71–78.

Silva Filho, D. da, Kim, E.-G. & Brédas, J. (2005). *Adv. Mater.* **17**, 1072–1076.

Simbrunner, J., Schrode, B., Hofer, S., Domke, J., Fritz, T., Forker, R. & Resel, R. (2021). *J. Phys. Chem. C*, **125**, 618–626.

Simões, R. G., Salzmann, I., Resel, R., Röthel, C. & Geerts, Y. H. (2018). *Cryst. Growth Des.* **18**, 4123–4129.

Skabara, P. J., Arlin, J. B. & Geerts, Y. H. (2013). *Adv. Mater.* **25**, 1948–1954.

Sokolov, A. N., Atahan-Evrenk, S., Mondal, R., Akkerman, H. B., Sánchez-Carrera, R. S., Granados-Focil, S., Schrier, J., Mannsfeld, S. C., Zoombelt, A. P., Bao, Z. & Aspuru-Guzik, A. (2011). *Nat. Commun.* **2**, 437.

Sosorev, A. Y. (2017). *Phys. Chem. Chem. Phys.* **19**, 25478–25486.

Spackman, M. A. (2013). *Phys. Scr.* **87**, 048103.

Spackman, M. A. & Jayatilaka, D. (2009). *CrystEngComm*, **11**, 19–32.

Spackman, M. A. & McKinnon, J. J. (2002). *CrystEngComm*, **4**, 378–392.

Stoeckel, M. A., Olivier, Y., Gobbi, M., Dudenko, D., Lemaur, V., Zbiri, M., Guilbert, A. A., D'Avino, G., Liscio, F., Migliori, A., Ortolani, L., Demitri, N., Jin, X., Jeong, Y., Liscio, A., Nardi, M., Pasquali, L., Razzari, L., Beljonne, D., Samorì, P. & Orgiu, E. (2021). *Adv. Mater.* **33**, 2007870.

Subramanian, S., Park, S. K., Parkin, S. R., Podzorov, V., Jackson, T. N. & Anthony, J. E. (2008). *J. Am. Chem. Soc.* **130**, 2706–2707.

Sundar, V. C., Zaumseil, J., Podzorov, V., Menard, E., Willett, R. L., Someya, T., Gershenson, M. E. & Rogers, J. A. (2004). *Science*, **303**, 1644–1646.

Sutton, C., Risko, C. & Brédas, J. (2016). *Chem. Mater.* **28**, 3–16.

Takimiya, K., Bulgarevich, K., Abbas, M., Horiuchi, S., Ogaki, T., Kawabata, K. & Ablat, A. (2021). *Adv. Mater.* **33**, 2102914.

Takimiya, K., Bulgarevich, K. & Kawabata, K. (2024). *Acc. Chem. Res.* **57**, 884–894.

Takimiya, K., Osaka, I., Mori, T. & Nakano, M. (2014). *Acc. Chem. Res.* **47**, 1493–1502.

Takimiya, K., Shinamura, S., Osaka, I. & Miyazaki, E. (2011). *Adv. Mater.* **23**, 4347–4370.

Tant, J., Geerts, Y. H., Lehmann, M., De Cupere, V., Zucchi, G., Laursen, B. W., Bjørnholm, T., Lemaur, V., Marcq, V., Burquel, A., Hennebicq, E., Gardebien, F., Viville, P., Beljonne, D., Lazzaroni, R. & Cornil, J. (2005). *J. Phys. Chem. B*, **109**, 20315–20323.

Tsurumi, J., Matsui, H., Kubo, T., Häusermann, R., Mitsui, C., Okamoto, T., Watanabe, S. & Takeya, J. (2017). *Nat. Phys.* **13**, 994–998.

Tsutsui, Y., Schweicher, G., Chattopadhyay, B., Sakurai, T., Arlin, J. B., Ruzié, C., Aliev, A., Ciesielski, A., Colella, S., Kennedy, A. R., Lemaur, V., Olivier, Y., Hadji, R., Sanguinet, L., Castet, F., Osella, S., Dudenko, D., Beljonne, D., Cornil, J., Samorì, P., Seki, S. & Geerts, Y. H. (2016). *Adv. Mater.* **28**, 7106–7114.

Virkar, A. A., Mannsfeld, S., Bao, Z. & Stingelin, N. (2010). *Adv. Mater.* **22**, 3857–3875.

Volpi, M., Jouclas, R., Liu, J., Liu, G., Catalano, L., McIntosh, N., Bardini, M., Gatsios, C., Modesti, F., Turetta, N., Beljonne, D., Cornil, J., Kennedy, A. R., Koch, N., Erk, P., Samorì, P., Schweicher, G. & Geerts, Y. H. (2023). *Adv. Sci.* **10**, 2301914.

Wang, C., Dong, H., Jiang, L. & Hu, W. (2018). *Chem. Soc. Rev.* **47**, 422–500.

Wedl, B., Resel, R., Leising, G., Kunert, B., Salzmann, I., Oehzelt, M., Koch, N., Vollmer, A., Duhm, S., Werzer, O., Gbabode, G., Sferrazza, M. & Geerts, Y. (2012). *RSC Adv.* **2**, 4404–4414.

Werzer, O., Kowarik, S., Gasser, F., Jiang, Z., Strzalka, J., Nicklin, C. & Resel, R. (2024). *Nat. Rev. Methods Primers*, **4**, 15.

Whittaker, S. J., Zhou, H., Spencer, R. B., Yang, Y., Tiwari, A., Bendesky, J., McDowell, M., Sundaram, P., Lozano, I., Kim, S., An, Z., Shtukenberg, A. G., Kahr, B. & Lee, S. S. (2024). *Cryst. Growth Des.* **24**, 613–626.

Winkler, A. (2016). *Surf. Sci.* **643**, 124–137.

Woodley, S. M. & Catlow, R. (2008). *Nat. Mater.* **7**, 937–946.

Xie, W., McGarry, K. A., Liu, F., Wu, Y., Ruden, P. P., Douglas, C. J. & Frisbie, C. D. (2013). *J. Phys. Chem. C*, **117**, 11522–11529.

Yamamura, A., Watanabe, S., Uno, M., Mitani, M., Mitsui, C., Tsurumi, J., Isahaya, N., Kanaoka, Y., Okamoto, T. & Takeya, J. (2018). *Sci. Adv.* **4**, eaao5758.

Yang, Y., Shtukenberg, A. G., Zhou, H., Ruzie, C., Geerts, Y. H., Lee, S. S. & Kahr, B. (2024). *Chem. Mater.* **36**, 881–891.

Yang, Y., Silva de Moraes, L., Ruzié, C., Schweicher, G., Geerts, Y. H., Kennedy, A. R., Zhou, H., Whittaker, S. J., Lee, S. S., Kahr, B. & Shtukenberg, A. G. (2022). *Adv. Mater.* **34**, 2203842.

Yoshida, H., Inaba, K. & Sato, N. (2007). *Appl. Phys. Lett.* **90**, 181930–181932.

Yu, P., Zhen, Y., Dong, H. & Hu, W. (2019). *Chem*, **5**, 2814–2853.

Zhang, X., Dong, H. & Hu, W. (2018). *Adv. Mater.* **30**, 1801048.

This article was originally published in *Acta Cryst.* (2024). C**80**, 601–611.

COMMENTARY

The structure of Chlamydomonas LOV1 as revealed by time-resolved serial synchrotron crystallography



Figure 1. Structure of *Chlamydomonas* LOV1 2.5 ms after light activation. The FMN-Cys57 thioether covalent adduct is clearly visible in the electron density (transparent blue). The FMN and Cys57 are marked. Residue numbers are marked (from 21 to 122) to help tracing the amino acid backbone from the N- to the C-terminus. Dotted blue line: the loop is removed to allow for an unperturbed view on the FMN binding pocket. Structure and structure factors obtained from PDB entry 8qia.

Marius Schmidt

A collaboration led by Joerg Standfuss, Paul Scherer Institute in Switzerland, and Przemyslaw Nogly from the Jagiellonian University in Krakov, Poland, investigated the reaction of a blue light photoreceptor domain derived from the phototropin of a single cellular organism. Results are published in an article in this issue of **IUCrJ** (Gotthard *et al.*, 2024). Phototropins are proteins found in plants, algae and fungi with homologs in bacteria. They are involved in various physiological responses from growth-towards-light (phototropism) to chloroplast light avoidance. The understanding of the light-activation reaction, and particularly that of the subsequent deactivation, plays an important role in controlling these physiological responses. Twenty-three years ago, the photoactive domain LOV2 from the maidenhair fern (*Adiantum capillus-veneris*) phytochrome/phototropin chimera Phy3 was characterized by Sean Crosson and Keith Moffat at the University of Chicago, USA (Crosson & Moffat, 2001). LOV (light–oxygen–voltage) domains are found in receptor proteins through all kingdoms of life. They are typically involved in regulating enzyme activity upon receiving an outside stimulus. Some proteins containing LOV domains are also found in humans, for example in cardiac potassium channels.

Phototropin LOV domains (LOV1 and LOV2) contain a flavin-mononucleotide (FMN) chromophore, each, that absorbs light in the blue–green region. Importantly, when light is absorbed, one of the FMN carbons (C4a) forms a covalent bond with a nearby cysteine residue of the LOV protein. For the fern LOV2 two different structures were determined, one in the dark and one under continuous light illumination (Crosson & Moffat, 2001, 2002). A few years later, Fedorov *et al.* extended these investigations to LOV1 of the phototropin from the single-cell green algae *Chlamydomonas reinhardtii* (Fedorov *et al.*, 2003). *Chlamydomonas* is biologically highly significant as a basic model for a photosynthetic organism.

In the study by Gotthard *et al.*, the photoreaction of the *Chlamydomonas* LOV1 was re-examined. The experiments were performed with time-resolved serial synchrotron crystallography (TR-SSX), where a large number of small crystals are transported into the X-ray interaction volume by a (viscous) jet and

exposed one by one to intense X-ray radiation. However, before the crystals are probed by X-rays they are excited by a 5 ms blue–green (λ = 488 nm) light pulse from a laser diode. The data were collected in a stroboscopic way. This means that once a jet volume containing crystals was excited, multiple exposures to X-ray pulses and corresponding detector readouts were recorded at increasing time delays. The serial crystallography approach has the advantage that radiation damage is minimized (although not avoided), which has been a potential issue with previous investigations on LOV proteins.

Since the yield of the excited photoproduct is low, multiple absorption events are particularly important to repeatedly activate the LOV1 to boost population transfer. The authors report six activation events on average during the 5 ms laser-light exposure. This results in difference electron density maps of exquisite quality, which could be easily interpreted. Fig. 1 shows the structure of LOV1 2.5 ms after light activation. The structure of the cysteinyl-FMN thioether covalent adduct is clearly visible. Upon adduct formation, the C4a carbon configuration changes from a planar sp^2 to a more tetrahedral sp^3-hybridized configuration, thereby distorting the structure of the isoalloxazine moiety of the FMN. The orientation of Cys52 is decisively different from that determined originally by Fedorov *et al.* It agrees more with the orientation observed by Crosson and Moffat earlier.

The paper also reports an important lesson learned when approximately Gaussian laser-light intensity profiles are employed together with stroboscopic data collection. For practical reasons, the fastest time point, which was the 2.5 ms time point in this case, should be excited by the maximum of the intensity profile. Crystals probed at later time points are transported a longer distance by the viscous jet into the X-ray interaction volume. These crystals are excited by subsequently smaller intensities from the flanks of the light intensity profile. This coercively means that the extent of population transfer to the covalently bound thioether adduct is smaller at later time points. The covalently bound adduct has a lifetime of several 100 s, yet the timescale probed in the paper is 400 ms (80 X-ray exposures for 5 ms each). On the measured timescale, a decay of the adduct species cannot be determined, yet an apparent decay of more than 70% is reported already at a pump–probe delay of 90 ms. This behavior can only be attributed to a smaller effective population transfer caused by less laser-light intensity from the flanks of the intensity profile. In addition, the 2.5 ms time point does not show the largest activation level. In fact, the largest concentration of the covalent adduct is observed at 22 ms. This means that the 22 ms time point was activated by the peak of the light intensity distribution and the 2.5 ms time point was excited by a slightly less, off-peak intensity. Nevertheless, important structural relaxations were discovered at time points longer than 32 ms after adduct formation as demonstrated by 19 time-resolved structures (up to 93 ms) deposited in the Protein Data Bank.

In summary, Gotthard *et al.* investigated the PHY1 activated state at numerous time delays, but with varying activation levels caused by different pump laser-light intensities. The structure of the FMN thio-ether covalent adduct determined by TR-SSX is different from that determined at cryo-temperatures. The results highlight the significance of room-temperature investigations in conjunction with SSX as an effective method to reduce radiation damage during data collection by distributing the X-ray dose over a large number of protein crystals.

References

Crosson, S. & Moffat, K. (2001). *Proc. Natl Acad. Sci. USA*, **98**, 2995–3000.

Crosson, S. & Moffat, K. (2002). *Plant Cell*, **14**, 1067–1075.

Fedorov, R., Schlichting, I., Hartmann, E., Domratcheva, T., Fuhrmann, M. & Hegemann, P. (2003). *Biophys. J.* **84**, 2474–2482.

Gotthard, G., Mous, S., Weinert, T., Maia, R. N. A., James, D., Dworkowski, F., Gashi, D., Furrer, A., Ozerov, D., Panepucci, E., Wang, M., Schertler, G. F. X., Heberle, J., Standfuss, J. & Nogly, P. (2024). *IUCrJ*, **11**, 792–808.

This article was originally published in *IUCrJ* (2024). **11**, 645–646.

COMMENTARY

AI-enhanced X-ray diffraction analysis: towards real-time mineral phase identification and quantification

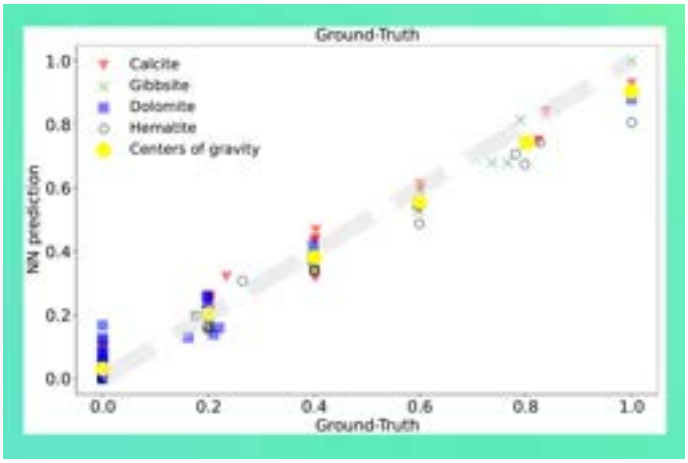


Figure 1. Scatter plot of the CNN model prediction versus the ground truth for mixtures composed of four mineral phases (calcite, gibbsite, dolomite and hematite). The training database takes into account the instrumental effects [DwIE in Simonnet *et al.* (2024)]. The centers of gravity are the weighted mean of each data points subset. Figure reproduced from Simonnet *et al.* (2024).

Nikolaos I. Prasianakis

There are a large number of scientific disciplines which benefit from advanced X-ray-based analytical techniques. The X-ray diffraction (XRD) method is a powerful technique which can provide qualitative and quantitative information about the crystallographic structure and composition of matter in a non-destructive way. Such information is crucial in several fields, such as in materials science for novel materials research, or in environmental and geological sciences where it improves the understanding of subsurface composition and chemistry, which is essential for resource exploitation and pollutant dispersion studies, to name a few.

The XRD techniques range from powder XRD, where the samples are provided in a homogeneous powder form, to XRD computed tomography (XRD-CT) where spatial investigation of heterogeneous samples in 2D and 3D is possible. At the same time, XRD techniques are paired with several synchrotron X-ray-based techniques and provide crucial complementary information (Allen, 2023). The working principle of XRD is based on the diffraction of X-rays resulting from their interaction with the crystalline planes of the considered material. The diffracted X-rays are collected by a specialized detector, where the diffraction pattern is recorded as a plot of the diffracted X-ray intensity versus the scattering angle. These diffraction patterns are subsequently analysed and compared with reference patterns. Each crystal is characterized by a unique fingerprint of peaks which allows the identification of multiple crystals within the same signal. Signal fitting to known patterns is a complex computationally demanding process, especially when multiple crystals are present. While powder XRD typically provides a single diffraction pattern, in XRD-CT there is one XRD pattern for each pixel within the considered 2D/3D domain resulting in multi-dimensional big data. The number of pixels within such a 3D tomogram can easily become very large ($>10^5$) introducing several challenges related to tomographic reconstruction, high-throughput data acquisition and their respective modelling (Hayashi *et al.*, 2015, 2019; Finegan *et al.*, 2020). More specifically, the model refinement computations are, due to the large number of the XRD-CT patterns that have to be processed, a few orders of magnitude slower than powder XRD computations. A potential solution to accelerate these computationally intensive processes is the application of artificial

intelligence (AI) techniques.

In recent years, developments in AI and machine learning have been quite impressive opening new avenues in numerical modelling and data interpretation. There are already several applications which take advantage of these advancements, ranging from the acceleration of reactive transport simulations using machine learning (Jatnieks *et al.*, 2016), to image and pattern recognition in the sense of ultrafast processing and detection which surpasses human capability (Ragone *et al.*, 2023; Boiger *et al.*, 2024; Omori *et al.*, 2023). More specifically, for XRD measurement interpretation, recent seminal works of Dong *et al.* (2021, 2023) and Lee *et al.* (2021) have implemented convolutional neural network (CNN) models to extract important information like phase identification and lattice parameters directly from XRD patterns. In Dong *et al.*, it is demonstrated that using a trained CNN model the results can be interpreted up to three orders of magnitude faster, while Lee *et al.* (2021) reported achieving the completion of the task in a few seconds instead of several hours, compared with the use of traditional techniques (Rietveld method).

In the same direction, there are the recent efforts for phase quantification using deep neural network processing of XRD patterns (Simonnet *et al.*, 2024; Poline *et al.*, 2024). In the article by Simonnet *et al.* (2024) in this issue of **IUCrJ**, the authors aim to introduce a CNN-based method for direct mineral phase quantification from the XRD signals. The training of these models requires a very large dataset and for that purpose pure XRD samples of four minerals and their mixtures are generated synthetically, using crystallographic information files. Interestingly, the authors incorporate the effect of the instrumental factors into the synthetic dataset, in order to increase the model realism and to accurately account for the exact experimental geometry, such as the wavelength function and the attenuation factor.

This approach results in a significant improvement in the accuracy and efficiency of the model in the considered real mineral mixture example, as shown in Fig. 1 (Simonnet *et al.*, 2024). Although the authors provide information, validation benchmarks and examples for a four-component system, the extension to systems composed of more than four minerals, which is common in practice, appears straightforward if the same methodology is followed. However, it should be noted that the number of training samples as well as the training efforts to build a more general model are expected to also increase hand in hand with the number of components, in order to maintain the same levels of accuracy.

It is of paramount importance and an excellent example of open research that the code has been made freely available as open-access software on the GitHub software development platform (GitHub – titouansimonnet/XRD_Proportion_Inference, https://github.com/titouansimonnet/XRD_Proportion_Inference). This repository and version control system includes well-documented input files, the code for generating the training datasets (synthetic XRD patterns), and the machine learning model architecture and parameters, as well as the test cases. This provides to the scientists in the community an excellent starting point to familiarize themselves with the tool, to use it, to optimize it and to extend it for the description of more complex systems.

AI-based tools enable ultrafast interpretation and processing of XRD patterns, significantly reducing the time required compared with traditional methods. The speed of interpretation and the resulting reduction in computational cost should not be underestimated. With these advancements, there is the potential to develop real-time experimental companions capable of interpreting and possibly reducing the dimensionality of the acquired data during the experiment. This opens new horizons such as conducting dynamic experiments with parallel XRD analysis, similar to Cai *et al.* (2020), and obtaining real-time high-resolution 3D information, which could be further used for the steering and adjustment of the experiment. Additionally, integrating real-time experimental data with highly sophisticated physical modelling algorithms can facilitate the development of digital twins of experiments, supporting the fitting of physical model parameters of interest and the exploration of parametric system responses within a single experiment.

References

Allen, A. J. (2023). *J. Appl. Cryst.* **56**, 787–800.

Boiger, R., Churakov, S. V., Ballester Llagaria, I., Kosakowski, G., Wüst, R. & Prasianakis, N. I. (2024). *Swiss J. Geosci.* **117**, 1–26.

Cai, L., Youngman, R. E., Baker, D. E., Rezikyan, A., Zhang, M., Wheaton, B., Dutta, I., Aitken, B. G. & Allen, A. J. (2020). *J. Non-Cryst. Solids*, **548**, 120330.

Dong, H. (2023). Doctoral Thesis, University College London.

Dong, H., Butler, K. T., Matras, D., Price, S. W. T., Odarchenko, Y., Khatry, R., Thompson, A., Middelkoop, V., Jacques, S. D. M., Beale, A. M. & Vamvakeros, A. (2021). *npj Comput. Mater.* **7**, 74.

Finegan, D. P., Vamvakeros, A., Tan, C., Heenan, T. M. M., Daemi, S. R., Seitzman, N., Di Michiel, M., Jacques, S., Beale, A. M., Brett, D. J. L., Shearing, P. R. & Smith, K. (2020). *Nat. Commun.* **11**, 631.

Hayashi, Y., Hirose, Y. & Seno, Y. (2015). *J. Appl. Cryst.* **48**, 1094–1101.

Hayashi, Y., Setoyama, D., Hirose, Y., Yoshida, T. & Kimura, H. (2019). *Science*, **366**, 1492–1496.

Jatnieks, J., De Lucia, M., Dransch, D. & Sips, M. (2016). *Eur. Geosci. Union Gen. Assem.* **97**, 447–453.

Lee, J. W., Park, W. B., Kim, M., Pal Singh, S., Pyo, M. & Sohn, K. S. (2021). *Inorg. Chem. Front.* **8**, 2492–2504.

Omori, N. E., Bobitan, A. D., Vamvakeros, A., Beale, A. M. & Jacques, S. D. M. (2023). *Philos. Trans. R. Soc. A Math. Phys. Eng. Sci.* **381**. https://doi.org/10.1098/RSTA.2022.0350.

Poline, V., Purushottam Raj Purohit, R. R. P., Bordet, P., Blanc, N. & Martinetto, P. (2024). *J. Appl. Cryst.* **57**, 831–841.

Ragone, M., Shahabazian-Yassar, R., Mashayek, F. & Yurkiv, V. (2023). *Prog. Mater. Sci.* **138**, 101165.

Simonnet, T., Grangeon, S., Claret, F., Maubec, N., Fall, M. D., Harba, R. & Galerne, B. (2024). *IUCrJ*, **11**, 859–870.

This article was originally published in *IUCrJ* (2024). **11**, 647–648.

COMMENTARY

Unity gives strength: combining Bertaut's and Belov's concepts and the formalism of aperiodic crystals to solve magnetic structures of unprecedented complexity

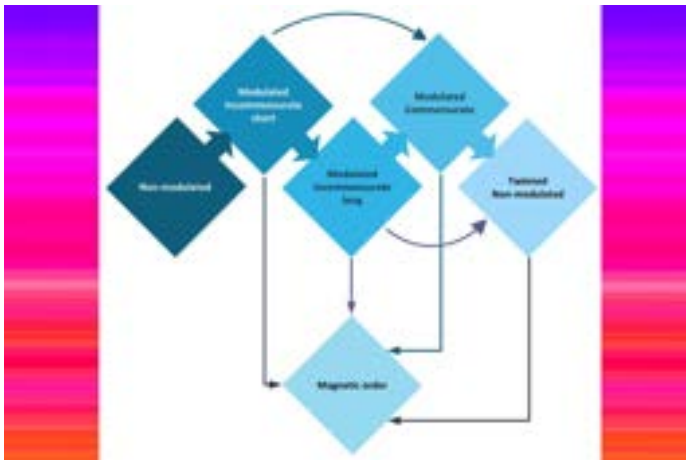


Figure 1. Pathways to reaching the magnetically ordered phase in the system studied by Geers *et al.* (2024). Possible crystal phase transition sequences are either direct (short arrows between the lozenges in the upper row) or indirect (curved arrows), depending on the substitution of Ni by Co. The magnetically ordered phase can be reached from any of the crystal phases linked to it by straight arrows.

Václav Petříček, Margarida Sousa Henriques

Crystal structure analysis from diffraction data is a method that has been around for over a hundred years. Collecting data for and then solving simple structures takes only a few hours and is a routine procedure that no longer surprises anyone. Yet structural analysis continues to fascinate us by opening up new avenues and possibilities. The paper by Geers *et al.* (2024) in this issue of **IUCrJ** is an excellent example of this, as it illustrates the tremendous progress that has been made in the last decade in solving magnetic structures from neutron diffraction data.

The article by Geers *et al.* is one of very few reports on modulated molecular frameworks. It summarizes the results of determining the modulated magnetic structure of the metal–organic coordination polymers $[CH_3NH_3]Co_xNi_{1-x}(HCOO)_3$, a series of compounds in which very unusual phase transitions have been observed. The authors describe how the magnetic ordering in the structures and magnetic phase transitions depend on the metal and its environment in the complex (Fig. 1). Furthermore, they show that it is possible to choose the pathway to the magnetic transition and tune the critical temperature and stability of the magnetic phase. It is remarkable how the magnetic state is reached via at least one modulated crystal phase. Strikingly, some phases show a combined nuclear and magnetic modulation at the lowest temperatures, indicating that a periodically deformed structure leads directly to a wave in the spin distribution. Therefore, the study is essential for understanding the interplay between the arrangement of atoms in the crystal and the magnetic moments.

The authors combine two seemingly different approaches to study the ordering of the magnetic moments in a crystal: representation analysis, based on irreducible representations of the initial paramagnetic phase as described by Bertaut (1968), and the description of magnetic ordering using magnetic groups as given by Belov *et al.* (1957). It has recently been shown that by combining these methods the arrangement of the atoms and magnetic moments in individual phases can be solved much more easily

and to a better degree. The fundamental problem for determining the proper, rather than the apparent, symmetry is that neutron diffraction combines diffraction effects from the atomic nuclei and from the magnetic moments. These can fully overlap in cases where the arrangement of the magnetic moments does not lead to a violation of translational symmetry. The violation of translational symmetry by the arrangement of the magnetic moments is commensurate when the propagation vector is half of one of the fundamental vectors of the primitive cell, but incommensurate when the propagation vector has general components. Commensurate cases are covered by magnetic space-group type IV. However, for incommensurate structures, it is necessary to use the superspace formalism introduced by de Wolff *et al.* (1981), which was later extended to magnetic structures by Perez-Mato *et al.* (2012) as magnetic superspace groups (MSSGs). These allow the symmetry of the crystal to be understood as including positional, occupation and magnetic modulations.

Determining the MSSG from experimental data is not easy at all. In most cases, the diffraction image simulates a symmetry that is higher than the real point symmetry because magnetic phase transitions lead, in most cases, to the existence of a number of magnetic domains with the same fractional volume. Moreover, systematic extinction of diffraction is complicated by the fact that the structure factor of the magnetic structure is an axial vector, and therefore all its components must meet the extinction conditions. The combination of representation analysis with the MSSG formalism helps to solve the situation, as implemented in the highly sophisticated tool ISODISTORT (Stokes *et al.*, 2023; Campbell *et al.,* 2006), which finds possible MSSGs based on knowledge of the initial structure and the propagation vector.

In the work of Geers *et al.*, the methods mentioned above are applied to the end members of the series of solid solutions, *i.e.* those containing only nickel or cobalt, measured at different temperatures. The differences in the behavior of these compounds are noteworthy, as shown in their Fig. 1. The first phase transformation has the same character for both crystals, in which an unmodulated structure transforms into a modulated one with the same superspace group and similar modulation vectors. A further decrease in temperature leads, in the case of the nickel compound, to a modulated structure where both the atomic position and magnetic moment of the nickel atom are modulated, while the cobalt compound undergoes two phase transitions: from the orthorhombic to a monoclinic group (twinned) and then to the magnetic space group $P2_1'/n'$.

Apart from the compounds containing only nickel or cobalt, the authors also studied in detail the solid solutions that contained a mixture of both metals (x = 0.25, 0.5 and 0.75) and discovered a full landscape of modulated and magnetic phases (see Fig. 5 in their paper). Finally, we would like to draw the reader's attention to the information provided in their supporting information, which serves as an excellent introduction to solving and refining magnetic structures.

In summary, the work of Geers *et al.* proves that the analysis of crystal structures by diffraction methods is still open to new challenges. It also hints at a possible role of modulated crystal structures as a controlling mechanism for spin degrees of freedom in these materials via selected crystal phase transitions.

References

Belov, N. V., Neronova, N. N. & Smirnova, T. S. (1957). *Kristallografiya*, **2**, 315–325.

Bertaut, E. F. (1968). *Acta Cryst.* A**24**, 217–231.

Campbell, B. J., Stokes, H. T., Tanner, D. E. & Hatch, D. M. (2006). *J. Appl. Cryst.* **39**, 607–614.

Geers, M., Fabelo, O., Cliffe, M. J. & Cañadillas-Delgado, L. (2024). *IUCrJ*, **11**, 910–920.

Perez-Mato, J. M., Ribeiro, J. L., Petricek, V. & Aroyo, M. I. (2012). *J. Phys. Condens. Matter*, **24**, 163201.

Stokes, H. T., Hatch, D. M. & Campbell, B. J. (2023). *ISODISTORT. ISOTROPY Software Suite.* Version 6.12.1. https://iso.byu.edu.

Wolff, P. M. de, Janssen, T. & Janner, A. (1981). *Acta Cryst.* A**37**, 625–636.

This article was originally published in *IUCrJ* (2024). **11**, 901–902.

ASSOCIATES NEWS

Japan-Taiwan Bilateral Seminar on Crystallography: "Frontier of Crystallography"



Hiroyoshi Matsumura, Kazuya Hasegawa

In November 2024, the Institute for Protein Research (IPR), the Research Center for Crystalline Materials Engineering (RCCME) and the Comprehensive Research Organization for Science and Society (CROSS) successfully hosted the Japan-Taiwan Bilateral Seminar on Crystallography: “Frontiers of Crystallography.” The event was held at the FUJI Hall, located in the EI (Emergent/Innovative) Engineering Building at Nagoya University, and brought together around 30 participants from Japan and Taiwan.

The Japan-Taiwan Bilateral Seminar on Crystallography, originally established in 1990, was temporarily suspended due to the COVID-19 pandemic but has now resumed. With the goal of advancing crystallography in both Japan and Taiwan and fostering ongoing personal connections, leading researchers were invited to engage in research exchanges.

In the opening remarks, Professor Kurisu from Osaka University and Professor Nei-Li Chan from National Taiwan University, who have maintained a close relationship over 20 years, provided their experience on the bilateral relationship. Professor Hasegawa from Nagoya University also introduced RCCME, highlighting the structural science conducted at the center. The scientific session featured high-level presentations by eight young researchers in fields such as structural biology, MicroED and functional small molecules, as outlined below:

(1) Naruhiko Adachi, Japan. "Setup and operation of 3DED/microED experiments at KEK and Tsukuba University."
(2) Yu-Yuan Hsiao, Taiwan. "Structural analysis of TREX1: From catalytic property identification to inhibitor development."
(3) Kazuki Kawahara, Japan. "Structural biology of the type IV pillus from enteric bacterial pathogens."
(4) Shih-Ming Lin, Taiwan. "Calcium-dependent modulation and lectin domain function in the activation of Vibrio campbellii α-hemolysin."
(5) Toshiyuki Sasaki, Japan. "Tailoring structural analysis of functional small-molecule crystals with X- ray and electron diffraction methods depending on crystal properties."
(6) Chyuan-Chuan Wu, Taiwan. "Structural basis of mitochondrial DNA degradation machinery."
(7) Yuya Hanazono, Japan. "Structural analysis of amide protons using high-resolution neutron crystallography."
(8) Wen-Ting Lo, Taiwan. "Structural basis of class II phosphoinositide 3-kinase regulation and

pharmacological inhibition."

At the end of the scientific session, Professor Nakagawa from Osaka University provided an overview of the upcoming AsCA 2025 conference, which will be held in Taipei next year and co-organized by Japan and Taiwan. In his closing remarks, Professor Sugiyama, President of CrSJ, highlighted the longstanding bilateral relationship in crystallography and underscored the importance of continued collaboration. Following the symposium, a banquet was held in Nagoya University’s cafeteria, where participants enjoyed lively discussions over beer and wine. This meeting showcased the strong ties built over three decades, with knowledge and camaraderie passed from generation to generation. We believe this symposium will contribute to the success of AsCA 2025.



OUTREACH

11th Polish Crystal Growing Competition for Schools 2024



Monika Oboz, Magdalena Szubka

The first edition of the Polish Crystal Growing Competition for Schools organized at the Institute of Physics of the University of Silesia in 2014 was inspired by Dr Hanna Dąbkowska, a member of the IUCr Commission for Crystal Growth. The competition immediately gained great popularity and, since 2014, has been held every year.

Over 220 participants from 45 different towns participated in this year's 11th edition of the competition, sending over 300 good-quality crystals.



The event was co-financed by the Silesian Voivodeship - Co-organizer of the European City of Science, Katowice 2024.

Traditionally, the jury selected three winners and distinguished over 20 works. The award ceremony occurred on June 13, 2024, during the "Crystals: order, beauty and utility" conference at the Institute of Physics of the University of Silesia in Katowice.

It was held under the patronage of the dean of the Faculty of Science and Technology, Professor Danuta Stróż, and director of the Institute of Physics of the University of Silesia, Professor Sebastian Pawlus.

During the conference, lectures were given by invited outstanding specialists from national research centers, such as the Institute of High Pressures of the Polish Academy of Sciences (UNIPRESS) and the Institute of Molecular Physics of the Polish Academy of Sciences.

At the awards gala, there was a presentation of the winners and participants distinguished in the competition and an award ceremony.

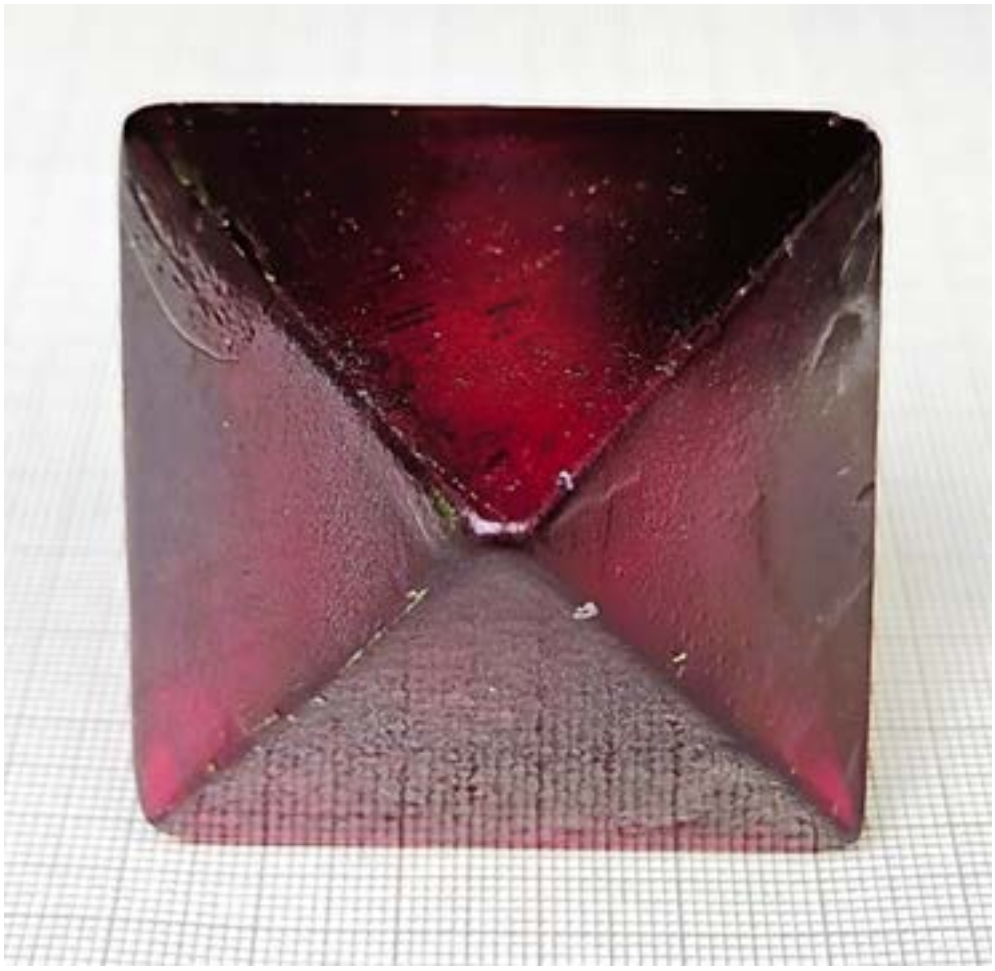
The conference ended with a poster session of the winners and authors of distinguished works, during which awards for the best poster were presented.

The conference and the competition awards gala took place during Crystal Week, part of the celebrations organized by an Academic Consortium of seven public universities as part of the European City of Science 2024, a title awarded to Katowice by the European Commission.

The Polish Crystal Growth Society and the Crystallography Committee of the Polish Academy of Sciences provided the patronage of the competition.



Joanna Ajdukiewicz, Teacher - Agata Bladoszewska, 1st Bilingual Secondary School named after Edward Dembowski, Gliwice, 1st place, $C_6H_8O_7$.



Wiktor Januszkiewicz, Teacher - Maria Rogozińska, Szymczak XXXV General Secondary School with Bilingual Departments named after Bolesław Prus, Warszawa, 2nd place, $K(Al,Cr)(SO_4)_2 \cdot 12H_2O$.



Bruno Głogowski, Teacher - Agnieszka Cacek, Primary School No. 221 with Integration Departments named after Barbara Bronisława Czarnowska, Warszawa, 3rd place, $KAl(SO_4)_2 \cdot 12H_2O$.

MEETING REPORT (IUCR SUPPORTED)

ACA2024 Meeting



K. Stevens

The 2024 American Crystallographic Association (ACA) Annual Meeting was held from 7-12 July 2024, at the Denver Marriott Tech Center in Denver, Colorado. This gathering of structural science professionals, including researchers and industry experts, provided a vibrant platform for scientific exchange, networking and exploring the latest advancements in crystallography. With attendance surpassing 600, and more than 400 oral and poster abstracts submitted, the growing relevance of structural science was incredibly evident. The meeting brought together seasoned scientists and early-career researchers who engaged in diverse sessions, workshops and social events.

We are grateful to our members whose donations have supported the ACA student travel grant, and we extend our thanks to the IUCr for their generous grant, both of which enabled us to award over 30 travel grants to early-career scientists, allowing them to attend and actively participate at ACA2024.



From left to right: Catherine Drennan presents her keynote address, attendees engage with virtual reality in the exhibit hall, and workshop participants collaborate.

A highlight of the meeting was the keynote address by Catherine Drennan, a prominent chemist and biochemist, who captivated attendees with her talk “Shake, Rattle & Roll: Capturing Snapshots of Proteins in Action”. Known for her passion for 'molecular storytelling', Dr Drennan shared insights into her laboratory’s use of X-ray crystallography and electron microscopy to capture enzymes in action, offering a remarkable glimpse into the molecular 'dances' that drive biochemical reactions.

Following the keynote, attendees gathered in the exhibit hall, where over 30 companies showcased products and services essential to structural science. Many of these exhibitors, including Thermo Fisher Scientific, Xenocs Inc., Rigaku Americas Corporation, DECTRIS Ltd, the American Institute of Physics, Bruker AXS, Quantum Detectors, Gatan, FEI Electron Optics BV (The Netherlands), Stoe Corporation,

MiTeGen, SPT Labtech, Stoe Corporation, Crystal Growth & Design, Formulatrix, MiTeGen, the Hampton Research Corp., Waters|Wyatt Technology, Anton Paar, NanoSoft, LLC and Altos Labs, among others, also supported the meeting as sponsors, helping to fund speaker travel and other essential expenses.



From left to right: the IUCr2026 booth distributing congress materials, the ACA Council in session, and a view of one of the session rooms.

The exhibit hall also featured a booth spotlighting the 27th Congress and General Assembly, to be held in Calgary, Alberta, Canada, from 11-18 August 2026. Hosted by the ACA, the Canadian National Committee for Crystallography (CNCC) and the US National Committee for Crystallography (USNC/Cr), the booth showcased exciting plans for the Congress in Calgary's vibrant setting.

ACA2024 hosted over 30 sessions covering a number of diverse structural science topics and five highly attended workshops, including Workshop 1: Advanced Structure Refinement with Olex2 & NoSpherA2; Workshop 2: Applications of Small Angle Scattering to Structural Biology: an Introduction; Workshop 3: Hands-on CryoEM Sample Preparation & Data Collection using CryoEM Merit Badges; Workshop 4: Simple & Advanced Single Crystal X-Ray Structure Refinement using ShelXle; and Workshop 5: Crystallographic & Cryo-EM Structure Solution with Phenix.

The Young Scientist Interest Group (YSIG) played an active role in supporting early-career researchers, organizing a mixer and the popular Three Minute Thesis (3MT) competition. This competition challenged young scientists to present their research in three minutes. Manju Ojha from the University of Maryland, Baltimore County, claimed first place with her presentation "Structure of saguaro cactus virus 3′ translational enhancer mimics 5′ cap for eIF4E binding". Nicholas Bragagnolo from York University earned second place for his talk "TraG-edy to Triumph: How Challenges in Crystallisation Efforts of TraG led to Success". In third place, Chhandosee Ganguly from the University of Oklahoma presented "Simple Techniques to Improve Particle Distribution and Data Quality for Dynamic Protein-Nucleic Acid Complexes".



From left to right: attendees board the bus after the YSIG mixer, poster presenters receive awards at the banquet, and ACA President Allen Oliver addresses the audience.

Beyond the scheduled early-career activities, the week was filled with engaging moments. Games unfolded spontaneously in the lobby, and one evening, an impromptu karaoke session infused a conference room with lively energy. Also, in a touching instance of mentorship, a young attendee sat captivated in the speaker-ready room as the seasoned presenter Larry Andrews rehearsed his slides. The young attendee stayed, drawn into Larry's presentation, as he graciously delivered his entire lecture just for this engaged listener.

Demonstrating a continuing commitment to inclusivity, the ACA hosted a session on the #IAmRemarkable initiative, co-chaired by ACA members Sandra Gabelli and Callie Saeher, empowering participants to celebrate their achievements and counter societal norms that often discourage self-promotion, particularly among under-represented groups. The session fostered an environment of encouragement and confidence.

The ACA recognized outstanding contributions this year by awarding over 15 poster prizes, including the IUCr Pauling Poster Prize to Madeline M. Glennon, a graduate student from the University of Notre Dame, for her poster titled “Structural Elucidation of an RNA Triple Helix in Complex with a Small Molecule”. Additionally, three major awards were celebrated: the Margaret C. Etter Early Career Award to Benjamin Frandsen of Brigham Young University, the M. J. Buerger Award to Thomas Albrecht-Schönzart from the Colorado School of Mines and the Bertram Eugene Warren Diffraction Physics Award to John Greeden of McMaster University.



From left to right: attendees enjoying the banquet, a snapshot from the poster session, and the ACA Meeting Committee addressing guests at the banquet.

For a comprehensive look at the ACA2024 program, please visit the ACA website’s 'Past Meetings' page. Recorded sessions will soon be available on the ACA History Portal for further insights. The ACA extends heartfelt gratitude to the 2024 Meeting Committee, poster session co-chairs, session chairs, workshop organizers, speakers and exhibitors for making this meeting possible. And to every attendee, thank you for being part of this extraordinary global scientific community.



From left to right: a spontaneous talk, new badges, and the 2024 SIG chairs kicking off preparations for the 2025 program.

Mark your calendars for our 75th Anniversary Meeting, happening 18-23 July 2025 at the Westin Chicago Lombard! In honor of this diamond anniversary, we will reflect on past meeting highlights, celebrate the field’s growth and recognize the remarkable contributions of our community. More details coming soon!

MEETING REPORT

SCANZ Crystal 35 Meeting Report – Going West!



Christopher Sumby

Crystal35, the 35th Biennial Conference of the Society of Crystallographers in Australia and New Zealand (SCANZ), was held from 27th to 29th October 2024 in Fremantle, Western Australia. The Crystal meetings tend to be held in the state where the SCANZ president resides, and this was no different, bringing us back to Western Australia for the second time in seven years for a meeting organised by Professor Charlie Bond and a team of local and interstate crystallographers and structural biologists. Crystal35 was held in Fremantle (Walyalup, the local Nyoongar peoples' name for the area), a seaside suburb of Perth. While close to Perth and Perth airport, Fremantle is a charming destination full of narrow streets lined with heritage buildings, close to historical and functioning dock areas, with great access to well-known local breweries and cafes.

Once again, the meeting was an excellent size for networking and scientific discussions with 128 attendees, and was a fantastic opportunity to catch up with much of the Australian and some of the New Zealand crystallographic community. Despite being a significant distance, the meeting was attended by a small contingent of New Zealand crystallographers, as well as international speakers from Japan, Singapore and South Africa. The organising committee of Charlie Bond, University of Western Australia (UWA), Chair; Mihwa Lee, University of Melbourne; Stephen Moggach, UWA; Joel Haywood, Curtin University; Rhys Grinter, Monash University; Stephanie Boer, ANSTO; Gemma Turner, UWA; Luke Smithers, UWA; and Crystal Cooper, UWA, developed a vibrant and diverse program with 21 invited speakers and a series of concurrent sessions with speakers selected from abstracts.

Highlights of the program included the 1987 Fund Lecture by Professor So Iwata (Kyoto University); the awarding of the 2023 and 2024 Sandy Mathieson Medals to Professor Neeraj Sharma (UNSW) and Professor Jack Clegg (University of Queensland), respectively; and the awarding of the 2024 Lawrence Bragg Medal to Professor Jenny Martin (University of Queensland and Griffith University). Professor Iwata also gave an excellent talk on time-resolved (4D) structure analysis of membrane proteins and its application to drug discovery. This included a discussion of the structures of membrane proteins, mainly G protein-coupled receptors (GPCRs) and transporters, and investigation of the complex structures of the receptor sites, which can be used for drug discovery.



Left to right: Professor Charlie Bond, SCANZ President, presenting the Bragg Medal to Emeritus Professor Jenny Martin, the 2024 Sandy Mathieson Medal to Professor Jack Clegg and the 2024 Sandy Mathieson Medal to Professor Neeraj Sharma. Photos by Chris Sumby.

Professor Sharma was the 2023 recipient of the Sandy Mathieson Medal, awarded for distinguished contributions to science involving X-ray, neutron or electron diffraction and/or imaging by a researcher within 15 years of the award of their PhD (https://scanz.iucr.org/__data/assets/pdf_file/0010/155791/Mathieson-Recipientsv2.pdf). Professor Sharma investigates the structure and function of batteries using synchrotron and neutron diffraction techniques, and gave us a talk spanning from fundamental battery science through to analysis and testing of commercial batteries, including batteries that had been subjected to a proximal explosion. Furthermore, Professor Clegg presented his team's recent work on flexible or bendy crystals, which helps rewrite some of the conventional wisdom of crystalline materials as being brittle and inflexible. Professor Clegg also showed the scope of potentially flexible materials, including the use of advanced single-crystal synchrotron measurements to understand the mechanism of bending and the location of the stored forces in these crystals.

The final named lecture, given on the final day of the meeting, was the Bragg Medal award for distinguished contributions to science involving X-ray, neutron or electron diffraction and/or imaging by Professor Martin. Professor Martin gave an engaging presentation starting from William Henry and William Lawrence Bragg and spanning her time in crystallography, including the early use of scientific computing, cakes inspired by crystallography and structural biology, and her contributions to gender equity and diversity in SCANZ and the IUCr.

A diverse group of keynote lecturers provided excellent coverage of all aspects of crystal growth and structure determination, including talks titled "CryoEM structures of the multimeric secreted NS1, a major factor for dengue hemorrhagic fever" (Professor Shee-mei Lok, Duke-NUS Medical School, Singapore), "Predicting crystal growth and morphology from accuracy to speed" (Professor Julian Gale, Curtin University), "Crystal engineering with multicomponent crystals" (Professor Delia Haynes, Stellenbosch University, South Africa) and "TRAPped in an elevator: amino-sugar uptake and utilisation by bacteria" (Professor Renwick Dobson, University of Canterbury, New Zealand).

Two excellent poster sessions were held, one at lunch on Sunday and the second in the evening on Monday, with 42 posters displayed over the course of the three days. Lots of discussion took place as presenters vied for five poster prizes, which were awarded at the close of the conference. Other highlights included the Rising Stars session, a lunchtime session hosted by beamline scientists from the Australian Synchrotron on the new beamlines (MX3, ADS and BioSAXS) coming online as the BRIGHT program reaches completion. The Rising Stars of the conference were Dr Charles Bayly-Jones (Monash University), Dr Isabelle Jones (Curtin University and UWA), Dr Katherine Davies (The Walter and Eliza Hall Institute of Medical Research and Melbourne University), Dr Hunter Windsor (UNSW) and Dr Rebecca Frkic (Australian National University).



The Rising Star session presenters bookended by the session chairs Dr Joel Haywood and Dr Josie Auckett (left), and the poster prize recipients with Dr Crystal Cooper and Professor Charlie Bond (right). Photos by Chris Sumby.

Crystal35 also provided an opportunity for a SCANZ business meeting. The focus of the meeting was changes to the SCANZ constitution to complete some steps to modernise it and to provide greater structure, certainty around the council terms, timing between Crystal meetings, and the addition of a new standing committee for outreach. The leadership of SCANZ now passes to the new president, Professor Chris Sumby (the author of this article) from the University of Adelaide, with the new vice-president being Professor Emily Parker (Professor of Chemical Biology at Victoria University of Wellington and Science Advisor to the MBIE - Ministry of Business, Innovation and Employment in New Zealand), and a committee comprising Professor Charlie Bond (past president), Associate Professor David Turner (secretary), Professor Jack Clegg (treasurer), Dr Michelle Miller (newsletter editor), and committee members Dr Lauren Macreadie, Dr James Hester and Professor Stephanie Gras. Further representation also comes via the National Committee for Crystallography (NCCr) representatives in Australia and New Zealand. At present, this includes Professor Kurt Krause from Otago University, the New Zealand NCCr representative, with the Australian role vacant.

Crystal35 was bookended by two excellent social events, with an informal mixer at the Ball & Chain, a restaurant and bar attached to the conference venue, on the Saturday night and a conference social at the Gage Roads Brewing Company on the Tuesday night. Many participants also took the opportunity to visit Rottnest Island, a 25-minute ferry ride from Fremantle, to see quokkas, a small wallaby-like marsupial, and to experience the stunning scenery of this protected nature reserve.

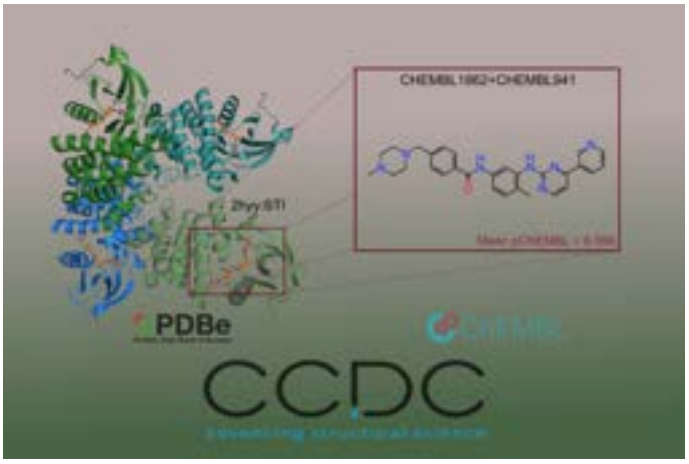


Clockwise from top left: Little Creatures brewery in Fremantle (photo: Chris Sumby), the pre-conference mixer at the Ball & Chain (photo: Charlie Bond), the conference venue (the Esplanade Hotel) (photo: Chris Sumby) and the conference social at Gage Roads Brewing Company (photo: Charlie Bond).

Christopher Sumby is located at The University of Adelaide.

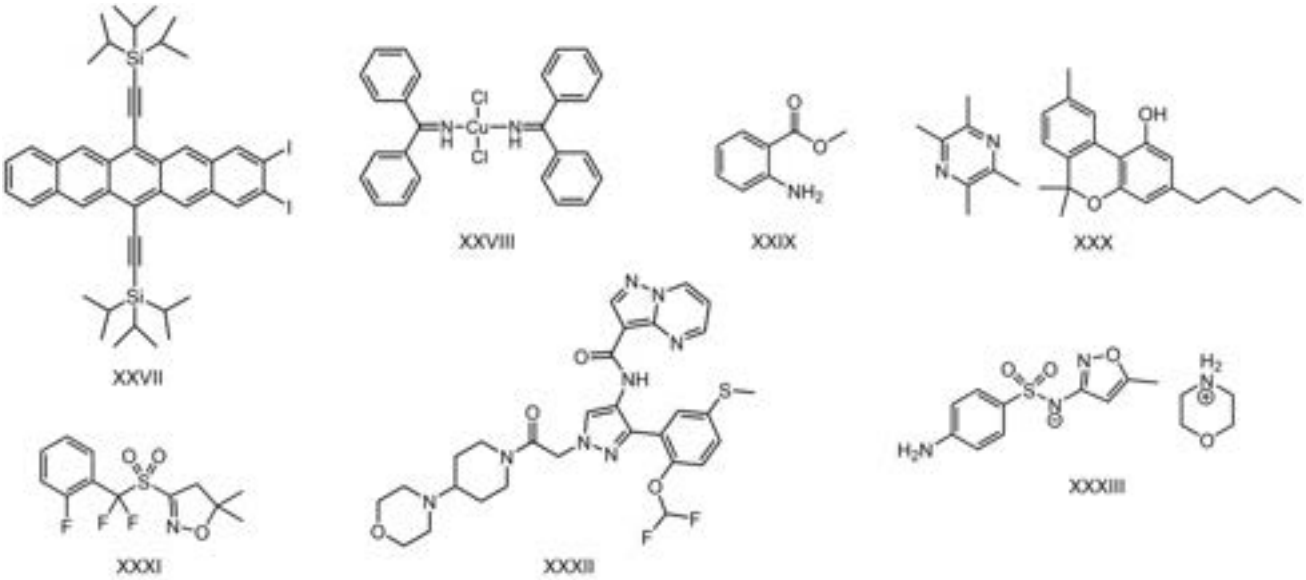
NOTICE

Results of the 7th CSP blind test published - overcoming pharmaceutical and other materials issues before they exist



Two scientific papers have been published detailing the findings from the 7th Crystal Structure Prediction (CSP) Blind Test (here and here). To coincide with these publications, the Cambridge Crystallographic Data Centre (CCDC) has released a CSP Blind Test database containing 171,679 entries from 207 different landscapes.

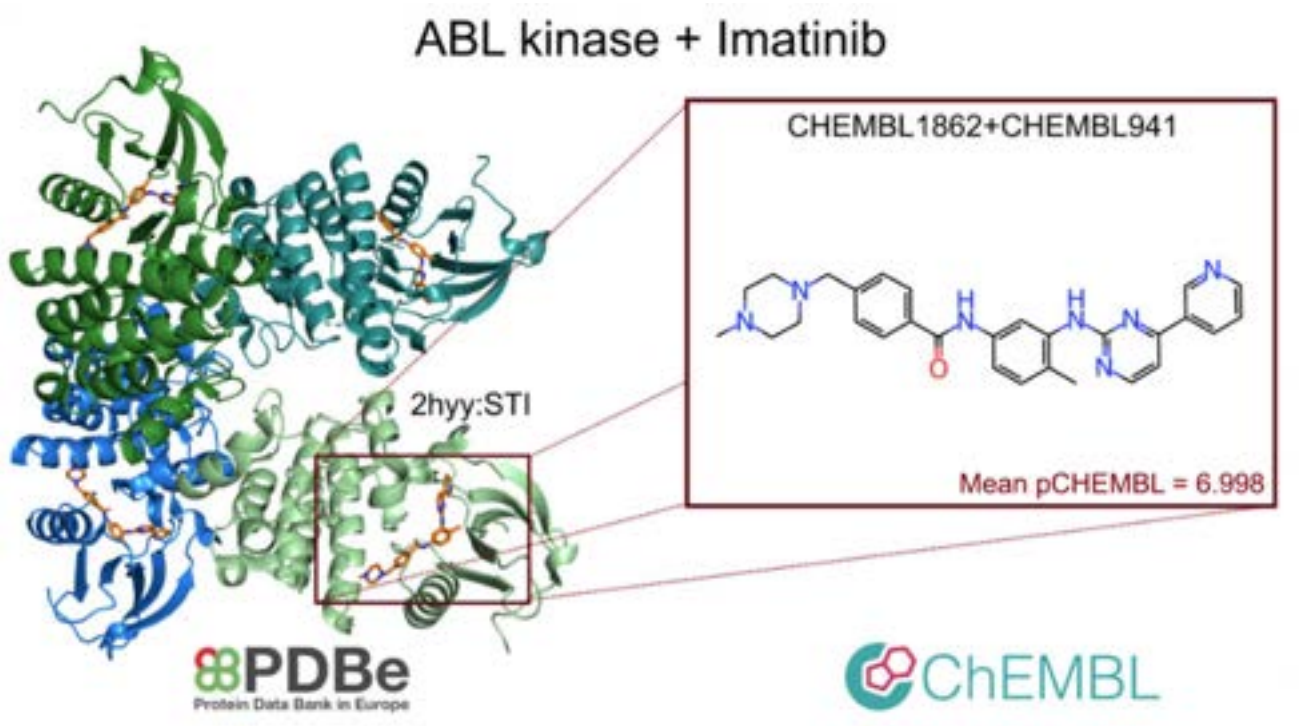
CSP predicts the most likely crystal structures to form from a given molecule, based on its 2D chemical structure. Most methods use informatics and computational science techniques. Predicting more stable structures leads to many benefits including improved manufacturing processes, patent protection and breaking, and the potential discovery of new improved materials. For more on this subject, click here.



Seven target systems of varying complexity featured in the 7th CSP Blind Test.

BioChemGraph - CSD data linked to PDBe, ChEMBL, and other sources via UniChem

In the era of data-driven biology, integrating information from different resources is essential yet often challenging. The BioChemGraph project addresses this challenge by creating infrastructure that consolidates structural, functional, and biochemical annotations for small molecules and their targets from key resources: the Protein Data Bank (PDB), the ChEMBL database and the Cambridge Structural Database (CSD). For more on this subject, click here.



Crystal structure of ABL kinase (PDB code 2hyy) in complex with imatinib. The simple report available as bioactivity_report_simple.tsv shows the mean pChEMBL value of 6.998, calculated from all available bioactivity data for this complex in ChEMBL. The full dataset can be accessed in bioactivity_report_full.tsv.

How to compare the packing of your polymorphs

Polymorphism is the ability of a compound to crystallize into multiple forms, which is important for pharmaceuticals since different polymorphs can affect a drug's bioavailability and efficacy. Comparing polymorphic structures can be complex, but tools like Crystal Packing Similarity and Structure Overlay in Mercury can help identify differences and similarities by examining packing environments and conformations. For more on this subject, click here.

Check out all of CCDC's latest blogs here.

New video: unlock crystal structure secrets with Mercury

This 5-minute video demonstrates how to use the Powder Pattern Simulator in Mercury. The Simulator is compatible with both CSD entries and structures in CIF format. Users with a CSD-Core license or higher (such as CSD-Materials, CSD-Discovery or CSD-Enterprise) have access to the option of adding a second wavelength in the simulation. Watch here, or below.

Events

In 2024, we hosted six free virtual workshops, attracting over 650 attendees from 61 different countries. Over 200 attendees achieved a perfect score of 100% on the post-workshop test. Thank you to everyone who joined us! We are preparing more virtual workshops for next year, with confirmed dates on the 11th and 25th of March and the 8th of April 2025.

The topics for these workshops will be announced soon, so please keep an eye on the events page of our website for updates or sign up for the CCDC newsletter to be the first to receive event announcements.

If you would like to suggest topics for our workshops, webinars and CSDU online training modules in 2025, please email us at hello@ccdc.cam.ac.uk.

Follow us on social media

Want to learn more about CCDC events, blogs, case studies and software updates? Follow us on LinkedIn, Facebook and X.

PRESS RELEASE

Setting the pace in non-ambient XRD: a new benchmark for environmental heating



Pioneers in non-ambient X-ray diffraction

While most X-ray diffraction (XRD) measurements are performed under ambient conditions (*i.e.* room temperature, ambient pressure), many processes, *e.g.* geological, catalytical or industrial ones, occur under non-ambient conditions. Non-ambient parameters, such as temperature, pressure, humidity or different gas atmospheres, can significantly alter a material's structure, property or reactivity. Since many of these changes are reversible, or occur stepwise with multiple intermediates, *in situ* investigation of materials under non-ambient conditions is an essential tool in establishing a detailed understanding of a material's properties.

When we introduced the HTK 10 High-Temperature Chamber at Anton Paar back in 1964, we made our mark in the history of non-ambient X-ray diffraction. The HTK 10 High-Temperature Chamber was capable of heating samples up to 1600°C in order to study their structural changes by X-ray diffraction during heating.

Prior to this, non-ambient X-ray diffraction of various materials was mainly done with homemade equipment, and there was no real commercial heating chamber available on the market. This changed when we entered the market 60 years ago. Since then, our knowledge and experience in X-ray diffraction - especially under non-ambient conditions - has steadily grown. This has led to our current broad portfolio of non-ambient X-ray diffraction attachments for studies between -190°C and +2300°C under different atmospheres (dry and humid) and pressures, as well as mechanical or electrical loads. Along with this complete portfolio, we also create customized solutions for our customers - something that has made Anton Paar the market leader in non-ambient XRD.

This year, we're proud to announce the launch of the HTK 1500 High-Temperature Chamber, the new benchmark of environmental heaters for high-temperature X-ray diffraction. The HTK 1500 allows for homogeneous heating of all types of sample materials, including crystalline powders and bulk samples, up to 1500°C. This makes it the only true environmental heater available on the market that reaches such high temperatures without any compromises in precision. The temperature sensor is located directly beneath the sample in a protective ceramic holder, guaranteeing highly repeatable and reliable temperature measurements. A fast and easy switch between reflection and transmission modes, by the use of a capillary extension, makes the HTK 1500 suitable for air-sensitive and organic powders and liquids. Sample spinning is also provided, which is crucial for improving data quality by overcoming preferred orientation. The sample carriers are made of chemically inert alumina, minimizing the risk of reactions with samples, even at high temperatures. A user-friendly slider for the sample holder allows for

quick and reproducible sample exchange.



The HTK 1500 is completely compatible with Anton Paar's XRDynamic 500 X-ray diffractometer. This combination offers high automation, including stage recognition, stage and sample alignment and realignment during heating, and easy connection of cooling water, vacuum, and gas lines. The seamless integration into the XRDynamic 500 control software ensures a user-friendly experience for high-temperature X-ray diffraction analysis.



https://www.anton-paar.com

info@anton-paar.com

FEATURE ARTICLE

Tribute to the support groups in the quasicrystal discovery – a 40-year anniversary



On November 3, 2011, at NIST, from left to right: Istvan Hargittai, William Boettinger, Frank Gayle, Francis Biancaniello, Stephen Ridder, Leonid Bendersky, Robert Schaefer and Balazs Hargittai. Photograph by Istvan Hargittai.

Istvan Hargittai

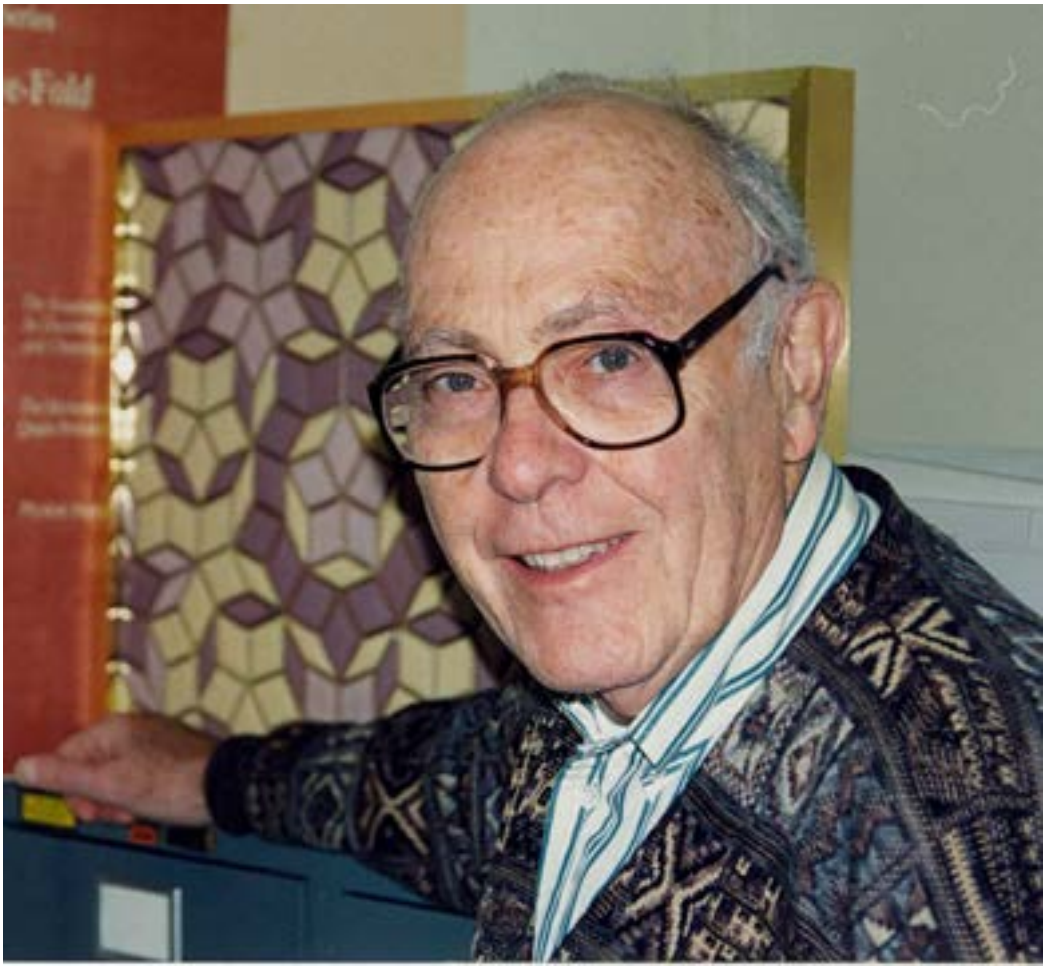
Forty years ago, in 1984, a brief communication in Physical Review Letters announced the discovery of quasicrystals (not yet using this term). Three scientists joined Dan Shechtman as co-authors. Previously, associates of the then National Bureau of Standards assisted Shechtman in his experiments. In 2011, Dan Shechtman received the Nobel Prize in Chemistry for the discovery of quasicrystals. There was no doubt that he deserved it and that he deserved the prize unshared. This personal review is dedicated to his 'support cast', the members of two groups that assisted his discovery and the publication reporting it.



Dan Shechtman, 1995, in the author's home in Budapest. Photograph by Istvan Hargittai.

Dan Shechtman's unshared Nobel Prize in 2011 was unequivocally appreciated by those familiar with his milestone discovery and his perseverance during the preceding years. Great scientific authorities had questioned the validity of the interpretation of his observation. The award signaled the official seal of approval of the existence of quasicrystals, which he announced in 1984 [1] but had observed in 1982 (see, *e.g.* [2−7]).

In 1981, Dan Shechtman of the Technion — The Israel Institute of Technology — went for his first sabbatical at the National Bureau of Standards (NBS; today, the National Institute of Standards and Technology, NIST, in Gaithersburg, Maryland). John W. Cahn (1928−2016), a senior scientist at NBS, initiated his appointment. The two first met in the late 1960s when Cahn visited the Technion, where Shechtman was an engineering student in the Department of Metallurgy. At the time, Cahn was already well known for his thermodynamics of materials [8]. Their next meeting was in 1972 when Shechtman was a postdoctoral fellow at the Aerospace Research Laboratories, Wright-Patterson Air Force Base, near Dayton, Ohio.



John W. Cahn, 1995, in Gaithersburg, Maryland, photograph by Istvan Hargittai.

Their “life-changing” meeting [8] happened in 1979 when Cahn and his wife stayed at the Technion for a longer period. By then, Shechtman had become an expert in electron microscopy and developed a method for studying metallic powders by transmission electron microscopy. His research focused on rapidly solidified metallic alloys, something a group at NBS had also been working on but not very successfully. Cahn thought that Shechtman would be a good addition to the group and invited him for a talk and then for a stay at NBS. Shechtman at NBS was supported by a joint program of the Defense Advanced Research Project Agency (DARPA) and the National Science Foundation (NSF). He had freedom in choosing and executing his research projects.

Shechtman first visited NBS in the summer of 1980 and gave a talk. Then, he returned with his family in August 1981 for “two magnificent years” [8]. In 1995 he remembered: “I started by studying rapidly solidified aluminum-iron alloys. I analyzed the phases present and the solidification patterns. I collaborated mainly with members of the metallurgy group, Bill Boettinger, Bob Schaefer, and Frank Biancaniello. We wrote a series of papers together and understood rapid solidification better. It was in April 1982, half a year after I had arrived, that I discovered the icosahedral phase.” ([2], p. 84) [Conversation with Dan Shechtman (1995). Balatonfüred, Hungary].



In 1984 at NBS, from left to right: Frank Biancaniello, John W. Cahn, Denis Gratias, Leonid Bendersky, Dan Shechtman and Robert Schaefer. Photograph by H. Mark Helfer/NIST; courtesy of NIST (colorized by the Editor).

Frank Biancaniello's role was especially important in Shechtman's studies. He was a technician, not yet a full-fledged researcher at the time (as he became soon afterward); his tasks included the preparation of the alloy samples of various compositions for the electron microscope–electron diffraction experiments. According to the other members of the group, Biancaniello was most enthusiastic about this project. He was happy to work many extra hours, including nights and weekends, and he was as skilled as he was devoted to this work. At Shechtman's initiative, the tests extended even outside the range of reasonable compositions — reasonable, that is, for expected practical applications. Biancaniello remembered [9]:

"Obviously, the quasicrystal discovery was the most important one culminating in Danny's Nobel. But many other exciting projects we worked on came to fruition over the years. I'm sure you have heard of some of the bulk metallic glass research being carried out over the years, with yield strengths on the order of 1 to 2 gigapascals with no ductility. Steve Ridder and I developed a High Nitrogen Stainless Steel with a yield strength of 1.1 gigapascals with an elongation of 60%, using so-called rapid solidification technology. I only mention this in an attempt to demonstrate how intellectually stimulating these thirty years were starting with working with Danny Shechtman and continuing on to recent times. As Bill Boettinger mentioned, we worked on many projects with Danny. Steve Ridder and I did more recent research with Danny using a quasicrystal for a wear-resistant coating while doing thermal spray studies."

Shechtman narrated in our 1995 conversation about some of the details of the seminal experiment ([2], p. 84):

"At first, I was studying rapidly solidified aluminum-iron alloy, which we thought had some commercial future. Eventually, it turned out that although rapid solidification research resulted in several useful products, it did not develop into a widespread technology. This, however, is not important for our story. In the aluminum-iron binary system, there was one metastable phase, Al_6Fe, which I studied. The

equivalent Al_6Mn in the aluminum-manganese system is a stable phase, and I wanted to compare some crystallographic features of the two. We started, therefore, to produce a series of aluminum-manganese alloys with increasing amounts of Mn in them. Eventually, I ran wild, from a practical point of view, since beyond several percent of manganese the rapidly solidified alloy becomes brittle and therefore useless. Among the alloy ribbons that I have prepared with Frank Biancaniello by melt spinning, there were alloys which contained over 25 weight percent manganese. On April 8, 1982, as I was studying by electron microscopy rapidly solidified aluminum alloy which contained 25% manganese, something very strange and unexpected happened. It is worthwhile to look at my TEM [transmission electron microscope] logbook records of that day. For plate number 1725 (Al-25% Mn) I wrote: '10 Fold ???'. There were ten bright spots in the selected area diffraction pattern, equally spaced from the center and from one another. I counted them and repeated the count in the other direction and said to myself: ‘There is no such animal’. In Hebrew: 'Ein Chaya Kazo'. I then walked out to the corridor to share it with somebody, but there was nobody there, so I returned to the microscope and, in the next couple of hours, performed a series of experiments. Most of the needed experiments were performed at that time. A few days later, all my work was complete, and everything was ready for the announcement. Then it took two years to publish it.”

This comment that “it took two years to publish it” signified a hard time for Shechtman. The delay was not only due to the disbelief of the scientific community that the dogma about the impossibility of fivefold symmetry (and other 'forbidden' symmetries) in the world of crystals should fall. It was also that no convincing model could be constructed for interpreting the unexpected observation. At the same time, sitting on a seminal observation, he felt the necessity of communicating it to the broader community of researchers. He produced a manuscript in co-authorship with Ilan Blech (b. 1936), one of his former professors at the Technion, who devised a model to interpret Shechtman’s observation. This also meant that in Ilan Blech Shechtman found someone who shared his conviction that it indeed was an observation of a heretofore unknown structure.

They submitted their manuscript to the *Journal of Applied Physics* (*JAP*) in the summer of 1984. The disappointing editorial decision came back with a review. The Editor of *JAP*, Lester Guttman, wrote [10]: “Our reviewer and we both believe that your paper will not reach the most appropriate audience through this journal, and we are therefore returning your manuscript. We wish to make it clear that this is not a comment on the technical quality of your work; rather, it is an attempt on our part to try to place papers where they will be of the greatest use to the greatest number of people.” As the manuscript was more of the nature of a report in metallurgy than in physics, eventually, it was published in a metallurgy journal, *Metallurgical Transactions* [11]. The name of the journal was later changed to *Metallurgical and Materials Transactions*. In the wake of Shechtman’s Nobel Prize, the editor of this journal invited Shechtman’s three co-authors of the *Physical Review Letters* paper to recount their experience in that co-authorship [12]. This account was followed by a reproduction of the 1985 Shechtman-Blech paper [11].

Even before Shechtman received the letter of rejection from *JAP*, he showed the manuscript to John W. Cahn. Shechtman did not do this too eagerly, as Cahn’s initial reaction when he showed him the April 8 observation was rather negative. In Cahn’s words [13] [Conversation with John W. Cahn (1995). NIST, Gaithersburg, Maryland]: “One day he came into my office, and said, ‘John, what do you think of a 10-fold axis?’ I said, ‘Don’t bother me, Danny, this is clearly twinning’, and he said, ‘I don’t think so’. Then we discussed a number of experiments to decide this question. I didn’t know much about twinning, but I did know that through twinning you could get unexpected symmetries.”

They did not talk again about Shechtman’s observation until mid-1984. In the meantime, Shechtman was back in Israel, and when he returned, he wanted to inform Cahn about the difficulties of publishing his April 8 observations. At the time, Cahn was attending a Gordon Conference in Aspen, Colorado, but when Shechtman’s word reached him, he flew back one day early from the conference. Shechtman showed him the manuscript that had been submitted to *JAP* but had not been rejected yet. We continue with Cahn’s own words [13]:

“I read this paper immediately and got very excited because I saw the data for the first time. I wasn’t convinced by the Blech model, but I was very much convinced by the experiments. It was obvious that it was not twinning, that it was something outside of what was known. I’m sure that had I seen the data in ’82, the same day when they were taken, we wouldn’t have wasted two years. On Friday, I met with Danny and said, this is a poorly written paper; you’re hiding this new phase. The entire paper was about experiments on aluminum–manganese. It started out by saying that we did this, we found this, and gave a list of the known periodic phases for each composition range, and buried, in half a paragraph, was a new phase, in the middle of an otherwise very conventional paper. My impression was that it was written that way to sneak it past the referee because everybody, except Blech, had told him that he had nothing. I remember that Friday going to the bosses [at NBS] and telling them that this is really something and it’s going to be big. I more or less said that we should mount a major effort; lots of people should shift because this has got to be investigated. At this stage I was not a co-author, and I did not expect to be a co-author. I told Danny that this is the wrong paper, but Danny told me that the paper had been submitted.”



Denis Gratias and Dan Shechtman in Shechtman’s office at the Technion, in January 2011, nine months before the announcement of Shechtman’s Nobel Prize. Shechtman is wearing his 'quasicrystal tie'. Photograph by Istvan Hargittai.

When the paper was rejected by *JAP* and published in *Metallurgical Transactions*, Cahn encouraged Shechtman to write “a proper paper”. To this, Shechtman said to Cahn [13]: “if you feel so strongly about it, can you write this paper?” To which Cahn replied: “Danny, this is your work; you’re making me an enormous gift.” Shechtman did not mind, and the two and a half journal-page paper was produced, though not before Cahn had invited a young French theoretician, Denis Gratias, to join them in writing the paper. Blech did not participate in producing this manuscript, but Shechtman added his name out of loyalty. Blech soon went into industry; he now lives in California. The others continued in research. Denis Gratias is currently a research director emeritus at the CNRS, the French National Center for Scientific Research. His highest recognition was his election to be a corresponding member of the French Academy

of Sciences in 1994.

John W. Cahn's co-authorship in the 1984 *Physical Review Letters* paper was an important event, but only one of several in his rich research career. He was born in Cologne, Germany, in a Jewish family. His father was a lawyer known for his anti-Nazi sympathy who narrowly escaped arrest upon the Nazi takeover in 1933. The family fled Germany and, after a few years in Holland, emigrated to the United States in 1939. They lived in New York City, and Cahn served in the US Army in Japan during its occupation. Cahn received a bachelor's degree in chemistry in 1949 at the University of Michigan and a PhD in physical chemistry in 1953 at the University of California Berkeley. For the next decade, he worked in chemical metallurgy at General Electric in Schenectady and became a professor of metallurgy at the Massachusetts Institute of Technology from 1964−1978, followed by his tenure at the NBS/NIST from 1977−2007. His research results in metallurgy, non-crystalline materials, and other areas of materials science and technology were manifested in numerous publications and named effects and equations. The development of his research interests has been summarized [14]. His achievements were recognized by numerous awards and other signs of appreciation. He was elected member of the US National Academy of Sciences in 1973 and the National Academy of Engineering in 1998. He received the National Medal of Science in 1998 and the Kyoto Prize in 2011.

When Cahn accepted Shechtman's assertion that his observation was a discovery of a heretofore unknown phenomenon, however great Cahn's authority was in materials science, there were more hurdles to overcome. In Cahn's words [13]:

"At NIST, we have an Editorial Review Board. Every paper from the Institute has to be reviewed internally before it can be sent out. This Review Board was afraid of another polywater. The Bureau of Standards had been burned by polywater[1] publications. The Board wanted to be on the right side this time and had asked local crystallographers to give them lectures about fivefold symmetry, why it can't be. They were spending a great deal of time. The Board was split. My Division Chief of Metallurgy, also an old friend, said to me, 'John, you have a wonderful reputation. Why ruin it by putting your name on something like such a paper.' I said, 'please, read this paper, it is very important and very exciting, and it's not a time to be conservative.' The Board took a very long time, they had lots of meetings, sometimes they came to me for advice but I was never present at these meetings. They carried an inquiry very carefully, and eventually they approved the paper. Finally, in mid-October, we could send off the manuscript. It came out three weeks after it was submitted."

After the paper was published, it generated enormous interest and an avalanche of publications. Foremost among them was a brief communication by Paul Steinhardt and Dov Levine of the University of Pennsylvania. They offered a plausible model and coined the name 'quasicrystal' [15].

As we have seen Shechtman had two supporting teams, one for his seminal experiment and one for its publication, with John W. Cahn bridging the two. The following years, however, Shechtman spent essentially as a lone hero of perseverance. There was a growing number of his supporters, but the dissenters could refer to the devastating opinion of Linus Pauling (1901−1994), arguably the most revered chemist of the time. In the fall of 1993, not long before his passing, I asked Pauling about quasicrystals. He dismissed it; not the experiment, not even the name, but the interpretation, and he did this in an uncompromising manner [16]: "As to the quasicrystals, you know that I contend that icosahedral quasicrystals are icosahedral twins of cubic crystals containing very large icosahedral complexes of atoms. It is not surprising that these crystals exist. The first one to be discovered was the MgZnAl compound reported by my associates and me in 1952. We did not observe quasicrystals of this compound, but they have been observed since then." Even after Pauling's death, many of his followers were reluctant to disrespect the memory of their Master by accepting Shechtman's discovery for what it was. The Nobel Prize in 2011 ended any such hesitation.

Although solid state structures have not been in my research interest except for comparison with gaseous structures, quasicrystals have fascinated me ever since I heard about them. Curiously, I had learned about the possibility of their existence as early as 1982. I organized a lecture series for Alan L.

Mackay of Birkbeck College at Eötvös University in Budapest and two of his presentations were about fivefold symmetry. Mackay warned us that if we believed the impossibility of fivefold symmetry in solid-state structures, as classical crystallography had taught us, we might let it pass us unrecognized even if we observed it (see, *e.g.* [17] (Conversations with Alan L. Mackay, October 1994, London) and [18]).

In 1987, I attended a crystallography meeting in Moscow in honor of Alexei Shubnikov's centennial [19]. There, Shechtman's discovery dominated the discussions in the coffee breaks. We met first in person in the early 1990s when I spent a month in Israel as a visiting professor at Ben-Gurion-University in Beer Sheva. This stay allowed me to give invited lectures at all major universities in Israel. During one of these presentations as I was talking at length about the significance of Shechtman's quasicrystals, suddenly someone in the audience stood up and said: "I am Danny Shechtman." Thus, our friendship began. In 1995, I was responsible for the scientific program of a crystallography meeting/school in Balatonfüred, Hungary, and quasicrystals received plenty of exposure with Shechtman as a star lecturer. There were other encounters but fast forward to January 2011 when at my initiative and, perhaps, at others' as well, there was a meeting at the Technion celebrating Shechtman and his discovery. This meeting happened nine months before the announcement of his Nobel Prize.

My son, Balazs, and I visited NIST on November 3 and 4, 2011, responding to an invitation for a presentation about Edward Teller and the other Hungarian 'Martians' of science. As our visit happened a few weeks after the announcement of Shechtman's Nobel Prize, I gave an impromptu talk about the quasicrystal discovery as well. We spent several hours with Shechtman's former colleagues, and we learned about the warm feelings they had toward Shechtman and their pride for having contributed to the discovery [5].

His former NIST colleagues have rarely figured in Shechtman's statements. In his two-minute speech at the festive Nobel banquet on December 10, 2011, of his two support groups, he mentioned only the names of his co-authors of the seminal paper [20]. There was no acknowledgments section in his Nobel lecture [21], which my wife and I attended in December 2011 in Stockholm. Neither was there one in his Gregory Aminoff lecture in 2000 in Stockholm, which we also attended. The latter was linked to the 'Symmetry 2000' conference. Alas, Shechtman did not produce his presentation for the volumes of the proceedings of that meeting [22], just as he never wrote up his Nobel lecture for publication either (but it can be watched as a video [21]). One can only speculate that he may have had some frustrating experience at NBS that he did not wish elaborating. He acknowledged though his joint work with NBS associates in our 1995 conversation when he told me: "I collaborated mainly with members of the metallurgy group, Bill Boettinger, Bob Schaefer, and Frank Biancaniello." ([2], p. 84).

References

[1] Shechtman, D., Blech, I., Gratias, D. & Cahn, J. W. (1984). Metallic phase with long-range orientational order and no translational symmetry. *Phys. Rev. Lett.* **53**, 1951–1953.

[2] Hargittai, B. & Hargittai, I. (2005). *Candid Science V: Conversations with Famous Scientists*, ch. 5, pp. 76-93. London: Imperial College Press.

[3] Hargittai, I. & Hargittai, M. (2000). *In Our Own Image: Personal Symmetry in Discovery*, pp. 157-172. New York: Kluwer/Plenum.

[4] Hargittai, I. (2011). Dan Shechtman's quasicrystal discovery in perspective. *Isr. J. Chem.* **51**, 1144–1152.

[5] Hargittai, I. (2011). *Struct. Chem.* **22**, 745–748. (This was based on an invited contribution to *IGGERET*, the Hebrew-language publication of the Israeli Academy of Sciences and Humanities.)

[6] Hargittai, B. & Hargittai, I. (2012). Quasicrystal discovery–from NBS/NIST to Stockholm. *Struct. Chem.* **23**, 301–306.

[7] Gratias, D. & Quiquandon, M. (2019). Discovery of quasicrystals: the early days. *C. R. Phys.* **20**, 803–816.

[8] Shechtman, D. (2016). My Memories of John Cahn, NIST.

[9] Biancaniello, F. (2011). Private communication by e-mail to I. Hargittai, November 3, 2011.

[10] Shechtman, D. (2011). Private communication by e-mail to I. Hargittai, December 26, 2011.

[11] Shechtman, D. & Blech, I. (1985). The microstructure of rapidly solidified Al_6Mn. *Metall. Trans. A*, **16A**, 1005-1012.

[12] Blech, I. A., Cahn, J. W. & Gratias, D. (2012). Reminiscences about a Chemistry Nobel Prize won with metallurgy: comments on D. Shechtman and I. A. Blech, Metall. Trans. A, 1985, Vol. 16A, pp. 1005–12. *Metall. Mater. Trans. A*, **43**, 3411–3422.

[13] Hargittai, I. & Hargittai, M. (2000). *In Our Own Image: Personal Symmetry in Discovery*, pp. 165-167. New York: Kluwer/Plenum.

[14] Bottinger, W. J., Handwerker, C. A. & Gayle, F. W. (2019). John W. Cahn. *Memorial Tributes*. Vol. 22, pp. 38-44. Washington, DC: National Academies Press.

[15] Levine, D. & Steinhardt, P. J. (1984). Quasicrystals: a new class of ordered structures. *Phys. Rev. Lett.* **53**, 2477–2480.

[16] Interview via e-mail with Linus Pauling in the fall of 1993. (1995). *Chem. Intell.* **1**(1); reproduced in Hargittai, I. (2000). *Candid Science: Conversations with Famous Chemists*, edited by M. Hargittai, pp. 2-7. London: Imperial College Press. (Actual quote, p. 6.)

[17] Hargittai, B. & Hargittai, I. (2005). *Candid Science V: Conversations with Famous Scientists*, ch. 4, pp. 56-75. London: Imperial College Press.

[18] Hargittai, I. (2017). Generalizing crystallography: a tribute to Alan L. Mackay at 90. *Struct. Chem.* **28**, 1–16.

[19] Hargittai, I. & Vainshtein, B. K. (1988). Editors. *Crystal Symmetries: Shubnikov Centennial Papers*. Oxford: Pergamon Press.

[20] Dan Shechtman – Banquet speech (2011). https://www.nobelprize.org/prizes/chemistry/2011/shechtman/speech/.

[21] Dan Shechtman – Nobel Lecture (2011). https://www.nobelprize.org/prizes/chemistry/2011/shechtman/lecture/.

[22] Hargittai, I. & Laurent, T. C. (2002). Editors. *Symmetry 2000, Part 1 and Part 2*. Proceedings from a symposium held at the Wenner-Gren Centre, Stockholm, September, 2000 (in two volumes). London: Portland Press.

1 For polywater, see https://en.wikipedia.org/wiki/Polywater.

Istvan Hargittai is located at the Budapest University of Technology and Economics, Hungary.

IUCR SUPPORTED EVENTS

IUCr supported meetings

These forthcoming meetings are supported by grants from the IUCr Calendar Committee.



11th Oct 2026 - 16th Oct 2026

Indaba10

Skukuza, Kruger National Park, South Africa



5th Dec 2026 - 10th Dec 2026

African Materials Research Society (AMRS 2026)

Nairobi, Kenya

MEETINGS CALENDAR

Meetings calendar

This is a list of meetings of interest to crystallographers occurring within the next twelve months, as recorded in the IUCr Calendar of Events. Please let us know of any that are missing by completing this form or sending an email to forthcoming.meetings@iucr.org.



Indaba10 South Africa 11th Oct 2026 - 16th Oct 2026



Synchrotron Radiation: Science, Knowledge, Innovations, Future (SKIF-2026) Russian Federation 18th Oct 2026 - 23rd Oct 2026



CCP-EM/Diamond Icknield Workshop United Kingdom 9th Nov 2026 - 13th Nov 2026



Instruct-ERIC hands-on workshop on Advanced cryo-FIB-SEM methods Germany 9th Nov 2026 - 13th Nov 2026



Crystal36-AXAA 2026 Meeting Australia 26th Nov 2026 - 2nd Dec 2026

African Materials Research Society (AMRS 2026) Kenya 5th Dec 2026 - 10th Dec 2026

Joint Polish-German Crystallographic Meeting 2027 Germany 15th Feb 2027 - 18th Feb 2027